

THESIS

WOOD-INDUCED STREAM CHANNEL COMPLEXITY AS A DRIVER OF TRANSIENT
STORAGE

Submitted by

Anna E. Marshall

Department of Geosciences

In partial fulfillment of the requirements

For the Degree of Master of Science

Colorado State University

Fort Collins, Colorado

Summer 2021

Master's Committee:

Advisor: Ellen Wohl

Ryan Morrison

Sara Rathburn

Copyright by Anna Elizabeth Marshall 2021

All Rights Reserved

ABSTRACT

WOOD-INDUCED STREAM CHANNEL COMPLEXITY AS A DRIVER OF TRANSIENT STORAGE

Rivers are naturally diverse, heterogeneous systems. This spatial heterogeneity is driven by inputs into a river corridor including water, sediment, large wood, coarse particulate organic material (CPOM), and dissolved loads, all of which interact with the river valley to create distinct forms of geomorphic complexity. Spatial heterogeneity within a river corridor drives surface exchange of water, sediment, and nutrients moving downstream and into transient storage zones. Transient storage is increased by features that enhance bed heterogeneity and surface flow separation, such as large wood. This thesis explores the role that wood-induced spatial heterogeneity has in facilitating zones of surface transport and storage. Specifically, I look at how discharge and logjam characteristics drive transient storage, as reflected in the movement of salt tracers and CPOM.

Logjams alter gradients in hydraulic head and create zones of flow-separation and low velocity along channel margins, which enhance storage of organic matter and solutes. Although research has shown that a single logjam in a channel increases transient storage, limited work has been done to understand the characteristics of logjams that enhance transient storage. Scientific gaps remain in understanding whether decreasing the downstream spacing of logjams or the logjam porosity drives an increase in transient storage. Here, I designed experiments for two constructed flume systems—one with a change in downstream logjam spacing and one with a change in logjam porosity—to understand the effects of logjam characteristics on transient

storage at different flows. More closely spaced logjams resulted in slower advection down the flume channel at low flows. At high flows and with changing porosities, there was no consistent effect of jam spacing or jam porosity on advective travel times. This likely points to the influence of a low Damkohler number, where high velocity and/or short reach length resulted in only a small amount of flow-path exchange with storage zones. In the future, a modified flume configuration with exaggerated scaling of discharge and porosity may be necessary to better distinguish the study effects.

Surface transient storage is also a physical control on CPOM transport and deposition. The details of surface transient storage determine when and if CPOM is deposited and remobilized. Yet, no studies have looked at how CPOM transport and storage vary in relation to shorter (diurnal) as well as longer (seasonal peak flow) variations in discharge. I physically sampled CPOM moving along the bed and in-suspension at stream reaches above and below a logjam as well as a location with no logjam. I sampled CPOM masses throughout a seasonal hydrograph and on a 24-hour diurnal timespan to examine how transport and deposition changed with flow. The majority of CPOM was transported in suspension following a clockwise hysteresis along the seasonal hydrograph. CPOM stored in the channel and overbank areas is more likely to be mobilized as stage rises and snowmelt runoff enters the channel, whereas the supply of CPOM is depleted as the snowmelt hydrograph continues. A similar hysteresis in CPOM transport did not occur during 24-hour diurnal fluctuations in discharge except at peak CPOM movement. CPOM peaked before discharge peaked on both the diurnal and seasonal hydrographs. CPOM transport in a logjam backwater occurred at a significantly lower rate than in reaches without logjams, suggesting logjams provide storage zones for CPOM.

Understanding the characteristics and processes of wood-induced spatial heterogeneity that facilitate zones of surface transport and storage has important management implications. Large wood and hyporheic restoration are increasingly used to enhance ecosystem services and functions in rivers, yet the specific characteristics of logjams remain poorly defined. Considering that CPOM is a primary energy source in the food webs of shaded forest streams, management designed to foster the sustainability of stream ecosystems can benefit from maintaining or creating features that enhance CPOM retention. Furthermore, designing logjams to restore a river reach with the goal of improving hydrologic function will provide greater value if the design incorporates reach-scale logjam characteristics that enhance transient storage.

ACKNOWLEDGEMENTS

This research has benefited from the minds and labor of many and I am continually grateful for the small village it took to see this project through. First, I would like to thank my advisor, Ellen Wohl, who has pushed me to keep asking question and run with ever-evolving research ideas. I have tremendous respect for Ellen's ability to move through a revolving door of research questions with speed and diligence and her mentorship and humor over the past two years have taught me a great deal. My fluvial family has also offered countless hours of conversation over new ideas and interpretation.

Financial support was provided for my M.S. through the National Science Foundation (NSF 1819068). This project was collaborative between the Colorado School of Mines and the Ohio State University and my work was continually enhanced by guidance and feedback from Kamini Singha and Audrey Sawyer as well as Karl Wilhelmsen and Sawyer McFadden during all phases of the project. Kamini and Audrey worked repeatedly with me to untangle flume results and served as continual sounding boards as I worked through interpreting those results. Sara Rathburn and Ryan Morrison, as my M.S. committee, have provided valuable insight in the planning phases of my project as well as feedback on my thesis. The third chapter of my thesis also benefited from anonymous feedback from two reviewers as part of the publication process.

The labor of carrying 50-lb bags of salt and equipment into the study area and running tracer tests in the field was shared by a large number of people including Kamini Singha, Audrey Sawyer, Ellen Wohl, Jackie Randall, Sawyer McFadden, Karl Wilhelmsen, Zach Kornse, Danny White, Marissa Karpack, Ian Gambill, Garrett Wright, John Kemper, Kaitlyn Berckmann, Sarah Lowe, Chloe Roth, Emily Iskin, Logan Rutt, and Luke Jacobsen. Additionally, Danny White,

Sawyer McFadden and Jackie Randall provided supplies and brainpower for setting up the flume. Emily Iskin supported me with a summer of help in the field and flume. David Merritt provided the sampling apparatus for measuring CPOM and Lucas Zeller helped establish a consistent methodology in the field.

I acknowledge that the land my field and flume work was conducted on is the traditional and ancestral homelands of the Arapaho, Cheyenne, and Ute Nations and recognize, with respect, the Indigenous peoples as original stewards of this land.

Finally, my family deserves perhaps the greatest thanks as the ones who sparked a never-ending curiosity and love of getting my feet wet at a young age. I dedicate this thesis to them.

TABLE OF CONTENTS

ABSTRACT.....	ii
ACKNOWLEDGEMENTS.....	v
CHAPTER 1: OVERVIEW.....	1
References.....	7
CHAPTER 2: CHARACTERIZING LOGJAMS AS DRIVERS OF TRANSIENT STORAGE AT DIFFERENT FLOW REGIMES IN A FLUME.....	10
Summary.....	10
1. Introduction.....	11
1.1 Transient Storage in Rivers.....	11
1.2 Logjams in Rivers.....	13
1.3 Linking Logjams and Transient Storage.....	15
1.4 Knowledge Gaps.....	16
1.5 Research Objective.....	17
2. Flume Methods.....	19
2.1 Initial Flume Set-Up Using Field Scaling and Electrical Resistivity.....	21
2.2 Changing Longitudinal Spacing.....	27
2.3 Changing Porosity.....	31
2.4 Analyzing Transient Storage Data.....	33
3. Results and Discussion.....	39
3.1 Overview of Data.....	39
3.2 Changing Longitudinal Spacing.....	39
3.3 Changing Porosity.....	43
3.4 Sources of Error and Future Work.....	44
4. Conclusions.....	48
References.....	50
CHAPTER 3: SEASONAL AND DIURNAL FLUCTUATIONS OF COARSE PARTICULATE ORGANIC MATTER TRANSPORT IN A SNOWMELT-DOMINATED STREAM.....	58
Summary.....	58
1.0 Introduction.....	59
2.0 Field Area.....	64

3.0 Methods.....	66
3.1 Sample collection and processing.....	66
3.2 Data analysis.....	68
4.0 Results.....	69
4.1 CPOM Transport (H1).....	70
4.2 Seasonal Hydrograph (H2).....	71
4.3 H3: Diurnal Cycle.....	72
4.4 H4: Local Storage Features.....	74
5.0 Discussion.....	75
6.0 Conclusions.....	77
References.....	79
SUPPLEMENTARY INFORMATION.....	84
Appendix I.....	84
Appendix II.....	86
Appendix III.....	96
Appendix IV.....	97
Appendix V.....	103
Appendix VI.....	107

CHAPTER 1: OVERVIEW

A river corridor consists of the channel, the floodplain, and the hyporheic zone beneath the channel into which stream flow moves downward and from which hyporheic water upwells. The spatial heterogeneity of a river corridor describes variation in geomorphic characteristics such as grain-size distribution, cross-sectional channel geometry, or planform. This spatial heterogeneity is driven by inputs into a river corridor including water, sediment, large wood, coarse particulate organic matter (CPOM), and dissolved load (Figure 1.1), all of which interact with the river valley to create distinct forms of geomorphic complexity (Wohl, 2016). Each of these characteristics can also vary through time. A single source of spatial heterogeneity in a river can create a myriad of additional heterogeneity that shapes a diverse river corridor. The introduction of a piece of wood or a logjam, for example, acts as a driver of physical complexity in a river. A logjam spanning a channel will create a backwater in which fine sediment and organic material are deposited, which in turn creates more 3-dimensional variation in sediment volume and grain-size distributions. Water will move at a slower velocity through the backwater, thus creating spatial variations in hydraulics.

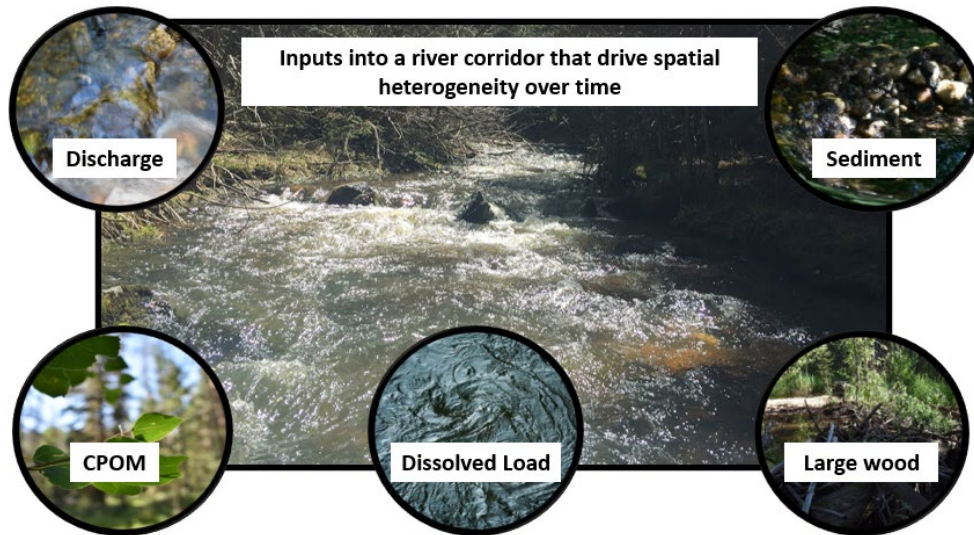


Figure 1.1. Inputs into a river corridor, which interact with the valley context to create spatial heterogeneity.

Spatial heterogeneity within a river corridor promotes retention of water, sediment, and nutrients moving downstream and into transient storage zones. Transient storage in streams consists of water connected to the surface flow that is delayed in its downstream transport by a stream feature (Zarnetske et al., 2007) (Figure 1.2). Along the surface, stream water in flux is stored in eddies along the margins of a spatially heterogeneous channel, in backwaters upstream from a logjam, or in floodplain sediment. Stream water in flux is also driven through subsurface flow paths vertically beneath the channel and laterally beneath the banks and by changes in pressure gradients caused by a stream feature (Cardenas & Wilson, 2007). These subsurface transient storage zones are located beneath or adjacent to the water column where stream water is forced into sediments via head gradients as flow through the porous media and then reenters the stream at some distance downstream (Harvey & Bencala, 1993) (Figure 1.2).

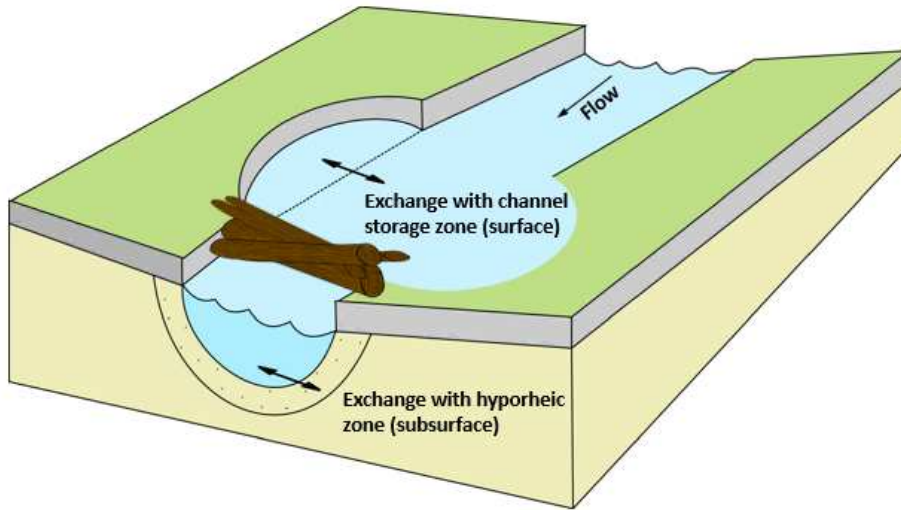


Figure 1.2. Stream-water flow path exchange with surface and subsurface transient storage zones.

Stream features that create spatial heterogeneity in the channel, such as wood, can promote lateral connectivity by forcing high flows onto the floodplain and increase vertical connectivity by increasing pressure gradients for flows moving between the surface and subsurface of the stream (Figure 1.2). Strong lateral and vertical connectivity and limited longitudinal connectivity can attenuate downstream fluxes of excess nutrients and fine sediment, both of which can be pollutants to streams. This 3-dimensional connectivity that promotes zones of transient storage has important implications for ecosystem health in a river. Storage of water fluxes in zones of transient storage for even a few minutes makes nutrients, in particular, more accessible to biota, starting with microbes and aquatic insects that form the base of the river food web (Battin et al., 2008). Connectivity among channel, floodplain, and hyporheic zone also has implications for ecosystem health beyond the river itself because rivers play such a critical role as migration corridors and preferred habitat for many terrestrial species, as well as aquatic and riparian species.

Spatial variations in storage features and temporal variations in discharge influence the transport of CPOM in the channel. CPOM can be transported downstream or stored by channel features such as logjams or eddies (Beckman & Wohl, 2014). Physical complexity, such as logjams or other boundary irregularities that create sites of lower velocity and shear stress, promotes storage and retention zones that can extend the residence time of CPOM during downstream transport (Bilby & Likens, 1980; Raikow et al., 1995; Lautz & Fanelli, 2008; Beckman & Wohl, 2014; Jochner et al., 2015; Livers & Wohl, 2016; Livers et al., 2018). Streams with lower wood loads (volume of wood per area) are significantly less retentive of CPOM and less physically complex than streams with abundant wood loads (Beckman & Wohl, 2014; Livers et al., 2018; Livers & Wohl, 2016).

This thesis explores the role that wood-induced spatial heterogeneity has in facilitating zones of surface transport and storage. I look at how discharge and specific characteristics of logjams drive transient storage and in turn how transient storage facilitates solute transport and the movement and deposition of coarse particulate organic matter (CPOM).

My investigation of the relative importance of logjam characteristics in influencing transient storage includes flume and field components. I look at how changing the longitudinal spacing of logjams as well as logjam porosity at varying discharges influences transient storage in a flume. In the field, I observe how CPOM transport and deposition change around logjams at varying discharges. Key terms for varying wood-induced spatial heterogeneity are included in Table 1.1.

Table 1.1 Wood terminology definitions used to describe spatial heterogeneity.

Term	Definition	Reference
Wood	Any size of woody material greater than 1 cm in diameter	Manners et al., 2007
Large wood (LW)	Wood >10 cm in diameter and 1m in length	Wohl et al., 2010
Coarse particulate organic matter (CPOM)	Any organic material that is less than 1 cm in diameter or is composed of non-woody organic material (i.e., leaves)	Marshall et al., 2021
Channel-spanning logjams (logjam or jam)	Any accumulation of fluvially transported wood with three or more wood pieces in contact with one another	Beckman & Wohl, 2014
Logjam porosity (Φ_j)	Interconnected void space between solids in the jam	Livers et al., 2020
Longitudinal spacing	Spacing of logjams moving consecutively downstream	Wohl & Beckman, 2014

As might be expected, previous work indicates that greater spatial heterogeneity within a channel equates to greater potential for transient storage (e.g., Gooseff et al., 2007). A growing body of recent research describes wood as a driver of channel spatial heterogeneity (e.g., Buffington & Montgomery, 1999; Collins et al., 2012; Faustini & Jones, 2003) and as a driver of transient storage (e.g., Ader et al., 2021; Kaufmann & Faustini, 2012; Sawyer et al., 2011; Sawyer & Cardenas, 2012). However, large gaps remain in understanding the relative importance of different logjam characteristics and varying flow regimes in creating transient storage because of the complex interactions among wood, hydraulics, and sediment dynamics. I address some of these gaps using two distinct sets of observations and analyses. Chapter 2 assesses the relative importance of different discharges and logjam characteristics, specifically longitudinal spacing and porosity, in influencing surface transient storage based on physical experiments in a flume. Chapter 3 addresses patterns of CPOM transport and deposition at varying distances downstream from logjams at different discharges in a mountain stream. This chapter is published as Marshall et al. (2021).

The broad goals of this work are to increase understanding of wood-induced stream channel complexity as a driver of transient storage and to understand how these features influence CPOM transport. Restoration to re-establish natural riverine function has grown into a multi-billion-dollar industry despite a lag in understanding how to place LW in rivers to improve specific processes or how to evaluate the function of natural LW (Roni et al, 2014; Grabowski et al., 2019). To design river restoration projects efficiently and effectively, more attention is needed toward studying the specific characteristics of LW that influence habitat and natural processes. In the past few decades, the importance of transient storage has become central to river science in an integrated view that recognizes the importance of vertical and lateral connections of rivers with surrounding floodplains and underlying aquifers (e.g., Stanford & Ward, 1993) as well as the flood pulses that drive additional exchanges (e.g., Poff et al., 2007). Numerous environmental challenges are influenced by transient storage, including water quality (e.g., O'Connor et al., 2010), river restoration (e.g., Marttila et al., 2018), and climate change (e.g., Meyer et al., 1999). Despite a growing scientific understanding, one challenge that river restoration practitioners and decisionmakers faces is the lack of best available science to draw upon to develop lines of evidence to support detailed placement and evaluation of wood in rivers to maximize processes such as transient storage. Limited understanding of logjam processes constrains our ability to design wood-based river restoration targeted to restore habitat and ecosystem function (Roni et al., 2014). This work represents a small step forward in understanding the intricacies of various drivers of transient storage in an effort toward restoring and increasing the natural function of river corridors.

References

- Ader, E., Wohl, E., McFadden, S., & Singha, K. (2021). Logjams as a driver of transient storage in a mountain stream. *Earth Surface Processes and Landforms*, esp.5057. <https://doi.org/10.1002/esp.5057>
- Battin, T. J., Kaplan, L. A., Findlay, S., Hopkinson, C. S., Marti, E., Packman, A. I., Newbold, J. D., & Sabater, F. (2008). Biophysical controls on organic carbon fluxes in fluvial networks. *Nature Geoscience*, 1(2), 95–100. <https://doi.org/10.1038/ngeo101>
- Beckman, N. D., & Wohl, E. (2014). Carbon storage in mountainous headwater streams: The role of old-growth forest and logjams. *Water Resources Research*, 50(3), 2376–2393. <https://doi.org/10.1002/2013WR014167>
- Bilby, R. E., & Likens, G. E. (1980). Importance of Organic Debris Dams in the Structure and Function of Stream Ecosystems. *Ecology*, 61(5), 1107–1113. <https://doi.org/10.2307/1936830>
- Buffington, J. M., & Montgomery, D. R. (1999). Effects of hydraulic roughness on surface textures of gravel-bed rivers. *Water Resources Research*, 35(11), 3507–3521. <https://doi.org/10.1029/1999WR900138>
- Cardenas, M. B., & Wilson, J. L. (2007). Dunes, turbulent eddies, and interfacial exchange with permeable sediments. *Water Resources Research*, 43(8), 8412. <https://doi.org/10.1029/2006WR005787>
- Collins, B. D., Montgomery, D. R., Fetherston, K. L., & Abbe, T. B. (2012). The floodplain large-wood cycle hypothesis: A mechanism for the physical and biotic structuring of temperate forested alluvial valleys in the North Pacific coastal ecoregion. *Geomorphology*, 139–140, 460–470. <https://doi.org/10.1016/j.geomorph.2011.11.011>
- Faustini, J. M., & Jones, J. A. (2003). Influence of large woody debris on channel morphology and dynamics in steep, boulder-rich mountain streams, western Cascades, Oregon. *Geomorphology*, 51(1–3), 187–205. [https://doi.org/10.1016/S0169-555X\(02\)00336-7](https://doi.org/10.1016/S0169-555X(02)00336-7)
- Gooseff, M. N., Hall, R. O., & Tank, J. L. (2007). Relating transient storage to channel complexity in streams of varying land use in Jackson Hole, Wyoming. *Water Resources Research*, 43(1), 1–10. <https://doi.org/10.1029/2005WR004626>
- Harvey, J. W., & Bencala, K. E. (1993). The Effect of streambed topography on surface-subsurface water exchange in mountain catchments. *Water Resources Research*, 29(1), 89–98. <https://doi.org/10.1029/92WR01960>
- Jochner, M., Turowski, J. M., Badoux, A., Stoffel, M., & Rickli, C. (2015). The role of log jams and exceptional flood events in mobilizing coarse particulate organic matter in a steep headwater stream. *Earth Surface Dynamics*, 3(3), 311–320. <https://doi.org/10.5194/esurf-3-311-2015>
- Kaufmann, P. R., & Faustini, J. M. (2012). Simple measures of channel habitat complexity

- predict transient hydraulic storage in streams. *Hydrobiologia*, 685(1), 69–95.
<https://doi.org/10.1007/s10750-011-0841-y>
- Lautz, L. K., & Fanelli, R. M. (2008). Seasonal biogeochemical hotspots in the streambed around restoration structures. *Biogeochemistry*, 91(1), 85–104. <https://doi.org/10.1007/s10533-008-9235-2>
- Livers, B., Lininger, K. B., Kramer, N., & Sendrowski, A. (2020). Porosity problems: Comparing and reviewing methods for estimating porosity and volume of wood jams in the field. *Earth Surface Processes and Landforms*, esp.4969. <https://doi.org/10.1002/esp.4969>
- Livers, B., & Wohl, E. (2016). Sources and interpretation of channel complexity in forested subalpine streams of the Southern Rocky Mountains. *Water Resources Research*, 52(5), 3910–3929. <https://doi.org/10.1002/2015WR018306>
- Livers, B., Wohl, E., Jackson, K. J., & Sutfin, N. A. (2018). Historical land use as a driver of alternative states for stream form and function in forested mountain watersheds of the Southern Rocky Mountains. *Earth Surface Processes and Landforms*, 43(3), 669–684. <https://doi.org/10.1002/esp.4275>
- Manners, R. B., Doyle, M. W., & Small, M. J. (2007). Structure and hydraulics of natural woody debris jams. *Water Resources Research*, 43(6). <https://doi.org/10.1029/2006WR004910>
- Marshall, A.E., Iskin, E.P., Wohl, E. (2021). Seasonal and diurnal fluctuations of coarse particulate organic matter transport in a snowmelt dominated stream. *River Research and Applications*. <https://doi.org/10.1002/rra.3802>
- Marttila, H., Turunen, J., Aroviita, J., Tammela, S., Luhta, P. L., Muotka, T., & Kløve, B. (2018). Restoration increases transient storages in boreal headwater streams. *River Research and Applications*, 34(10), 1278–1285. <https://doi.org/10.1002/rra.3364>
- Meyer, J. L., Sale, M. J., Mulholland, P. J., & Poff, N. L. (1999). Impacts of Climate Change on Aquatic Ecosystem Functioning and Health. *Journal of the American Water Resources Association*, 35(6), 1373–1386. <https://doi.org/10.1111/j.1752-1688.1999.tb04222.x>
- O'Connor, B. L., Hondzo, M., & Harvey, J. W. (2010). Predictive Modeling of Transient Storage and Nutrient Uptake: Implications for Stream Restoration. *Journal of Hydraulic Engineering*, 136(12), 1018–1032. [https://doi.org/10.1061/\(ASCE\)HY.1943-7900.0000180](https://doi.org/10.1061/(ASCE)HY.1943-7900.0000180)
- Poff, N. L. R., Olden, J. D., Merritt, D. M., & Pepin, D. M. (2007). Homogenization of regional river dynamics by dams and global biodiversity implications. *Proceedings of the National Academy of Sciences of the United States of America*, 104(14), 5732–5737. <https://doi.org/10.1073/pnas.0609812104>
- Raikow, D. F., Grubbs, S. A., & Cummins, K. W. (1995). Debris dam dynamics and coarse particulate organic matter retention in an Appalachian mountain stream. *Journal of the North American Benthological Society*, 14(4), 535–546. <https://doi.org/10.2307/1467539>
- Roni, P., Beechie, T., Pess, G., & Hanson, K. (2014). Wood placement in river restoration: Fact, fiction, and future direction. *Canadian Journal of Fisheries and Aquatic Sciences*, 72(3), 466–478. <https://doi.org/10.1139/cjfas-2014-0344>

- Sawyer, A. H., Bayani Cardenas, M., & Buttles, J. (2011). Hyporheic exchange due to channel-spanning logs. *Water Resources Research*, 47(8). <https://doi.org/10.1029/2011WR010484>
- Sawyer, A. H., & Cardenas, M. B. (2012). Effect of experimental wood addition on hyporheic exchange and thermal dynamics in a losing meadow stream. *Water Resources Research*, 48(10). <https://doi.org/10.1029/2011WR011776>
- Stanford, J. A., & Ward, J. V. (1993). An Ecosystem Perspective of Alluvial Rivers: Connectivity and the Hyporheic Corridor. *Journal of the North American Benthological Society*, 12(1), 48–60. <https://doi.org/10.2307/1467685>
- Wohl, E. (2016). Spatial heterogeneity as a component of river geomorphic complexity. *Progress in Physical Geography: Earth and Environment*, 40(4), 598–615. <https://doi.org/10.1177/0309133316658615>
- Wohl, E., & Beckman, N. (2014). Controls on the longitudinal distribution of channel-spanning logjams in the Colorado Front Range, USA. *River Research and Applications*, 30(1), 112-131.
- Wohl, E., Cenderelli, D. A., Dwire, K. A., Ryan-Burkett, S. E., Young, M. K., & Fausch, K. D. (2010). Large in-stream wood studies: a call for common metrics. *Earth Surface Processes and Landforms: The Journal of the British Geomorphological Research Group*, 35(5), 618-625.
- Zarnetske, J. P., Gooseff, M. N., Brosten, T. R., Bradford, J. H., McNamara, J. P., & Bowden, W. B. (2007). Transient storage as a function of geomorphology, discharge, and permafrost active layer conditions in Arctic tundra streams. *Water Resources Research*, 43(7), 7410. <https://doi.org/10.1029/2005WR004816>

CHAPTER 2: CHARACTERIZING LOGJAMS AS DRIVERS OF TRANSIENT STORAGE AT DIFFERENT FLOW REGIMES IN A FLUME

Summary

Logjams are a key component of natural streams. Flow paths around logjams create pressure gradients along the riverbed that drive surface water-groundwater exchange as well as create zones of surface transient storage in logjam backwaters and marginal eddies. A logjam itself can vary in size, shape, and porosity, depending on the wood matrix and composition of organic material, but how these specific characteristics of a logjam drive transient storage remains largely unknown. Here, I focus on investigating how different characteristics of logjams, specifically longitudinal spacing and porosity, influence transient storage. I use a salt tracer at different flow regimes in a flume to create breakthrough curves of the tracer concentration over time. Instream breakthrough curves from specific conductivity data can be used to characterize transient storage by calculating the temporal moments of the curve and using those moments as statistical descriptors of the tracer distribution over time. In this study, I use mean arrival time and skew to understand patterns of advection and dispersion in the movement of the solute mass. Higher values of skewness and mean arrival time indicate greater retention, and I used the values here as a metric of increased transient storage. I predicted an increase in transient storage as (i) longitudinal spacing between logjams decreased, (ii) more fine material was added to a jam, and (iii) flow increased. Overall, the tracer moved more slowly through the system as logjams were placed closer together. Results suggest more transient storage at low flow, likely due to slower advection through the logjams. Flume runs at high flow had no trend as jams were added, suggesting that the velocity is too high for exchange with the bed material. Results from the flume runs with changing jam porosity could not be physically interpreted because the travel

time of the solute mass was so quick. Thus, flume scaling was not effective in distinguishing the effects of changing logjam characteristics and changing flow. Understanding how logjam characteristics drive transient storage has important management implications for rivers in forested, or historically forested, environments. Restoration to re-establish natural riverine function has grown into a multi-billion-dollar industry, yet limited understanding of logjam processes constrains our ability to design wood-based river restoration targeted to restore habitat and ecosystem function. To design river restoration projects efficiently and effectively, more attention is needed toward studying the specific characteristics of logjams that critical processes.

1. Introduction

1.1 Transient Storage in Rivers

Stream water flow paths with significantly reduced downstream velocity in comparison to flow in the thalweg of the stream can be defined as transient storage zones (Bencala, 1983; Harvey et al., 1996). Transient storage can be generally segregated into surface transient storage (STS), where water flow paths are stored in surface sites of flow separation and low velocity, and subsurface transient storage via hyporheic exchange (HTS), where flow paths originate and terminate in the surface channel but flow through the subsurface. These two types of transient storage can be increased by features that enhance spatial heterogeneity and thus surface flow separation and downwelling from pressure gradients. Examples of such features include variation in cross-sectional geometry and bedforms (Bencala, 1983; Harvey & Bencala, 1993; Kasahara & Wondzell, 2003; Ensign & Doyle, 2005; Gooseff et al., 2007), logjams (Hester & Doyle, 2008; Sawyer et al., 2011; Marttila et al., 2018; Ader et al., 2021), and 3D spatial heterogeneity of alluvial thickness and grain-size distribution (Harvey et al., 1996).

Transient storage has numerous positive implications for river corridor ecosystem services and processes. Transient storage influences stream biogeochemical cycling by increasing the residence time of stream solutes and the opportunity for microbial uptake (Fischer et al., 2005; Battin et al., 2008; Tonina & Buffington, 2009; Harvey & Gooseff, 2015; Marttila et al., 2018). Solute in streams are subject to downstream transport by advection and dispersion and can also be retained within a reach by transient storage processes. Transient storage zones are important areas of nutrient and pollutant processing in rivers because they extend residence times and increase exposure with biochemically reactive surfaces (Harvey & Wagnert, 2000; Hall et al., 2002; Ensign & Doyle, 2005; Stewart et al., 2011). Zones of transient storage have been identified as a sink for pollutants, preventing them from reentering surface water downstream. The movement of stream water into the subsurface additionally provides a vector for dissolved oxygen to come into direct contact with both oxidative and highly reducing biogeochemical conditions. Zones of transient storage provide increased habitat diversity for microbial and macroinvertebrate communities (Mulholland et al., 2004; Hester & Gooseff, 2010). By facilitating heat exchange with relatively constant temperature groundwater, transient storage zones act as a buffer for water temperature fluctuations and a zone of thermal refugia. This temperature dynamic is an important driver of habitat heterogeneity in streams: it has direct influence on macroinvertebrate and fish survival during low flow and high flows. Transient storage, through altering flow paths and increasing floodplain roughness, creates attenuation as well as enhanced base flows (Herzog et al., 2018). Additionally, zones of transient storage serve as accumulation zones for coarse particulate organic matter, which supports benthic food chains (Marshall et al, 2021).

1.2 Logjams in Rivers

An extensive scientific literature documents the numerous beneficial physical and ecological functions created by logjams in a river corridor (e.g., Ruiz-Villanueva et al., 2016; Wohl et al., 2017, 2019; Swanson et al., 2021). Logjams create zones of flow separation that enhance storage of sediment, organic matter, and solutes, and attenuate downstream fluxes of surface water (Buffington & Montgomery, 1999; Hassan et al., 2005; Wohl & Scott, 2017). By increasing hydraulic resistance, logjams can alter the magnitude and the type of bedforms present in a channel (MacFarlane & Wohl, 2003; Curran & Wohl, 2003; Yochum et al., 2012, 2014), as well as channel planform, migration rate, and channel-floodplain connectivity (Hickin & Nanson, 1984; Piégay & Gurnell, 1997; Wohl, 2011; Collins et al., 2012). Logjams also enhance habitat diversity and retention of nutrients, increasing biomass and biodiversity (Benke & Wallace, 1990; Hyatt & Naiman, 2001; Roni, 2003; Ballinger et al., 2009).

Logjams are commonly categorized by whether they formed in situ around an immobile key piece or in transport at a site of reduced conveyance for large wood (Abbe & Montgomery, 2003). In situ or autochthonous jams are composed of LW that has not moved from the point where it first entered the channel, although it may have rotated, or the channel may have moved. Transport or allochthonous jams are composed of LW that has moved some distance downstream by fluvial processes. Studies in Rocky Mountain streams observed that although individual pieces of wood move in streams during most years, the location of logjams and the wood load stay relatively constant (e.g., Wohl & Goode, 2008; Wohl and Scamardo, 2021). All of the logjams observed in this thesis are in situ and were formed around a relatively immobile piece or pieces of LW.

The longitudinal density of logjams, or successive downstream spacing of jams within channels at the reach- to network-scales, is influenced by local controls of valley geometry and associated wood recruitment and fluvial transport capacity (Wohl & Beckman, 2014). Numerous studies have shown that logjams tend to be non-randomly distributed in relation to potential control variables (e.g., Abbe & Montgomery, 2003; Wohl & Cadol, 2011; Wohl & Beckman, 2014; Pfeiffer & Wohl, 2018). A logjam itself can vary in size, shape, and porosity depending on the wood matrix and composition of woody material. A common approach for estimating wood volume involves measuring the logjam volume and then estimating the logjam porosity, or fraction of void space (Φ_j) versus filled space ($1 - \Phi_j$), within the logjam volume to determine the wood volume (Livers et al., 2020). This approach uses the following equation, where ‘jam volume’ (JV) is the volume of the jam that includes wood, void space, and other solids and ‘wood volume’ (WV) is the total apparent volume of wood within a jam, regardless of piece size:

$$\Phi_j = 1 - \left(\frac{WV}{JV}\right) \quad (1)$$

Porosity can influence the degree to which logjams alter stream channel hydraulics, with a less porous jam creating greater backwater effects, local bed and bank erosion, and habitat, while a more porous jam has less overall influence on local hydraulics and habitat (Manners et al., 2007; Dixon, 2016; Ventres-Pake et al., 2020). Some jams have more poorly sorted piece sizes due to the processes of deposition or the supply of fine organic material, resulting in lower porosity. Although smaller wood pieces are not commonly measured in studies conducted by physical scientists (ecologists are more likely to quantify small wood), the ability of logjams to trap small wood (e.g., Millington & Sear, 2007) exerts an important control on jam porosity and creation of a backwater that retains fine sediment and organic matter. Spreitzer et al. (2019) recently explored the influence of jam sorting and organizational structure on porosity, but

patterns are difficult to distinguish because reported porosity values are based on varied enclosing volumes of jams. Jams with wood pieces aligned and oriented in a similar way likely have lower porosity than jams in which wood pieces are randomly oriented and unorganized (Spreitzer et al., 2019).

1.3 Linking Logjams and Transient Storage

Among the beneficial effects of logjams is the potential for direct enhancement of surface and subsurface transient storage. The connectivity of river networks is controlled in large part by the hydraulic forces that dissipate water's energy as it interacts with geomorphic and biological roughness elements, such as logjams (Prestegard, 1983; Jackson et al., 2013), which resist the flow and force water to move laterally through pathways across the channel and beneath the surface (Harvey & Gooseff, 2015). By obstructing flow and increasing hydraulic resistance within the channel, logjams can influence surface transient storage by creating low-velocity zones within the channel (Gippel, 1995), and subsequently enhancing the formation of backwater pools (Richmond & Fausch, 1995; Kaufmann & Faustini, 2012; Beckman & Wohl, 2014; Livers & Wohl, 2016). Logjams can also increase surface transient storage by deflecting flow toward the channel bed and creating scour pools that enhance residual pool volume (Fausch & Northcote, 1992; Ensign & Doyle, 2005; Mao et al., 2008) as well as by deflecting flow toward the channel banks and creating marginal eddies (Zhang et al., 2019).

Logjams also create indirect effects on surface and subsurface transient storage. Logjams plays an important role in trapping and storing sediment in most rivers in forested ecosystems (Wohl & Scott, 2017), which creates secondary effects on transient storage. By deflecting flow, logjams locally enhance entrainment of bed material and scour of the channel bed and banks

(Buffington et al., 2002). Studies of the effects of logjams on floodplain sediment dynamics emphasize how the obstructions created by logjams can result in changes in bedforms via overbank flows and vertical accretion or bank erosion, channel avulsion, and formation of secondary channels (e.g., Sear et al., 2010; Wohl & Scott, 2017). Logjams commonly create high spatial variability in average bed grain size and alluvial thickness upstream and downstream of a jam (Massong & Montgomery, 2000). Advective pumping, induced by streamflow over a spatially heterogeneous, permeable bed, leads to a distribution of pore-water flow paths in the streambed (Wörman et al., 2002), which enhances the magnitude of subsurface transient storage via hyporheic exchange (Lautz et al., 2006; Hester & Doyle, 2008; Fanelli & Lautz, 2008; Sawyer et al., 2011; Sawyer & Cardenas, 2012).

1.4 Knowledge Gaps

Existing research demonstrates that logjams create nonlinear effects on stream metabolism (e.g., Day & Hall, 2017); spatial heterogeneity of physical channel characteristics (e.g., Livers & Wohl, 2016; Livers et al., 2018), including channel and floodplain planform (e.g., Buffington & Montgomery, 1999; Wohl, 2011); retention of particulate organic matter (e.g., Beckman & Wohl, 2014, Marshall et al., 2021); and aquatic habitat and biomass (e.g., Herdrich et al., 2018; Venarsky et al., 2018). Existing research also demonstrates that streams with significantly lower wood loads are significantly less retentive and physically complex than streams with abundant large wood and logjams (Wilcox et al., 2011; Wohl & Beckman, 2014; Livers & Wohl, 2016; Livers et al., 2018). However, although previous studies strongly suggest that large wood can increase surface transient storage (D'Angelo et al., 1993; Stofleth et al., 2008), the effects of varying wood load on surface transient storage have not been explicitly quantified with the exception of Kaufmann and Faustini (2012), who found a linear increase in

surface transient storage with an increasing quantity of wood. Less attention has been given to the characteristics of logjams that influence transient storage and, consequently, there is a lack of understanding as to what qualities of a logjam most influence hydrologic function. This knowledge is particularly important in a management context as wood is becoming increasingly used to restore function to rivers. The function of constructed logjams can be amplified if they are adequately designed to maximize processes such as transient storage.

1.5 Research Objective

My objective is to assess the relative importance of logjam characteristics and different discharges in influencing surface transient storage using a laboratory flume. Specifically, I varied (i) the longitudinal spacing of logjams, (ii) the porosity of a single logjam, and (iii) the discharge.

The geomorphologic complexity of streams with numerous logjams makes it challenging to quantify transient storage in the field at consistent scales and with the necessary variation in logjam characteristics. Scaled flume experiments offer an alternative approach to understand the interacting effects of logjams and channel morphologic complexity on transient storage. The fundamental physical drivers of transient storage, including substrate properties, surface water discharge, channel planform, and wood characteristics, can be isolated and studied under controlled experimental conditions in laboratory flumes, allowing the manipulation of variables one at a time (Endreny et al., 2011). Although previous studies have examined surface transient storage in relation to wood load (Kaufmann & Faustini, 2012) and the effects of an individual jam or piece of wood on transient storage (Sawyer et al., 2011, 2012; Sawyer & Cardenas, 2012; Sparacino et al., 2019; Ader et al., 2021), the work presented here is unique in examining the potential effects of logjam characteristics at varying flow regimes on transient storage.

To investigate logjam characteristics as a driver of transient storage at different flow regimes, I conducted two sets of experiments. The first set focuses on the effect of successive additions of logjams, from a single jam to multiple jams that were progressively more closely spaced longitudinally over the same length of flume. I envision the effect of jam spacing on surface transient storage as being analogous to the effect of the spacing of bed roughness elements on the distribution of velocity and flow resistance in a channel (Wohl & Ikeda, 1998). The ratio of distance between obstacles (length) to the height of obstacles governs how much the obstacles disrupt velocity fields and influence resistance. Obstacles that are widely spaced relative to their height create minimal resistance, as do closely spaced obstacles. Obstacles with a length/height ratio of 9-18 create the maximum flow resistance because flow separation created by each obstacle has just ended when the next obstacle is encountered (Wohl & Ikeda, 1998). Applying this analogy to logjams and surface transient storage is imperfect because flow resistance also depends on flow depth and because jams are permeable and thus have flow through as well as over them. However, I expect that single or very widely spaced jams will create only local and relatively minor effects on transient storage. As logjams increase in quantity and become more closely spaced, I hypothesize that they maximize surface transient storage because pressure gradients and backwater pools associated with an upstream logjam interfere with those associated with the logjam downstream.

The second experiment focuses on how changing the porosity of a single logjam at high and low flow influences transient storage. I expect that transient storage generally declines as flow increases, regardless of jam porosity. I also expect that lowering the porosity of a jam will increase transient storage. As more relatively small organic material is added, the jam will become more impermeable to flow paths moving through it. Consequently, greater backwaters

and pressure gradients pushing flow over the top of the jam are likely to occur, magnifying the transient storage zone.

2. Flume Methods

Flume experiments took place at Colorado State University's Engineering Research Center using a 9-m long and 1.2-m wide flume, with a rectangular cross section and smooth sidewalls. Flow is delivered to the flume via pipes and pumps from a reservoir of water. A cobble-filled baffle dissipates flow energy at the upstream end of the flume and a reinforced 250-micron mesh screen at the downstream end of the flume acts to catch any mobilized sediment.

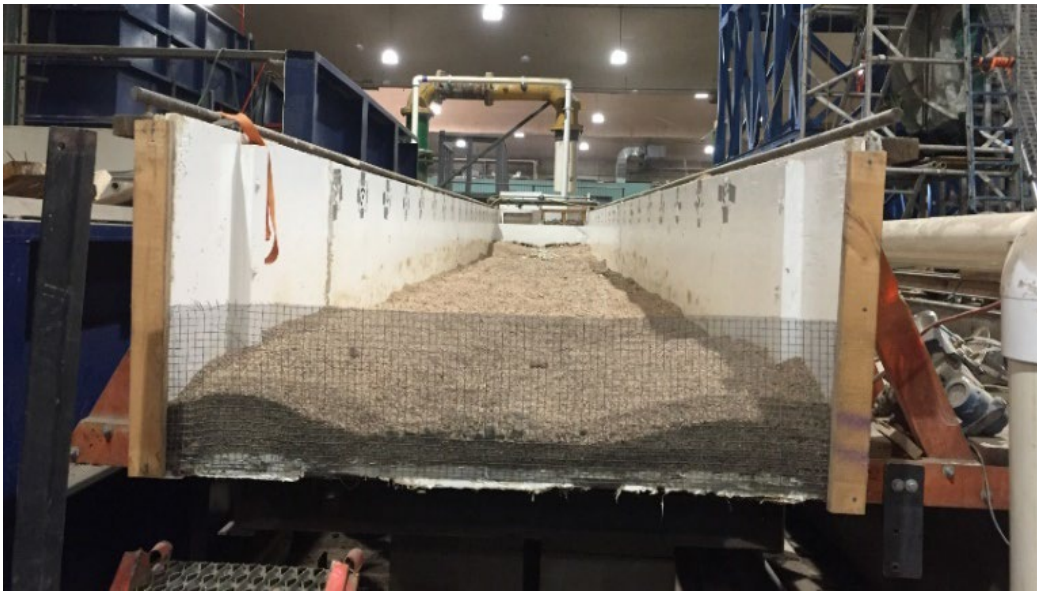


Figure 2.1. Upstream view of the flume (9-m long, 1.2-m wide) at CSU's Engineering Research Center.

In this study, I focused on designing tracer experiments to characterize the physical transient storage properties of a stream. The use of stream tracers in advancing and integrating surface exchange flows and floodplain processes in river corridors is growing as a methodology and stream tracers have become a widely used tool for analyzing the transport characteristics of complex stream systems (e.g., Singha & Gorelick, 2005; Jackson et al., 2013; Wollheim et al.,

2014). In a typical stream tracer experiment, a conservative tracer solution is injected into the stream and solute concentrations are sampled at a downstream location. As the tracer mass moves downstream, it is acted upon by four basic transport processes: (1) advection, which describes the rate at which the tracer mass moves downstream; (2) dispersion, which accounts for the mixing processes in the stream that cause the tracer mass to spread; (3) groundwater inflow, which serves to increase the rate of flow and to dilute the tracer; and (4) storage-zone exchange or diffusion, which describes the movement of solute between the active channel and stagnant or slowly moving zones in the stream or in the subsurface (Wagner & Harvey, 1997) (Figure 2.2). At some point downstream the tracer is sampled, providing a history of in-stream tracer concentrations. Here, I used sodium chloride (NaCl) as a tracer to explore the dynamics of logjam characteristics as drivers of surface transient storage on the basis of the observed tracer concentration history.

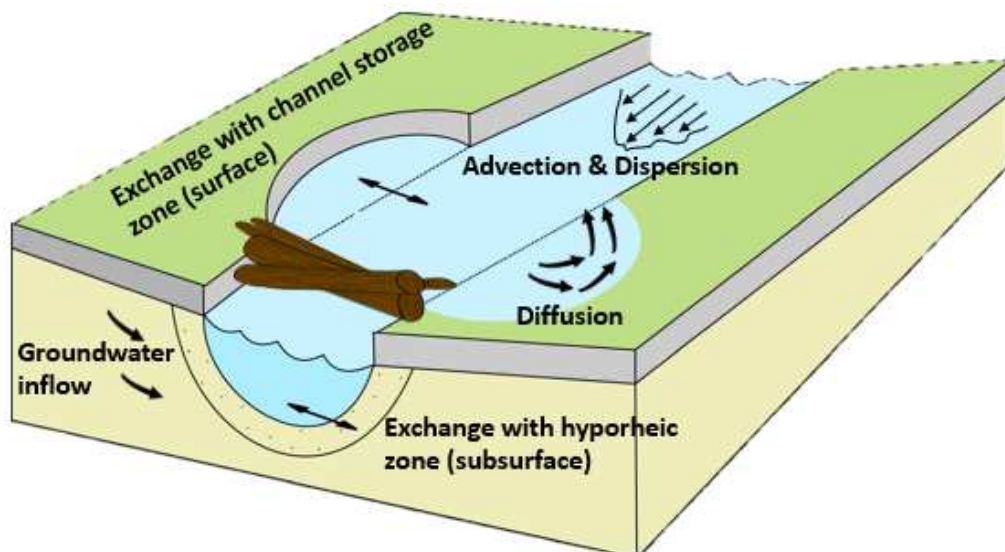


Figure 2.2. Transport processes, which act upon the solute tracer as it moves downstream. Processes include advection, dispersion, diffusion, and groundwater inflow. These processes result in exchange between surface and subsurface transient storage zones.

Over 100 flume trials were run as the experimental design approach was refined and the total number of logjams and logjam porosity were manipulated at varying flows in order to quantify the effects of changes in logjam characteristics on transient storage at fluctuating discharges. Three experiments were conducted in the flume environment at varying discharges: 1) replicating field conditions and methodologies from Ader et al. (2021) and Doughty et al. (2020) to assess surface and subsurface transient storage; 2) changing the longitudinal spacing of logjams in a single channel to explore the effect on surface transient storage; and 3) changing the porosity of a single jam to explore the effect on surface transient storage.

2.1 Initial Flume Set-Up Using Field Scaling and Electrical Resistivity

Initial conditions in the flume included a single channel and multithread channel, to represent the varying channel planform of the study field site, Little Beaver Creek, located in the Front Range of Colorado (refer to Chapter 3 for detailed description of study area). A companion study, as described in Doughty et al. (2020) and Ader et al. (2021), looked at reach-scale changes in transient storage at Little Beaver Creek associated with the presence of simple and complex logjams as well as meandering and anabranching channels. The flume set-up was configured to mirror the planform and longitudinal spacing of logjams in the field reaches (Figure 2.3). These flume conditions were numerically simulated by Wilhelmsen et al. (in press).

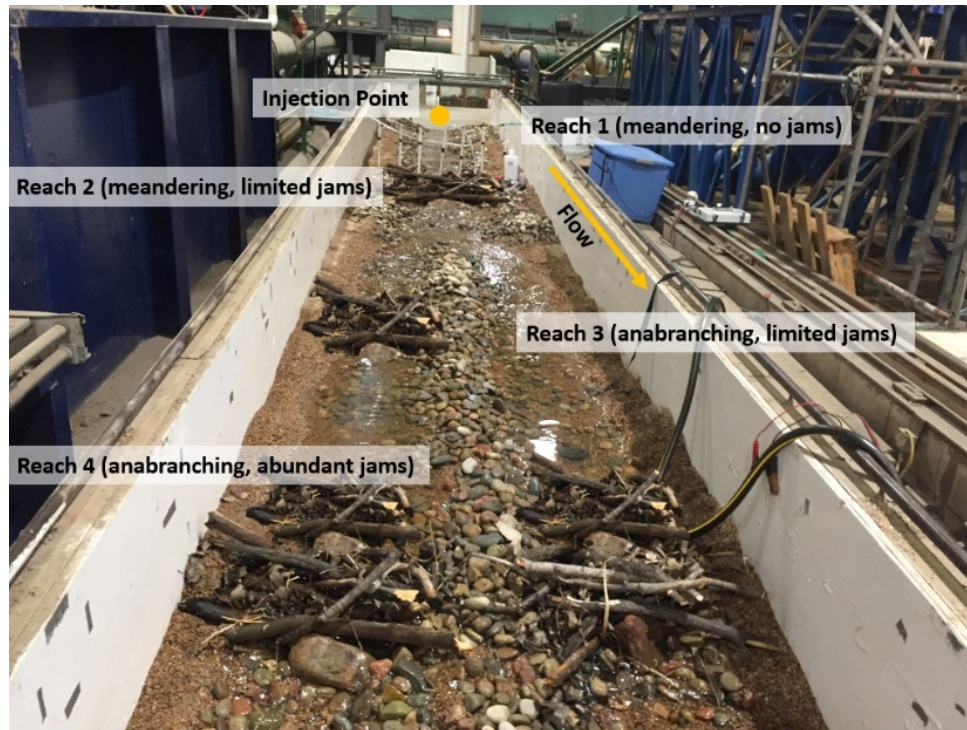


Figure 2.3. Upstream view of initial flume configuration. Yellow dot indicates the salt tracer injection point.

All four study reaches delineated in the field were included within the length of the 9-m long and 1.2-m wide flume (Figure 2.3). Flume attribute scaling here focused on maintaining the channel planform and logjam presence of Little Beaver Creek. The overall slope of the flume was 0.01 m/m, or 1% based on an average field slope. Reach lengths and spacing were uniform with 1-m long with 1-m spacing between each reach within the flume. This allowed me to address how adding consecutive jams into a reach influenced transient storage. The first 1.5 m of the flume was designated as a mixing zone, with an additional 1.5-m segment at the bottom of the flume allocated to prevent any backwater effect caused by the sediment screen. The single channel reaches in the flume were 40 cm wide and the multithread channels were 35 cm wide, or collectively 70 cm wide (Figure 2.3). These values were scaled based on the average channel width to valley width of Little Beaver Creek relative to the width of flume walls. Sediment sizing was based on maintaining an

immobile bed. Coarse sand was used as a 12-cm-thick subsurface layer, with a d_{16} of 1.8 mm, d_{50} of 3.3 mm, and d_{84} of 5.0 mm. A pebble top coat with a d_{16} of 7.5 mm, d_{50} of 12.7 mm, and d_{84} of 19.0 mm was added as a surface layer. The total depth of sediment was scaled to represent the average depth-to-bedrock at Little Beaver Creek. A summary of all flume attributes is included as Table 2.1.

Table 2.1. Measurements of flume attributes including grain size, sediment depth, reach length and widths, and slope.

Attribute	Flume Measurement
d_{50} , subsurface (mm)	3.3
d_{50} , surface (mm)	12.7
Sediment depth (cm)	14
Reach length (m)	1
Channel width, meandering (cm)	40
Channel width, anabranching (cm)	70
Slope (%)	1

Three discharges representing snowmelt peak flow, the receding limb of the snowmelt hydrograph, and base flow in Little Beaver Creek were scaled to the size of the flume channel based on average 2019 and 2020 field flows using a scaling factor of 100 (Table 2.2). For each flume run, the discharge was set manually by adjusting valves on the pipes delivering water to the flume until the target low, medium, or high discharge value was attained from a flow meter with $\pm 0.2\%$ accuracy. Because I sought to examine the effect of a range of flow conditions on flow resistance, exact scaling of Froude number between the flume model and Little Beaver Creek was not applied. Flow for all flume runs was fully turbulent, allowing relaxation of Reynolds number scaling (Peakall et al., 1996).

Table 2.2. Field and flume average discharges.

Discharge Category	Average Field Discharge (m³/s)*	Average Flume Discharge (m³/s)
High	1	0.01
Medium	0.5	0.005
Low	0.1	0.001

*Field measurements as reported in Ader et al. (2020) at Little Beaver Creek

For the field-scaled flume runs, I started with ramped pieces of large, channel-spanning wood pinned in place by immobile boulders. Wood pieces collected in the field were introduced upstream with a high flow to simulate riparian LW recruitment. Coarse particulate organic matter (CPOM), mainly in the form of leaves, pine needles, and bark, was added to the flow upstream of the wood jams and allowed to deposit on and within the jam in order to reduce the porosity of each jam. Flume runs were carried out by sequentially adding jams from downstream to upstream. Given the scaling of the flume relative to the field, the most complex reach (reach 4, multithread, with abundant jams) was run prior to the wood additions of the meandering (reach 2) and multithread (reach 3) limited-jam reaches. This ensured that the logjams above reach 4 were not influencing transient storage in reach 4.

Measurements of transient storage in the flume mirrored the methodology used by Doughty et al. (2020) at Little Beaver Creek to image both subsurface and surface transient storage using sodium chloride (NaCl) as a tracer. The injection of a highly conductive fluid, such as dissolved NaCl, acts as a tracer by increasing the conductivity of flow paths. In turn, conductivity measurements provide a multidimensional image of the salt tracer distribution in transient storage zones through time (Ward et al., 2010a, 2010b; Toran et al., 2013a; Ward et al., 2014). Specific conductivity was measured at 10-second intervals during the tracer test using fluid electrical

conductivity loggers (HOBO U-24, Onset Computing). One conductivity logger was deployed upstream of the NaCl injection point to measure background fluid conductivity, and two or four conductivity loggers, based on single or multithread channel configuration, were deployed 0.3-m upstream and downstream of the logjam in the experimental study reach.

An IRIS Syscal Pro Resistivity Meter (IRIS) was used to collect discrete subsurface measurements since the conductivity loggers do not separate surface and subsurface readings. The IRIS was connected to seven electrodes across the 1.2-m width of the flume above and below each of the four reaches (Figure 2.4). For each tracer test, dissolved NaCl was injected at a constant rate into the middle of the channel upstream of all study reaches for two hours per flume trial following one hour of background data collection. Complete mixing of the tracer into the stream was assumed and electrical resistivity measurements were collected for up to 24 hours post injection. Conductivity loggers were employed for the same duration as the IRIS above and below the active study reach as well as at the upstream control reach and above the injection point (Figure 2.5). A minimum of one replicate was run for all flume runs. A control line was run during every flume trial below the injection point but above the uppermost logjam and a conductivity logger recorded data at the control line.



Figure 2.4. Flume configuration set for IRIS. Electrodes attached to PVC are connected by wires to the IRIS to image the subsurface flow.

Preliminary analysis from the in-stream data (surface transient storage measurements collected from the conductivity loggers) and bulk data (subsurface transient storage measurements collected from the IRIS electrical resistivity meter) showed unexplainable variation between the bulk and in-stream tailing patterns in BTCs as well as unexplainable variation between bulk replicates for the same run. Given the lack of continuity observed between the bulk data in the flume, and no discernible explanation for the discrepancies, the project team concluded that using ER as a method for subsurface transient storage measurements in the flume was not a viable option for the experimental set-up. Thus, results from the initial flume runs based on field conditions and methodologies are not included in this thesis and subsequent experimental runs did not utilize ER as a subsurface transient storage measure. The rest of this chapter discusses surface transient storage results from the conductivity loggers.

2.2 Changing Longitudinal Spacing

Previous studies suggest that in-stream wood can increase surface transient storage (e.g., Kaufmann & Faustini, 2012), but the nature of that relationship remains poorly defined. In this experiment, I explored the relationship between wood quantity and transient storage by changing the longitudinal spacing of logjams during high and low discharges.

Limited changes to the flume configuration occurred between the initial flume set-up referenced in Section 2.1 and changing the longitudinal spacing of logjams in the flume. A 30-cm-wide single thread channel was constructed along the entire 9-m length of the flume using the same surface and subsurface sediment as the initial flume set-up (Table 2.1). Discharges here reflect a high flow scenario scaled to seasonal snowmelt peaks and a low flow scenario scaled to base flow, both from a representative stream. Natural wood pieces and CPOM were configured into a channel-spanning jam prior to the start of each set of flume runs (Figure 2.5). All jams were constructed to an approximate standard size based on the number of wood pieces and CPOM volume, but the exact size varied between jams. Downstream spacing between jams decreased and once a jam was added to the flume it was not removed during subsequent runs.

Conductivity loggers were placed at the upper and lower extents of the flume, approximately 1.5-m from the tracer mixing zone at the top of the flume and from the mesh screen at the bottom of the flume to account for tracer mixing as well as any potential downstream backwater effects from the mesh sediment screen. An additional conductivity logger was deployed upstream of the NaCl injection point to measure background fluid conductivity. The first logjam was constructed at the uppermost extent of the flume, ~ 0.6-m from the upstream conductivity logger location (Figure 2.6). A second logjam was constructed at the bottommost extent of the

flume, approximately 0.6-m above the downstream conductivity logger location (Figure 2.6). Jam(s) 4 and 5 were placed directly in-between Jam 1 and 2 (Figure 2.6).

Pulse injections of NaCl were added at an injection concentration of 0.1 kg/l in the upstream mixing zone of the flume at the start of each flume run. Specific conductivity was measured at 10-second intervals during the tracer test using fluid electrical conductivity loggers (HOBO U-24, Onset Computing) at the locations depicted in Figure 2.5. Changes in instream conductivity with time following tracer injection represent the combined effects of surface transient storage in the channel (e.g., backwaters, eddies) and subsurface transient storage via hyporheic exchange. The HOBO loggers collected data for 30 minutes following the pulse to allow ample time for the flume to return to background solute concentrations. Four flume scenarios were run with the quantity of logjams increasing at a rate of 1, 2, 4, and 5 jams in order to decrease the longitudinal spacing of jams in the 9-m length of channel (Figure 2.5). Each flume scenario was run at high ($0.01 \text{ m}^3/\text{s}$) and low flow ($0.001 \text{ m}^3/\text{s}$) and replicates were completed for all flume runs.

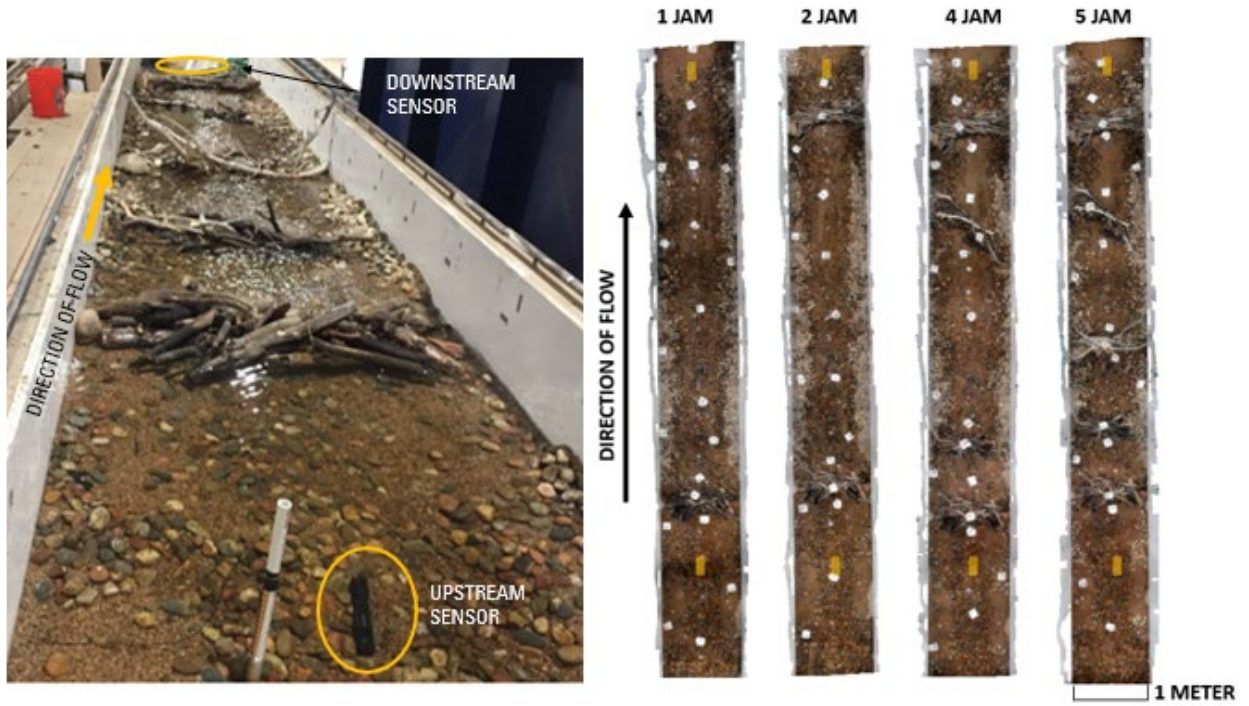


Figure 2.5. Logjam and channel configuration for each set of flume runs, shown from an oblique view on readers' left and birdseye view on readers' right. Note the 4 jam flume run includes the addition of two new jams. Yellow circles indicate sensor placement.

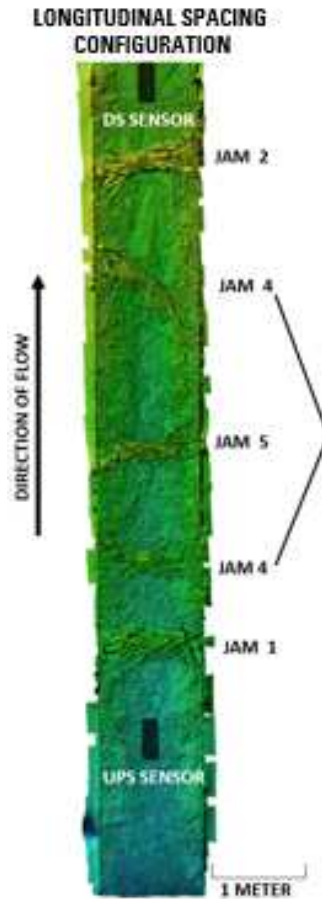


Figure 2.6. Logjam configuration in the flume and order of flume runs. Labels are placed next to the logjams that were added for the corresponding labeled flume run. Blue shading indicates lower elevation.

A digital elevation model (DEM) before and after each set of flume runs (i.e., at 1, 2, 4, and 5 jams) was constructed using structure-from-motion (SfM). Images were captured at regular downstream intervals with a camera mounted at consistent elevation. SfM uses multi-view computer vision methods that detect and match features between images to estimate the three-dimensional structure, camera locations, and angles simultaneously. Agisoft Metashape (Agisoft PhotoScan Professional, 2020) was used to process the images and create DEMs of the various flume runs for comparison. Dense point clouds from each flume run were aligned in Cloud Compare (CloudCompare, 2020) to aid in aligning DEMs for differencing. The resulting DEMs

have a resolution of less than 1 mm. DEM before and after raster layers were differenced in ArcGIS Pro.

2.3 Changing Porosity

Estimating accurate porosity values remains a challenge given the large variability in jam characteristics likely caused by different depositional processes and environments. Although many studies have reported wood volume and/or Φ_j , there is no established, consistent method to estimate these variables for jams, and accuracy assessment of the methods is lacking in most studies (Livers et al., 2020). In this experiment, I can more accurately measure porosity by manipulating the logjam in order to observe the relationship between porosity and surface transient storage. One channel-spanning logjam was constructed across a single 40-cm channel in the flume, maintaining the same channel characteristics as the additive jam experiment set-up described in Section 2.2 (Figure 2.7). Natural LW, twigs, and CPOM in the form of pine needles and crushed leaves were used as the jam materials. A volume of total wood and CPOM was measured prior to jam construction using water displacement as a proxy for wood volume and a graduated cylinder for CPOM volume. Flume runs were divided into high, medium, and low porosity (Table 2.3). The study logjam started at a high porosity with LW only (Figure 2.8). High porosity flume runs were completed at high ($0.01 \text{ m}^3/\text{s}$) and low flow ($0.001 \text{ m}^3/\text{s}$), in addition to replicates of each run. Following high porosity replicates, twigs were added to the LW jam to create a medium porosity jam. Medium porosity flume runs were completed at high ($0.01 \text{ m}^3/\text{s}$) and low flow ($0.001 \text{ m}^3/\text{s}$), in addition to replicates of each run following the same pulse injection set-up and run time. Upon completion of medium porosity replicates, CPOM was added to the LW and twigs jam to reduce jam porosity (Figure 2.8). Low porosity flume runs were

completed at high ($0.01 \text{ m}^3/\text{s}$) and low flow ($0.001 \text{ m}^3/\text{s}$), in addition to replicates of each run following the same pulse injection set-up and run time.

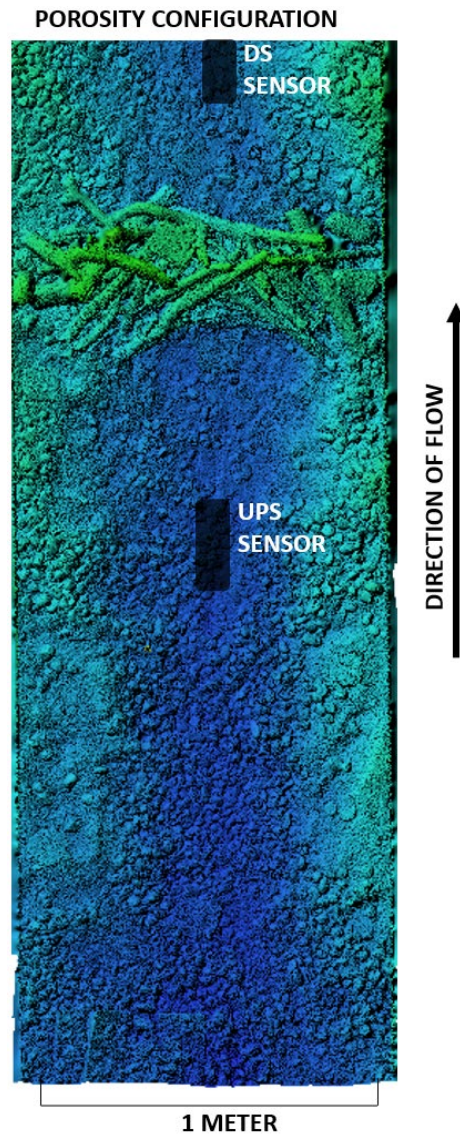


Figure 2.7. Flume configuration for porosity runs. Blue shading indicates lower elevation.

Table 2.3. Calculated porosity based on volume calculations LW, twigs, and CPOM.

Porosity Category	Porosity (%)	Composition
High	70	LW only
Medium	68	LW and twigs
Low	64	LW, twigs, and CPOM

* Note, porosity changes were lower than expected based on the organic matter added, as further discussed in results.



Figure 2.8. Comparison of visual porosity with LW only (high porosity, at left) versus LW, twigs, and CPOM (low porosity, at right).

A pulse injection 0.1 kg/l of dissolved NaCl was added at the upstream mixing zone of the flume. Specific conductivity was measured at 10-second intervals during the tracer test using conductivity loggers at the locations depicted in Figure 2.7. Changes in instream conductivity with time following tracer injection represent the combined effects of surface transient storage in the channel (e.g., backwaters, eddies) and subsurface transient storage via hyporheic exchange. The specific conductivity loggers collected data for 30 minutes following the pulse to allow ample time for the flow to return to background conductivity levels.

2.4 Analyzing Transient Storage Data

Conductivity data were plotted against time as breakthrough curves (BTCs) to observe the concentration of NaCl over the duration of the flume run. BTCs can be characterized through four central moments: area under the curve (M_0), mean arrival time (M_1), temporal variance

(M_2), and skewness (M_3) (Gupta and Cvetkovic, 2000; Harvey and Gorelick, 1995) (Table 2.4).

An example BTC is included as Figure 2.9.

Table 2.4. Temporal Moments used to characterize BTCs

Moment	Equation	Interpretation
Area under the curve (M_0)		How much mass has passed location
Mean arrival time (M_1)	2	Timescale at which half of the mass has already passed and half of the mass is yet to arrive; this timescale is related to advection
Temporal variance (M_2)	3	Spreading around the mean relative to advective time
Skewness (M_3)	4	How symmetrical or asymmetrical is the distribution; more skew indicates more transient storage

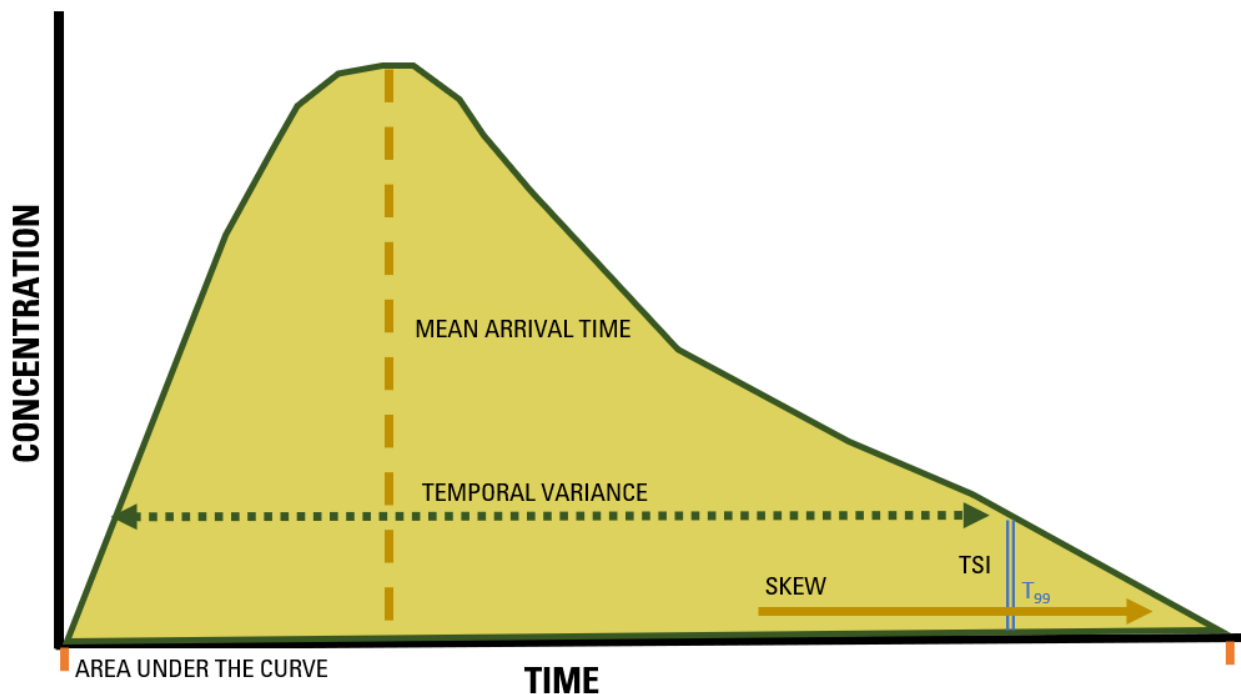


Figure 2.9. Example BTC showing the temporal moments as descriptors of the curve. The temporal moments help describe patterns of transient storage.

To estimate temporal moments, the background conductivity was removed from the data before calculations. The zeroth moment ($\text{mg}\cdot\text{s}/\text{L}$) is the total tracer mass passing the observation point per unit of discharge. To find the total mass passing the observation point, or area under the BTC, the zeroth moment was multiplied by the average flow. The mean arrival time (\bar{t}) of the injected tracer at the point of observation is commonly used to describe advection patterns and is calculated using:

$$\bar{t} = \frac{M_1}{M_0} \quad (2)$$

The variance of the pulse describes the spread of the BTC and is related to the second, first, and zeroth temporal moments:

$$\sigma^2 = \frac{M_2}{M_0} - \left(\frac{M_1}{M_0}\right)^2 \quad (3)$$

Skew is calculated from the lower order moments. Skew calculated from instream measurements is commonly used to describe transient storage within the channel and in underlying aquifer materials (e.g., Lees et al., 2000; Doughty et al., 2020). Skew describes the dispersion patterns, but also includes advection from lower order moments. The statistical moment of skewness represents the asymmetry of the BTC based on solute retention and can be used as a proxy for the rate of transient storage (Nordin & Troutman, 1980). Higher values of skewness indicate a larger degree of tailing behavior exhibited in the BTC, and therefore, a higher amount of transient storage. Skew is calculated using:

$$\mu_3 = \frac{M_3}{M_0} - 3\sigma^2 \frac{M_1}{M_0} - \left(\frac{M_1}{M_0}\right)^3 \quad (4)$$

Skew and mean arrival time values from the flume runs were used for two sets of analyses: 1) comparisons of number of jams per length of channel to amount of transient storage

and 2) comparisons of porosity of a single jam to transient storage. All temporal moments were calculated in Matlab (MATLAB, 2020). Flume run times were truncated to include one minute of background data prior to the pulse NaCl injection and a total time of 20 minutes to provide comparable skew values. Conductivity readings in the flume returned to background levels in under 10 minutes, so truncation did not cut off tailing behavior of the BTCs.

The transient storage index (TSI) was also calculated for comparison in understanding trends in BTCs. TSI is the relationship between the time elapsed between the peak tracer concentration at the upstream and downstream points of interest and the time at which 99% of the recovered tracer mass passed by the solute observation point (Mason et al., 2012; Ward et al., 2018). TSI is calculated using:

$$TSI = t_{99} - t_{peak} \quad (5)$$

TSI and skew are both commonly used metrics for transient storage. The primary difference between the metrics lies in a difference in sensitivity to mass. In skew calculations, mass is not weighted as heavily, while in TSI, mass is more equally weighted with time. Therefore, using the TSI equation might calculate more mass under the initial BTC whereas skew focuses on the tailings of the BTC. Given that patterns in TSI matched those of skew, TSI was not used in any analysis.

Tracer tests are influenced by Damkohler numbers. For a given tracer test design, the uncertainties in solute mass transfer between the surface and subsurface and storage-zone parameter estimates are strongly dependent on the experimental Damkohler number, DaI , which is a dimensionless combination of the rates of exchange between the stream and storage zones, the stream-water velocity, and the stream reach length of the experiment (Wagner and Harvey,

1997) (Equation 6). While Damkohler numbers are typically estimated through models rather than data, a Damkohler number can be calculated using the following equation:

$$DaI = \frac{\alpha \left(1 + \frac{A}{A_s}\right) L}{v} \quad (6)$$

where L is the length of the stream reach over which the experiment is performed, v is the average stream water velocity over that reach, A is the stream area, A_s is the storage area, and α is the exchange coefficient.

Parameter uncertainties are lowest at DaI values on the order of 1.0. When DaI values are much less than 1.0 (owing to high velocity, long exchange timescale, and/or short reach length), parameter uncertainties are high because only a small amount of tracer interacts with storage zones in the reach. For the opposite conditions ($DaI > 1.0$), solute exchange rates are fast relative to stream-water velocity and all solute is exchanged with the storage zone over the experimental reach (Wagner and Harvey, 1997). This creates a “goldilocks” scenario in a flume environment, where too much or too little flow velocity results in a lack of mass transfer in the system. While I cannot physically calculate a Damkohler number for the flume because the mass transfer rate is unknown, the relative effect of a Damkohler number can still be observed.

As with many studies that produce natural data, this dataset is non-normally distributed. The statistical data analysis thus requires alternative approaches that do not assume data normality or equal variance. I used RStudio to perform the statistical analyses (R Core Team, 2020). To investigate how skew and mean arrival time changed with differing logjam characteristics and flow, I used a rank transform as a nonparametric factorial analysis. Skew or mean arrival time, as the response variables, were rank transformed prior to analysis and then the rank transformed response was used in an ANOVA (type III). I used Emmeans to test the

significance of the interaction between number of jams or porosity and flow as well as the main effects of flow and jams or porosity (Table 2.5). An alpha of 0.05 was used in all statistical analyses.

Table 2.5. Response and predictor variables for statistical analysis.

Response	Predictor
Skew	# of logjams
Mean arrival time	Discharge
	Porosity

Two to three flume trials were completed for each flume configuration (e.g., one jam, high flow). A small sample size (n=2-3) makes statistical interpretation challenging with any flume runs with errors in the replicates. Thus, the standard deviation of skew and mean arrival time for three flume run replicates was used as a proxy for uncertainty. This resulted in an uncertainty threshold based on standard deviation of > 0.003 for mean arrival time and $> 8.15^{-6}$ for skew. Any samples falling outside the uncertainty threshold were excluded from the data analysis but are included in Appendix I. For flume configurations with three replicates, one replicate was simply removed if the value was outside the uncertainty threshold. For flume configurations with only two replicates, I relied on field notes and videos of the flume runs to determine and justify which run had erroneous data and needed to be removed from analysis. The figures in the subsequent sections include graphical representation of the full dataset as well as the dataset once uncertainty was removed.

Conductivity loggers were placed at the upstream and downstream ends of the experimental flume runs, but the location of the upstream sensor was in a backwater for all flume runs. Thus, upstream results are included in the discussion, but analyses focus on the data from the site downstream of the logjam, which depict both surface and subsurface transient storage.

3. Results and Discussion

3.1 Overview of Data

Results and subsequent discussion are split into two flume experiments addressing changes in logjam quantity and changes in the porosity of a single logjam. Analyses are centered around the temporal moments that describe the distribution of specific conductivity breakthrough curves (BTCs) over time (see Appendix II for BTCs). I use mean arrival time and skew in this thesis to explore transport processes relating to changing logjam characteristics and transient storage.

As mentioned in the methods (Section 2.4), an uncertainty threshold based on the standard deviation of replicates was used to discard unrepeatable results. Two data points remain per each grouping of flume runs (e.g., 1 jam, downstream, low flow) in analyses. However, the one- and two-jam flume configurations had replicate runs that were erroneous due to inconsistencies in tracer start times or injections, which required further removing replicates beyond the uncertainty threshold. Data points that necessitated removal beyond the uncertainty threshold are included in Appendix I. For data transparency, all data points are still plotted.

3.2 Changing Longitudinal Spacing

Data from the changing the longitudinal spacing of logjams show how transient storage changes as more logjams are added, based on high and low flow scenarios. DEMs depicting changes in longitudinal spacing are shown in Figure 2.10. BTCs for all flume runs with changing longitudinal jam spacing are included in Appendix II.

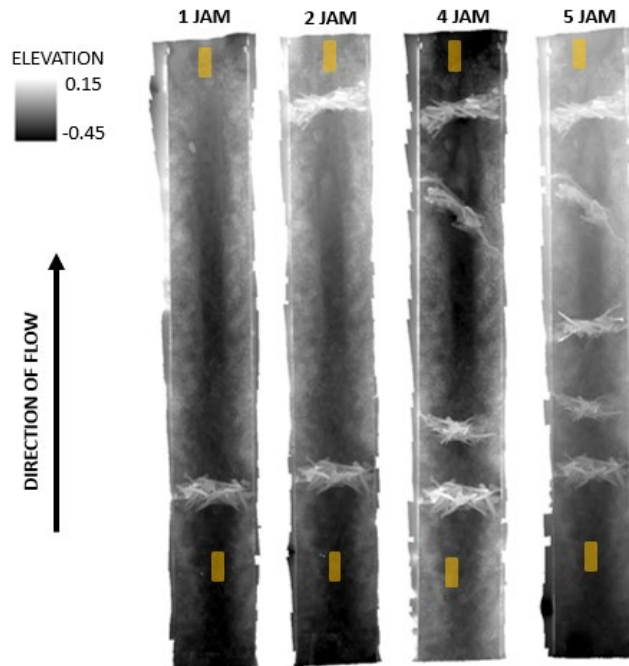


Figure 2.10. DEMs of each flume configuration following both high and low flow runs. Gray shading represents elevation in meters relative to reference points on the surface of the channel bed. Sensor locations are shown with yellow rectangles.

Q1: As the longitudinal spacing of logjams changes, what happens to transient storage at a point?

Figure 2.11c shows that more closely spaced logjams resulted in slower advection down the flume channel at low flow. There is an increase in mean arrival time with reduced longitudinal spacing at low flow, indicating slower advection as more jams are added under the same discharge conditions. In other words, more logjams in the flume resulted in slower movement of the tracer down channel. This slower transport of the tracer with increasing logjams makes sense given that, with each logjam, the localized velocity flow paths decrease and storage behind the logjam increases. There is a significant increase in mean arrival time as the number of jams increases by more than a single jam (i.e., going from 1 jam to 4 jams, 2 jams to 4 jams etc.) (Rank Transform, $p < 0.05$), but the increase in mean arrival time with the addition of a

single jam is not statistically significant (i.e., going from 1 jam to 2 jams or from 4 jams to 5 jams) (Rank Transform, $p > 0.05$). This suggests that more closely spaced logjams resulted in slower advection travel times down the flume channel. However, the decrease in advection time is not a significant change with the addition of a single logjam (Rank Transform, $p < 0.05$).

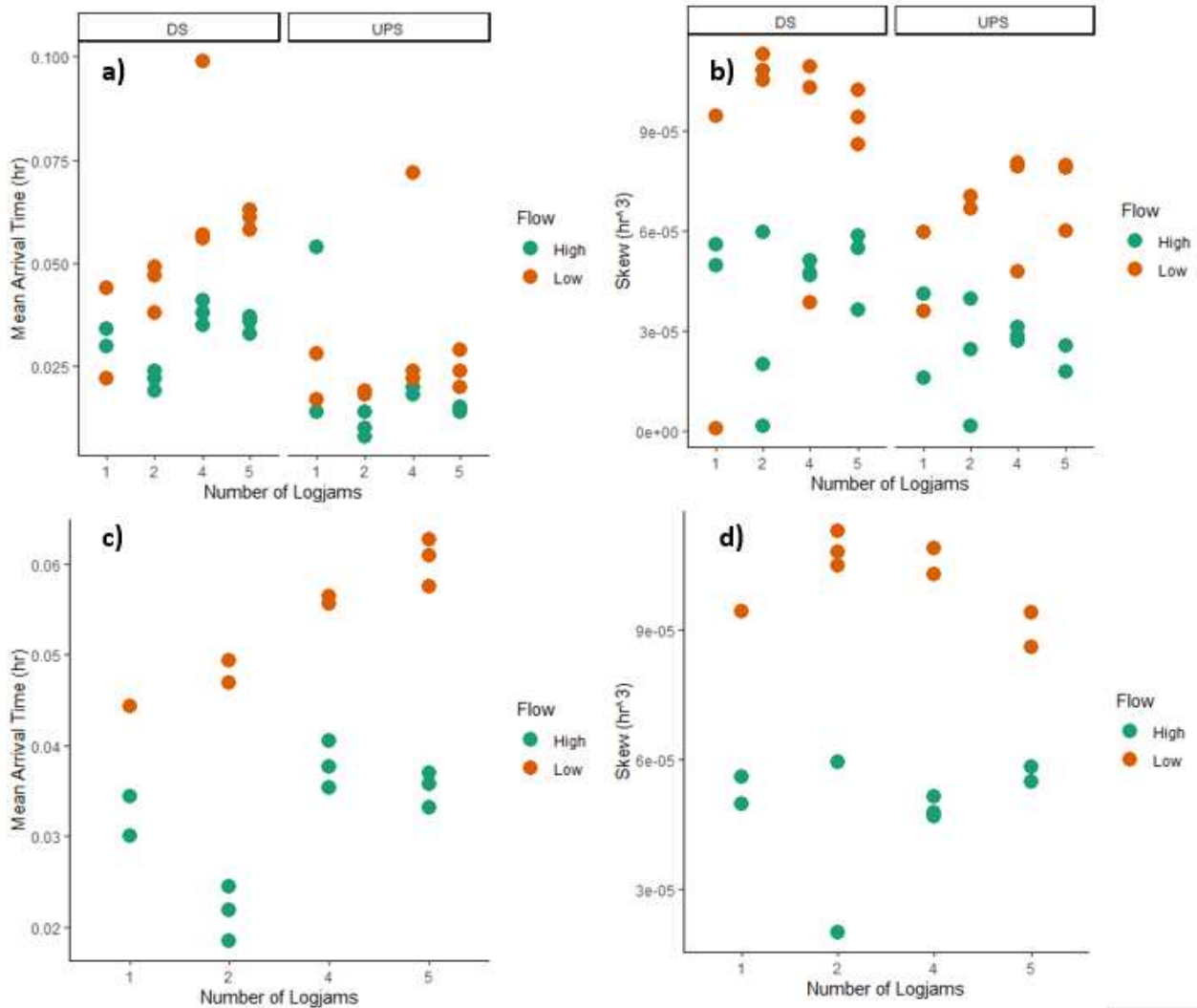


Figure 2.11. Mean arrival time and skew values plotted for all flume runs (including replicates) as longitudinal spacing changes and more jams are added. Each logjam configuration was run at high and low flow scenarios and flow is indicated in the figure by color (green for high flow, orange for low flow). Plots a and b show all data from conductivity loggers placed at upstream (UPS) and downstream (DS) locations. Plots c and d show the data used for all analyses (i.e., downstream location only and without erroneous replicate data).

At high flow, there is no trend in mean arrival time with an increasing number of logjams (Rank Transform, $p > 0.05$). This lack of increasing mean arrival time under this flow regime despite an increase in jams suggests that, with greater submergence of jams and other sources of flow resistance, the configuration of the flume channel offers similar or less predictable resistance to flow regardless of the number of jams. In other words, there is no consistent effect of number of jams on advective travel times. Some of the salt mass is also able to bypass the logjams via overtopping or preferential flow paths around the logjams, as observed during high flow runs.

Figure 2.11d suggests that the number of logjams does not significantly influence the magnitude of transient storage in the flume channel, as described by skew (Rank Transform, $p > 0.05$ for all jams). At both low and high flow, there is no trend in skew as the longitudinal density of logjams changes. At high flow, this likely indicates that the Damkohler number is much less than 1.0, given the high stream-water velocity combined with a short reach length, which results in only a small amount of tracer interacting with storage zones and thus limited solute mass transfer. It is worth noting here that the order of logjam placement relative to the sensor location could confound the interpretation. For example, Jam 2 was placed closest to the sensor and thus has the highest downstream skew value. Jam 4 was the second closest jam to the downstream sensor and has the second highest downstream skew value.

Q2: As flow changes, what happens to transient storage at a point?

Transient storage is statistically different between high and low flow (Rank Transform, $p < 0.05$). Figures 2.11c and 2.11d show higher values of both mean arrival time and skew at low flow compared to high flow for any given number of logjams. For mean arrival time, results

indicate slower advection through the logjams at low flow. I expect that, at a greater discharge, the velocity would also be greater, and vice versa.

Greater skew at low flow is counter to my original hypothesis as well as to the field data (Ader et al., 2021). However, these results in a flume can be explained by of the simplification of the system. Transient storage is typically greater at high flow in the field because flow paths are able to access the floodplain for storage. The flume limits the ability for water to access a floodplain and leads to a more homogeneous flow field, despite the presence of backwater pools. Moreover, the velocity is too fast at high flow in the flume, resulting in a DaI number that likely much less than 1.0. Therefore, solutes are flushed by advection before substantial exchange can occur with transient storage zones, leading to an insensitivity of skew to transient storage.

Q3: As location above or below a jam changes, what happen to transient storage at a point?

At low flow, upstream transient storage is significantly less than downstream transient storage (Rank Transform, $p=0.007$). This is as expected given the more evolved flow field as the tracer moves downstream. Because measurements are taken from the mobile zone, I expect to have more skew downstream of the logjam. Once again, the high flow scenario does not have sufficient hydraulic resistance and transient storage to increase the DaI to a level that would more accurately represent conditions in a real channel and thus facilitate interpretation of the results.

3.3 Changing Porosity

Temporal moments and BTCs for the porosity flume runs are included as Appendix III and IV, respectively. The results from the porosity flume runs cannot be physically interpreted with confidence given how fast the solute tracer moved through the system. Specifically, the

scaling used in the flume was not effective in distinguishing the effects of changing jam porosity. Organic matter added to the jam to decrease porosity was less effective than expected at changing the porosity enough to distinguish study effects at “high”, “medium”, and “low” porosity. Travel time for the tracer, regardless of flow, was too fast to distinguish changes based on porosity. Results and discussion are included in Appendix V.

3.4 Sources of Error and Future Work

This thesis utilized experimental methods to explore a novel question. The methodology offers an opportunity to ask additional questions as well as provide methodological refinement in future experiments. First, tracer experiments are not uniquely sensitive to surface or subsurface storage processes (Harvey et al., 1996), which limits physical interpretations and transferability of results. This study aimed to parse out surface and subsurface processes in the initial experiment set-up by using an IRIS for geophysical electrical resistivity (ER) imaging. To compare temporal trends in BTCs using the IRIS for bulk readings and conductivity probes for fluid readings, I analyzed the temporal moments of the fluid and bulk apparent conductivity data sets to detect similar behaviors. However, trends in temporal moments were not consistent between the surface and subsurface methodologies, and I was unable to provide any explanation for the variation. Future work to determine a feasible ER methodology and a companion flume configuration could provide valuable insight on patterns of hyporheic exchange in the subsurface.

The flume configuration presents an opportunity for further refinement of the physical model set-up to study the effects of logjam characteristics on transient storage. Flume flows and channel elements were scaled from Little Beaver Creek, a representative stream with logjams and transient storage. However, the relative scaling of the flume presented challenges in the data

interpretation. Specifically, the high flow scenario resulted in a low Damkohler number where water was moving too quickly over a short distance, so that the salt tracer did not have an opportunity to interact with surface or subsurface storage zones. Thus, the results from high flow runs were physically uninterpretable at times. Because of COVID-related delays and limited access to the experimental facilities, challenges in scaling were not identified with the experimental design until flume runs were completed. Future iterations of these experiments would benefit from using lower discharges for all flume runs. For example, the existing low flow could become the new high flow and an even lower new low flow could be run. Proposed future scaling of flume runs is included in Table 2.6.

Table 2.6. Proposed future scaling of flume attributes to improve study effects.

Flume Attribute	Current Scaling	Future Scaling
Porosity	High= 70%	High= 70%
	Medium= 68%	Medium= 50%
	Low= 65%	Low= 30%
Flow	High= 0.01 m ³ /s	High= 0.001 m ³ /s
	Low= 0.001 m ³ /s	Low= 0.0001 m ³ /s

As mentioned in Section 3.2, a flume is different than a field environment, particularly at high flow, in the limited ability for flow to access the floodplain. In the field, transient storage is often greater at high flow because flow paths are able to access the floodplain for storage. The simplified flume environment limits the ability for water to access a floodplain and leads to a more homogeneous flow field. As flow increases, water largely remains within the active channel as it flows downstream given limited ability for lateral movement, which leads to challenges in interpreting high flow results. The upstream sensor was placed less than 0.5-m

above the logjam in the flume and thus was always in a backwater and below the injection point. To make methods as simple as possible, ideally, the upstream sensor would be placed even farther upstream to confirm that upstream skew does not change (i.e., it is just an inlet condition) and interpretation of results would only consider downstream skew.

The flume experiment with changing porosities offers many lessons learned and opportunity for further refinement of the configuration. As mentioned in section 3.3, the scaling used in the flume was not effective in distinguishing the study effects. Travel time for the tracer, regardless of flow, was too fast to distinguish changes based on porosity. In other words, the tracer moved through the short flume reach too quickly to distinguish between changes in porosity. Sensors were placed less than 0.5-m above and below a single logjam. Thus, the “study reach” from upstream to downstream sensor was less than a meter in total distance. The results suggested that the tracer moves through the entire flume system very quickly, so when confined to a very small reach length (and high discharges), the results are not interpretable.

Additionally, the amount of material added between flume runs to change the porosity did not appear to be enough to show clear patterns in results. Future jam configurations should include larger changes in porosity between runs (i.e., changes by about 10-20% porosity) achieved by adding a greater quantity of organic material. This study decreased the porosity approximately 5% from high to low porosity and although that did increase the backwater, it was not sufficient to significantly influence transient storage. Future work will include re-running porosity flume runs with modified scaling in tandem with a numerical model and multiple pulse salt-conductivity measurements at Little Beaver Creek (see Table 3.1 for future scaling).

Outside of the flume configuration, there are many topics within this thesis that could continue to be explored. Porosity, as a logjam characteristic, has many important implications for

river form and function. Despite understanding of its importance, the actual measurement of porosity remains challenging. Most studies rely on a visual estimate of porosity, which is subjective and does not account for internal jam structure. Within the flume, I was able to constrain porosity measurements by physically measuring wood volumes and controlling the logjam parameters. Yet, most studies do not have the ability to re-construct jams, particularly in a field setting. Continued work to examine how to automate or objectively estimate porosity measurements has broad applications for river science and management. Spreitzer et al. (2019) most recently conducted an application of SfM photogrammetry in a laboratory setting by using a multi-angled approach to capture the jam at varying points-of-view. There are currently practical limits on using photogrammetric techniques to assess logjam porosity. SfM can be used to scan the outer contours of LW accumulations but cannot practically assess the wood content and porosity. Details of the outer deposit are captured in high resolution, but the core of the deposit remains occluded, resulting in only an estimation of porosity. I collected photos for all porosity flume runs to further explore SfM techniques to estimate porosity in the future.

The field site used for this project additionally provides a unique setting for investigating naturally-occurring changes in logjam characteristics. A beaver dam was built on top of one of the study logjams during the course of our field measurements at Little Beaver Creek. The change to the logjam increased the backwater storage of water, fine sediment, and particulate organic matter in a similar fashion to the constructed logjam with decreasing porosity in the flume. In summer 2021, the study area was affected by wildfire, which further provides an interesting natural progression of fine material added to the logjam. Future work at this site will provide a unique field study looking at changing porosity and how that influences transient storage under different natural processes. Following the fire season, temperature stakes were

installed above the study logjam as well as a series of logjams within burned and unburned reaches of Little Beaver Creek. These temperature measurements will ideally tell a story of some of the subsurface transient storage processes. Cumulatively, this work will relate the functionality of wood accumulations (size relative to active channel, location with respect to active channel, and porosity) to understanding the local and reach-scale geomorphic effects of logjams.

4. Conclusions

Results from flume experiments provide insight into how logjam characteristics influence transient storage, which can be used to advance both scientific research and practice. The presence of channel-spanning logjams facilitates more opportunities for solute retention and processing in zones of transient storage, especially at lower flow rates, when hydrologic retention peaks. The mean arrival time of the solute tracer increases with the number of jams in a reach, indicating slower advection time as more jams are added in the system. More transient storage occurs downstream of a logjam, which is expected given the more evolved flow field as the tracer moves downstream. High flow results in the flume do not show consistent patterns in transient storage and present challenges to physical interpretation of the results given the low Damkohler number. This lack of increasing skew or mean arrival time under this flow regime despite an increase in jams suggests that under greater submergence of jams and other roughness elements, the flume offers similar or less predictable resistance to flow regardless of the number of jams. In summary, my results suggest that adding more wood into a river system increases surface transient storage, although the effects of differing flows could not be distinguished. Although the results from the porosity flume runs cannot be physically interpreted with confidence given how fast the solute tracer moved through the system, areas of further research

include investigating porosity with more organic inputs in a flume and exploring automation methods for calculating porosity.

These results can be interpreted to provide recommendations for placing large wood for the purpose of increasing transient storage in a management context. One of the benefits of using a physical model is that it allowed for isolating study effects in a manner that is not feasible in the field. From the observed differences in surface transient storage between stream segments with greater and lesser amounts of large wood, I can infer that river management designed to foster surface transient storage can effectively focus on retaining wood (either by continuing recruitment and transport or fixing engineered logjams in place). Increased logjam quantity enhances transient storage, which in turn improves stream health and makes a case for river managers to implement wood in river restoration designs.

References

- Abbe, T. B., & Montgomery, D. R. (2003). Patterns and processes of wood debris accumulation in the Queets river basin, Washington. *Geomorphology*, 51(1–3), 81–107. [https://doi.org/10.1016/S0169-555X\(02\)00326-4](https://doi.org/10.1016/S0169-555X(02)00326-4)
- Ader, E., Wohl, E., McFadden, S., & Singha, K. (2021). Logjams as a driver of transient storage in a mountain stream. *Earth Surface Processes and Landforms*, esp.5057. <https://doi.org/10.1002/esp.5057>
- AgiSoft PhotoScan Professional (Version 1.7.0) (Software). (2020). Retrieved from <http://www.agisoft.com/downloads/installer/>
- Ballinger, A., Nally, R. Mac, & Lake, P. S. (2009). Decay state and inundation history control assemblage structure of log-dwelling invertebrates in floodplain forests. *River Research and Applications*, 26(2), n/a-n/a. <https://doi.org/10.1002/rra.1254>
- Battin, T. J., Kaplan, L. A., Findlay, S., Hopkinson, C. S., Marti, E., Packman, A. I., Newbold, J. D., & Sabater, F. (2008). Biophysical controls on organic carbon fluxes in fluvial networks. *Nature Geoscience*, 1(2), 95–100. <https://doi.org/10.1038/ngeo101>
- Beckman, N. D., & Wohl, E. (2014). Carbon storage in mountainous headwater streams: The role of old-growth forest and logjams. *Water Resources Research*, 50(3), 2376–2393. <https://doi.org/10.1002/2013WR014167>
- Bencala, K. E. (1983). Simulation of solute transport in a mountain pool-and-riffle stream with a kinetic mass transfer model for sorption. *Water Resources Research*, 19(3), 732–738. <https://doi.org/10.1029/WR019i003p00732>
- Benke, A. C., & Wallace, J. B. (1990). Wood dynamics in Coastal Plain blackwater streams. *Canadian Journal of Fisheries and Aquatic Sciences*, 47(1), 92–99. <https://doi.org/10.1139/f90-009>
- Buffington, J. M., Lisle, T. E., Woodsmith, R. D., & Hilton, S. (2002). Controls on the size and occurrence of pools in coarse-grained forest rivers. *River Research and Applications*, 18(6), 507–531. <https://doi.org/10.1002/rra.693>
- Buffington, J. M., & Montgomery, D. R. (1999). Effects of hydraulic roughness on surface textures of gravel-bed rivers. *Water Resources Research*, 35(11), 3507–3521. <https://doi.org/10.1029/1999WR900138>
- CloudCompare (version 2.10) (GPL software). (2019). Retrieved from <http://www.cloudcompare.org/>
- Collins, B. D., Montgomery, D. R., Fetherston, K. L., & Abbe, T. B. (2012). The floodplain large-wood cycle hypothesis: A mechanism for the physical and biotic structuring of temperate forested alluvial valleys in the North Pacific coastal ecoregion. *Geomorphology*, 139–140, 460–470. <https://doi.org/10.1016/j.geomorph.2011.11.011>
- Curran, J. H., & Wohl, E. E. (2003). Large woody debris and flow resistance in step-pool channels, Cascade Range, Washington. *Geomorphology*, 51(1–3), 141–157. [https://doi.org/10.1016/S0169-555X\(02\)00333-1](https://doi.org/10.1016/S0169-555X(02)00333-1)

- D'Angelo, D. J., Webster, J. R., Gregory, S. V., & Meyer, J. L. (1993). Transient Storage in Appalachian and Cascade Mountain Streams as Related to Hydraulic Characteristics. *Journal of the North American Benthological Society*, 12(3), 223–235. <https://doi.org/10.2307/1467457>
- Day, N. K., & Hall, R. O. (2017). Ammonium uptake kinetics and nitrification in mountain streams. *Freshwater Science*, 36(1), 41–54. <https://doi.org/10.1086/690600>
- Dixon, S. J. (2016). A dimensionless statistical analysis of logjam form and process. *Ecohydrology*, 9(6), 1117–1129. <https://doi.org/10.1002/eco.1710>
- Doughty, M., Sawyer, A. H., Wohl, E., & Singha, K. (2020). Mapping increases in hyporheic exchange from channel-spanning logjams. *Journal of Hydrology*, 587, 124931. <https://doi.org/10.1016/j.jhydrol.2020.124931>
- Endreny, T., Lautz, L., & Siegel, D. I. (2011). Hyporheic flow path response to hydraulic jumps at river steps: Flume and hydrodynamic models. *Water Resources Research*, 47(2), 2517. <https://doi.org/10.1029/2009WR008631>
- Ensign, S. H., & Doyle, M. W. (2005). In-channel transient storage and associated nutrient retention: Evidence from experimental manipulations. *Limnology and Oceanography*, 50(6), 1740–1751. <https://doi.org/10.4319/lo.2005.50.6.1740>
- Fanelli, R. M., & Lautz, L. K. (2008). Patterns of Water, Heat, and Solute Flux through Streambeds around Small Dams. *Ground Water*, 46(5), 671–687. <https://doi.org/10.1111/j.1745-6584.2008.00461.x>
- Fausch, K. D., & Northcote, T. G. (1992). Large woody debris and salmonid habitat in a small coastal British Columbia stream. *Canadian Journal of Fisheries and Aquatic Sciences*, 49(4), 682–693. <https://doi.org/10.1139/f92-077>
- Fischer, H., Kloep, F., Wilzcek, S., & Pusch, M. T. (2005). A river's liver - Microbial processes within the hyporheic zone of a large lowland river. *Biogeochemistry*, 76(2), 349–371. <https://doi.org/10.1007/s10533-005-6896-y>
- Gippel, C. J. (1995). Environmental Hydraulics of Large Woody Debris in Streams and Rivers. *Journal of Environmental Engineering*, 121(5), 388–395. [https://doi.org/10.1061/\(asce\)0733-9372\(1995\)121:5\(388\)](https://doi.org/10.1061/(asce)0733-9372(1995)121:5(388))
- Gooseff, M. N., Hall, R. O., & Tank, J. L. (2007). Relating transient storage to channel complexity in streams of varying land use in Jackson Hole, Wyoming. *Water Resources Research*, 43(1), 1–10. <https://doi.org/10.1029/2005WR004626>
- Gupta, A., & Cvetkovic, V. (2000). Temporal moment analysis of tracer discharge in streams: Combined effect of physicochemical mass transfer and morphology. *Water Resources Research*. <https://doi.org/10.1029/2000WR900190>
- Hall, R. J. O., Bernhardt, E. S., & Likens, G. E. (2002). Relating nutrient uptake with transient storage in forested mountain streams. *Limnology and Oceanography*, 47(1), 255–265. <https://doi.org/10.4319/lo.2002.47.1.0255>
- Harvey, C. F., & Gorelick, S. M. (1995). Temporal Moment-Generating Equations: Modeling

- Transport and Mass Transfer in Heterogeneous Aquifers. *Water Resources Research*.
<https://doi.org/10.1029/95WR01231>
- Harvey, J., & Gooseff, M. (2015). River corridor science: Hydrologic exchange and ecological consequences from bedforms to basins. In *Water Resources Research* (Vol. 51, Issue 9, pp. 6893–6922). Blackwell Publishing Ltd. <https://doi.org/10.1002/2015WR017617>
- Harvey, J. W., & Bencala, K. E. (1993). The Effect of streambed topography on surface-subsurface water exchange in mountain catchments. *Water Resources Research*, 29(1), 89–98. <https://doi.org/10.1029/92WR01960>
- Harvey, J. W., Wagner, B. J., & Bencala, K. E. (1996). Evaluating the Reliability of the Stream Tracer Approach to Characterize Stream-Subsurface Water Exchange. *Water Resources Research*, 32(8), 2441–2451. <https://doi.org/10.1029/96WR01268>
- Harvey, J. W., & Wagnert, B. J. (2000). Zones Interactions between. In *Streams and Ground Waters*. Elsevier Inc. <https://doi.org/10.1016/B978-0-12-389845-6.50002-8>
- Hassan, M. A., Hogan, D. L., Bird, S. A., May, C. L., Gomi, T., & Campbell, D. (2005). Spatial and Temporal Dynamics of Wood in Headwater Streams of the Pacific Northwest. *Journal of the American Water Resources Association*, 41(4), 899–919. <https://doi.org/10.1111/j.1752-1688.2005.tb03776.x>
- Herdrich, A. T., Winkelman, D. L., Venarsky, M. P., Walters, D. M., & Wohl, E. (2018). The loss of large wood affects rocky mountain trout populations. *Ecology of Freshwater Fish*, 27(4), 1023–1036. <https://doi.org/10.1111/eff.12412>
- Herzog, S. P., Higgins, C. P., Singha, K., & McCray, J. E. (2018). Performance of engineered streambeds for inducing hyporheic transient storage and attenuation of resazurin. *Environmental science & technology*, 52(18), 10627-10636.
- Hester, E. T., & Doyle, M. W. (2008). In-stream geomorphic structures as drivers of hyporheic exchange. *Water Resources Research*, 44(3). <https://doi.org/10.1029/2006WR005810>
- Hester, E. T., & Gooseff, M. N. (2010). Moving beyond the banks: Hyporheic restoration is fundamental to restoring ecological services and functions of streams. In *Environmental Science and Technology* (Vol. 44, Issue 5, pp. 1521–1525). UTC. <https://doi.org/10.1021/es902988n>
- Hickin, E. J., & Nanson, G. C. (1984). Lateral Migration Rates of River Bends. *Journal of Hydraulic Engineering*, 110(11), 1557–1567. [https://doi.org/10.1061/\(asce\)0733-9429\(1984\)110:11\(1557\)](https://doi.org/10.1061/(asce)0733-9429(1984)110:11(1557))
- Hyatt, T. L., & Naiman, R. J. (2001). The Residence Time of Large Woody Debris in the Queets River, Washington, USA. In *Ecological Applications* (Vol. 11, Issue 1). John Wiley & Sons, Ltd. [https://doi.org/10.1890/1051-0761\(2001\)011\[0191:TRTOLW\]2.0.CO;2](https://doi.org/10.1890/1051-0761(2001)011[0191:TRTOLW]2.0.CO;2)
- Jackson, T. R., Haggerty, R., Apte, S. V., & O'Connor, B. L. (2013). A mean residence time relationship for lateral cavities in gravel-bed rivers and streams: Incorporating streambed roughness and cavity shape. *Water Resources Research*, 49(6), 3642–3650. <https://doi.org/10.1002/wrcr.20272>

- Kasahara, T., & Wondzell, S. M. (2003). Geomorphic controls on hyporheic exchange flow in mountain streams. *Water Resources Research*, 39(1), SBH 3-1-SBH 3-14. <https://doi.org/10.1029/2002wr001386>
- Kaufmann, P. R., & Faustini, J. M. (2012). Simple measures of channel habitat complexity predict transient hydraulic storage in streams. *Hydrobiologia*, 685(1), 69–95. <https://doi.org/10.1007/s10750-011-0841-y>
- Lautz, L. K., Siegel, D. I., & Bauer, R. L. (2006). Impact of debris dams on hyporheic interaction along a semi-arid stream. *Hydrological Processes*. <https://doi.org/10.1002/hyp.5910>
- Lees, M. J., Camacho, L. A., & Chapra, S. (2000). On the relationship of transient storage and aggregated dead zone models of longitudinal solute transport in streams. *Water Resources Research*, 36(1), 213–224. <https://doi.org/10.1029/1999WR900265>
- Livers, B., & Wohl, E. (2016). Sources and interpretation of channel complexity in forested subalpine streams of the Southern Rocky Mountains. *Water Resources Research*, 52(5), 3910–3929. <https://doi.org/10.1002/2015WR018306>
- Livers, B., Wohl, E., Jackson, K. J., & Sutfin, N. A. (2018). Historical land use as a driver of alternative states for stream form and function in forested mountain watersheds of the Southern Rocky Mountains. *Earth Surface Processes and Landforms*, 43(3), 669–684. <https://doi.org/10.1002/esp.4275>
- MacFarlane, W. A., & Wohl, E. (2003). Influence of step composition on step geometry and flow resistance in step-pool streams of the Washington Cascades. *Water Resources Research*, 39(2), 1037. <https://doi.org/10.1029/2001WR001238>
- Manners, R. B., Doyle, M. W., & Small, M. J. (2007). Structure and hydraulics of natural woody debris jams. *Water Resources Research*, 43(6). <https://doi.org/10.1029/2006WR004910>
- Mao, L., Uyttendaele, G. P., Iroumé, A., & Lenzi, M. A. (2008). Field based analysis of sediment entrainment in two high gradient streams located in Alpine and Andine environments. *Geomorphology*, 93(3–4), 368–383. <https://doi.org/10.1016/j.geomorph.2007.03.008>
- Marshall, A.E., Iskin, E.P., Wohl, E. (2021). Seasonal and Diurnal Fluctuations of Coarse Particulate Organic Matter Transport in a Snowmelt Dominated Stream. River Research and Applications. In production. <https://doi.org/10.1002/rra.3802>
- Marttila, H., Turunen, J., Aroviita, J., Tammela, S., Luhta, P. L., Muotka, T., & Kløve, B. (2018). Restoration increases transient storages in boreal headwater streams. *River Research and Applications*, 34(10), 1278–1285. <https://doi.org/10.1002/rra.3364>
- Mason, S. J. K., McGlynn, B. L., & Poole, G. C. (2012). Hydrologic response to channel reconfiguration on Silver Bow Creek, Montana. *Journal of Hydrology*, 438–439, 125–136. <https://doi.org/10.1016/j.jhydrol.2012.03.010>
- Massong, T. M., & Montgomery, D. R. (2000). Influence of sediment supply, lithology, and wood debris on the distribution of bedrock and alluvial channels. *Bulletin of the Geological Society of America*, 112(4), 591–599. [https://doi.org/10.1130/0016-7606\(2000\)112<591:IOSSLA>2.0.CO;2](https://doi.org/10.1130/0016-7606(2000)112<591:IOSSLA>2.0.CO;2)

- MATLAB. (2020). version 9.7.0 (R2020a). Natick, Massachusetts: The MathWorks Inc.
- Millington, C. E., & Sear, D. A. (2007). Impacts of river restoration on small-wood dynamics in a low-gradient headwater stream. *Earth Surface Processes and Landforms*, 32(8), 1204–1218. <https://doi.org/10.1002/esp.1552>
- Mulholland, P. J., Valett, H. M., Webster, J. R., Thomas, S. A., Cooper, L. W., Hamilton, S. K., & Peterson, B. J. (2004). Stream denitrification and total nitrate uptake rates measured using a field ¹⁵ N tracer addition approach. *Limnology and Oceanography*, 49(3), 809–820. <https://doi.org/10.4319/lo.2004.49.3.0809>
- Nordin, C. F., & Troutman, B. M. (1980). Longitudinal dispersion in rivers: The persistence of skewness in observed data. *Water Resources Research*, 16(1), 123–128. <https://doi.org/10.1029/WR016i001p00123>
- Peakall, J., Ashworth, P., Best, & Jim. (1996). Physical Modelling in Fluvial Geomorphology: Principles, Applications and Unresolved Issues. *The Scientific Nature of Geomorphology: Proceedings of the 27th Binghamton Symposium in Geomorphology*, 221–234.
- Pfeiffer, A., & Wohl, E. (2018). Where Does Wood Most Effectively Enhance Storage? Network-Scale Distribution of Sediment and Organic Matter Stored by Instream Wood. *Geophysical Research Letters*, 45(1), 194–200. <https://doi.org/10.1002/2017GL076057>
- Piégay, H., & Gurnell, A. M. (1997). Large woody debris and river geomorphological pattern: Examples from S.E. France and S. England. *Geomorphology*, 19(1–2), 99–116. [https://doi.org/10.1016/s0169-555x\(96\)00045-1](https://doi.org/10.1016/s0169-555x(96)00045-1)
- Prestegard, K. L. (1983). Bar resistance in gravel bed streams at bankfull stage. *Water Resources Research*, 19(2), 472–476. <https://doi.org/10.1029/WR019i002p00472>
- R Core Team (2020). R: A language and environment for statistical computing. R Foundation for Statistical Computing, Vienna, Austria. URL <https://www.R-project.org/>.
- Richmond, A. D., & Fausch, K. D. (1995). Characteristics and function of large woody debris in subalpine Rocky Mountain streams in northern Colorado. *Canadian Journal of Fisheries and Aquatic Sciences*, 52(8), 1789–1802. <https://doi.org/10.1139/f95-771>
- Roni, P. (2003). Responses of Benthic Fishes and Giant Salamanders to Placement of Large Woody Debris in Small Pacific Northwest Streams. *North American Journal of Fisheries Management*, 23(4), 1087–1097. <https://doi.org/10.1577/m02-048>
- Ruiz-Villanueva, V., Piégay, H., Gurnell, A. A., Marston, R. A., & Stoffel, M. (2016). Recent advances quantifying the large wood dynamics in river basins: New methods and remaining challenges. In *Reviews of Geophysics* (Vol. 54, Issue 3, pp. 611–652). Blackwell Publishing Ltd. <https://doi.org/10.1002/2015RG000514>
- Sawyer, A. H., Bayani Cardenas, M., & Buttles, J. (2011). Hyporheic exchange due to channel-spanning logs. *Water Resources Research*, 47(8). <https://doi.org/10.1029/2011WR010484>
- Sawyer, A. H., Bayani Cardenas, M., & Buttles, J. (2012). Hyporheic temperature dynamics and heat exchange near channel-spanning logs. *Water Resources Research*, 48(1).

<https://doi.org/10.1029/2011WR011200>

- Sawyer, A. H., & Cardenas, M. B. (2012). Effect of experimental wood addition on hyporheic exchange and thermal dynamics in a losing meadow stream. *Water Resources Research*, 48(10), 10537. <https://doi.org/10.1029/2011WR011776>
- Sear, D. A., Millington, C. E., Kitts, D. R., & Jeffries, R. (2010). Logjam controls on channel:floodplain interactions in wooded catchments and their role in the formation of multi-channel patterns. *Geomorphology*, 116(3–4), 305–319. <https://doi.org/10.1016/j.geomorph.2009.11.022>
- Singha, K., & Gorelick, S. M. (2005). Saline tracer visualized with three-dimensional electrical resistivity tomography: Field-scale spatial moment analysis. *Water Resources Research*, 41(5), 1–17. <https://doi.org/10.1029/2004WR003460>
- Sparacino, M. S., Rathburn, S. L., Covino, T. P., Singha, K., & Ronayne, M. J. (2019). Form-based river restoration decreases wetland hyporheic exchange: Lessons learned from the Upper Colorado River. *Earth Surface Processes and Landforms*, 44(1), 191-203.
- Spreitzer, G., Tunncliffe, J., & Friedrich, H. (2019). Using Structure from Motion photogrammetry to assess large wood (LW) accumulations in the field. *Geomorphology*, 346, 106851. <https://doi.org/10.1016/j.geomorph.2019.106851>
- Stewart, R. J., Wollheim, W. M., Gooseff, M. N., Briggs, M. A., Jacobs, J. M., Peterson, B. J., & Hopkinson, C. S. (2011). Separation of river network-scale nitrogen removal among the main channel and two transient storage compartments. *Water Resources Research*, 47(10). <https://doi.org/10.1029/2010WR009896>
- Stofleth, J. M., Shields Jr, F. D., & Fox, G. A. (2008). Hyporheic and total transient storage in small, sand-bed streams. *Hydrological Processes*, 22(12), 1885–1894. <https://doi.org/10.1002/hyp.6773>
- Swanson, F. J., Gregory, S. V., Iroumé, A., Ruiz-Villanueva, V., & Wohl, E. (2021). Reflections on the history of research on large wood in rivers. *Earth Surface Processes and Landforms*, 46(1), 55–66. <https://doi.org/10.1002/esp.4814>
- Tonina, D., & Buffington, J. M. (2009). Hyporheic Exchange in Mountain Rivers I: Mechanics and Environmental Effects. *Geography Compass*, 3(3), 1063–1086. <https://doi.org/10.1111/j.1749-8198.2009.00226.x>
- Toran, L., Nyquist, J. E., Fang, A. C., Ryan, R. J., & Rosenberry, D. O. (2013). Observing lingering hyporheic storage using electrical resistivity: Variations around stream restoration structures, Crabby Creek, PA. *Hydrological Processes*. <https://doi.org/10.1002/hyp.9269>
- Venarsky, M. P., Walters, D. M., Hall, R. O., Livers, B., & Wohl, E. (2018). Shifting stream planform state decreases stream productivity yet increases riparian animal production. *Oecologia*, 187(1), 167–180. <https://doi.org/10.1007/s00442-018-4106-6>
- Ventres-Pake, R., Nahorniak, M., Kramer, N., O’Neal, J., & Abbe, T. (2020). Integrating Large Wood Jams into Hydraulic Models: Evaluating a Porous Plate Modeling Method. *JAWRA Journal of the American Water Resources Association*, 56(2), 333–347. <https://doi.org/10.1111/1752-1688.12818>

- Wagner, B. J., & Harvey, J. W. (1997). Experimental design for estimating parameters of rate-limited mass transfer: Analysis of stream tracer studies. *Water Resources Research*, 33(7), 1731–1741. <https://doi.org/10.1029/97WR01067>
- Ward, A. S., Gooseff, M. N., Fitzgerald, M., Voltz, T. J., & Singha, K. (2014). Spatially distributed characterization of hyporheic solute transport during baseflow recession in a headwater mountain stream using electrical geophysical imaging. *Journal of Hydrology*, 517, 362–377. <https://doi.org/10.1016/j.jhydrol.2014.05.036>
- Ward, A. S., Gooseff, M. N., & Singha, K. (2010a). Imaging hyporheic zone solute transport using electrical resistivity. *Hydrological Processes*. <https://doi.org/10.1002/hyp.7672>
- Ward, A. S., Gooseff, M. N., & Singha, K. (2010b). Characterizing hyporheic transport processes - Interpretation of electrical geophysical data in coupled stream-hyporheic zone systems during solute tracer studies. *Advances in Water Resources*, 33(11), 1320–1330. <https://doi.org/10.1016/j.advwatres.2010.05.008>
- Ward, A. S., Morgan, J. A., White, J. R., & Royer, T. V. (2018). Streambed restoration to remove fine sediment alters reach-scale transient storage in a low-gradient fifth-order river, Indiana, USA. *Hydrological Processes*, 32(12), 1786–1800. <https://doi.org/10.1002/hyp.11518>
- Wilcox, A. C., Wohl, E. E., Comiti, F., & Mao, L. (2011). Hydraulics, morphology, and energy dissipation in an alpine step-pool channel. *Water Resources Research*, 47(7), 7514. <https://doi.org/10.1029/2010WR010192>
- Wilhelmsen, K., Sawyer, A.H., Marshall, A.E., McFadden, S., Singha, K., Wohl, E. (2021). Interacting Influence of Log Jams and Branching Channels on Hyporheic Exchange Revealed through Laboratory Flume and Numerical Modeling Experiments. *Water Resources Research*. In press.
- Wohl, E., & Beckman, N. (2014). Controls on the longitudinal distribution of channel-spanning logjams in the Colorado front range, USA. *River Research and Applications*, 30(1), 112–131. <https://doi.org/10.1002/rra.2624>
- Wohl, E. E., & Ikeda, H. (1998). The effect of roughness configuration on velocity profiles in an artificial channel. *Earth Surface Processes and Landforms*, 23(2), 159–169. [https://doi.org/10.1002/\(SICI\)1096-9837\(199802\)23:2<159::AID-ESP829>3.0.CO;2-P](https://doi.org/10.1002/(SICI)1096-9837(199802)23:2<159::AID-ESP829>3.0.CO;2-P)
- Wohl, E. (2011). Threshold-induced complex behavior of wood in mountain streams. *Geology*, 39(6), 587–590. <https://doi.org/10.1130/G32105.1>
- Wohl, E., & Cadol, D. (2011). Neighborhood matters: Patterns and controls on wood distribution in old-growth forest streams of the Colorado Front Range, USA. *Geomorphology*, 125(1), 132–146. <https://doi.org/10.1016/j.geomorph.2010.09.008>
- Wohl, E., & Goode, J. R. (2008). Wood dynamics in headwater streams of the Colorado Rocky Mountains. *Water Resources Research*, 44(9), 9429. <https://doi.org/10.1029/2007WR006522>
- Wohl, E., Hall, R. O., Lininger, K. B., Sutfin, N. A., & Walters, D. M. (2017). Carbon dynamics of river corridors and the effects of human alterations. *Ecological Monographs*, 87(3), 379–

409. <https://doi.org/10.1002/ecm.1261>

- Wohl, E., Kramer, N., Ruiz-Villanueva, V., Scott, D. N., Comiti, F., Gurnell, A. M., Piegay, H., Lininger, K. B., Jaeger, K. L., Walters, D. M., & Fausch, K. D. (2019). The Natural Wood Regime in Rivers. *BioScience*, *69*(4), 259–273. <https://doi.org/10.1093/biosci/biz013>
- Wohl, E., & Scott, D. N. (2017). Wood and sediment storage and dynamics in river corridors. *Earth Surface Processes and Landforms*, *42*(1), 5–23. <https://doi.org/10.1002/esp.3909>
- Wohl, E., & Scamardo, J.E. (2021). The resilience of logjams to floods. *Hydrological Processes*, *35*, e13970.
- Wollheim, W. M., Harms, T. K., Peterson, B. J., Morkeski, K., Hopkinson, C. S., Stewart, R. J., Gooseff, M. N., & Briggs, M. A. (2014). Nitrate uptake dynamics of surface transient storage in stream channels and fluvial wetlands. *Biogeochemistry*, *120*(1–3), 239–257. <https://doi.org/10.1007/s10533-014-9993-y>
- Wörman, A., Packman, A. I., Johansson, H., & Jonsson, K. (2002). Effect of flow-induced exchange in hyporheic zones on longitudinal transport of solutes in streams and rivers. *Water Resources Research*, *38*(1), 2-1-2–15. <https://doi.org/10.1029/2001WR000769>
- Yochum, S. E., Bledsoe, B. P., David, G. C. L., & Wohl, E. (2012). Velocity prediction in high-gradient channels. *Journal of Hydrology*, *424–425*, 84–98. <https://doi.org/10.1016/j.jhydrol.2011.12.031>
- Yochum, S. E., Bledsoe, B. P., Wohl, E., & David, G. C. L. (2014). Spatial characterization of roughness elements in high-gradient channels of the Fraser Experimental Forest, Colorado, USA. *Water Resources Research*, *50*(7), 6015–6029. <https://doi.org/10.1002/2014WR015587>
- Zhang, N., Rutherford, I., & Ghisalberti, M. (2019). *Effect of instream logs on bank erosion potential: a flume study with a single log*. <https://doi.org/10.1080/24705357.2019.1634499>

CHAPTER 3: SEASONAL AND DIURNAL FLUCTUATIONS OF COARSE PARTICULATE ORGANIC MATTER TRANSPORT IN A SNOWMELT-DOMINATED STREAM¹

Summary

We measured coarse particulate organic matter (CPOM) transport along a wood-rich, pool-riffle mountain stream in the Southern Rockies of Colorado, USA to examine how spatial variations in storage features and temporal variations in discharge influence the transport of CPOM. Ecologists have found that the majority of annual CPOM export occurs during periods of high discharge. More recently, geomorphologists have begun to examine the transport of CPOM as bedload. There has been, however, little direct sampling of CPOM to evaluate how shorter (diurnal) and longer (seasonal peak flow) variations in discharge affect CPOM transport, and no examination of where CPOM is transported in the water column (primarily in suspension or as bedload). We collected CPOM moving as bedload, in suspension (at 0.6 of the flow depth), and at the surface to evaluate CPOM transport processes. Samples were collected at three sites: (1) in the backwater pool upstream from a channel-spanning logjam; (2) immediately downstream from the logjam; and (3) in a riffle about 10 bankfull-channel-widths downstream from any channel-spanning logjams. During sample sets, we collected samples over 15-minute increments at approximately 4-hour intervals over a 24-hour period. Seven sample sets were distributed over a period of two months that spanned the rise, peak, and recession of the annual snowmelt flood. We found that the majority of CPOM is transported in suspension following a clockwise hysteresis loop in which CPOM peaks prior to discharge during the seasonal hydrograph.

¹ Published as Marshall et al., 2021, River Research and Applications

1.0 Introduction

Coarse particulate organic matter (CPOM) spanning a diameter of 1 mm to 10 cm (Tank et al., 2010) is critical to the physical and ecological processes of stream ecosystems. Leaves, branches, wood fragments, and other allochthonous material composing CPOM enter the channel via fluvial transport from upstream, litter fall from riparian vegetation, wind, bank erosion, tree fall, and overland transport from the adjacent riparian and upland zones (Webster et al., 1994; Wallace et al., 1995; Jochner et al., 2015). Once in the channel, CPOM can be transported downstream or stored by channel features such as logjams or eddies (Beckman & Wohl, 2014) and decomposed by abrasion, leaching, microbial processing, and macroinvertebrate feeding (Tank et al., 2010).

In shaded forest streams with limited autochthonous primary production in the form of instream photosynthesis, CPOM forms the basis of stream food webs (Fisher & Likens, 1972; Tank et al., 2010) and ecologists regard CPOM inputs as a terrestrial subsidy to the stream ecosystem (Fisher and Likens, 1972). The fluvial transport of CPOM is one of the forms in which carbon is exported annually from a forested basin (Piégay et al., 1999; Battin et al., 2008; Worrall et al., 2014). Accumulations of CPOM can influence the porosity and permeability of the stream bed and thus hyporheic exchange (Harvey & Gooseff, 2015), as well as the porosity and permeability of logjams within the channel and therefore the physical effects of such logjams on channel hydraulics and sediment transport (Livers et al., 2020).

The physical morphology of a stream determines whether CPOM is simply routed through a stream reach or retained by either the channel boundary or in-channel structure (Gorecki et al., 2006; Small et al., 2008; Livers & Wohl, 2016; Pfeiffer & Wohl, 2018). Whether moving in contact with the stream bed or in suspension, CPOM is typically of lower density than

mineral sediment and is therefore more readily transported. Physical complexity, such as large wood (LW, defined here as downed, instream wood ≥ 1 m in length and ≥ 10 cm in diameter) or other boundary irregularities that create sites of lower velocity and shear stress, promotes storage and retention zones that can extend the residence time of CPOM during downstream transport (Bilby & Likens, 1980; Raikow et al., 1995; Lautz & Fanelli, 2008; Beckman & Wohl, 2014; Jochner et al., 2015; Livers & Wohl, 2016; Livers et al., 2018). Streams with lower wood loads (volume of wood per area) are significantly less retentive of CPOM and less physically complex than streams with abundant wood loads (Beckman & Wohl, 2014; Livers & Wohl, 2016; Livers et al., 2018). Even transient CPOM storage on timescales of hours provides opportunities for microorganisms to develop as attached biofilms or suspended aggregates and to metabolize carbon and other nutrients for energy and growth (Battin et al., 2008). Headwater streams are particularly important in CPOM dynamics because of their proximity to upland sources of CPOM and their limited transport capacity for large wood (Battin et al., 2008; Beckman & Wohl, 2014; Pfeiffer & Wohl, 2018).

Ecological investigations of CPOM dynamics have focused on its contribution to stream energy budgets (e.g., Fisher and Likens, 1972) and on the specific characteristics of CPOM inputs (e.g., Molinero and Pozo, 2004); the mass balance between inputs and outputs (e.g., Cummins et al., 1983); rates and processes of CPOM decomposition (e.g., Whiles and Wallace, 1997); and retention mechanisms and residence time (e.g., Aumen et al., 1983). Although previous work has demonstrated that transport of CPOM strongly reflects discharge (e.g., Webster et al., 1994; Wallace et al., 1995; Goebel et al., 2003) and that the majority of annual CPOM export can occur during floods (e.g., Newbold et al., 1997), there has been little direct

sampling of CPOM transport across a seasonal hydrograph and no examination of whether CPOM is transported primarily in suspension or as bedload.

More recently, geomorphologists have started to examine CPOM transport, documenting rapid changes in CPOM bedload transport rates with increasing flow in small streams (e.g., Turowski et al., 2013; Bunte et al., 2016, Iroumé et al., 2020) and substantial transport during periods of intense precipitation and storms over large catchments (e.g., Hilton et al., 2008; Ramos Scharrón et al., 2012). In snowmelt runoff regimes, nearly all of the annual CPOM export (97%) may be concentrated during the seasonal high flow (Bunte et al., 2016). Previous studies have employed bedload traps to sample CPOM (e.g., Bunte et al., 2016; Iroumé et al., 2020) and the question of how to extrapolate from bedload samples to whole-stream transport of CPOM requires untested assumptions (Bunte et al., 2016) because the relative proportions of CPOM carried as bedload and suspended load remain unknown. Bunte et al. (2016) documented seasonal hysteresis in bedload CPOM transport in a snowmelt stream, with generally clockwise relations and higher CPOM transport on the rising limb of the snowmelt hydrograph, but little is known about how CPOM transport varies in relation to shorter (diurnal) as well as longer (seasonal peak flow) variations in discharge.

Previous work on suspended and bedload sediment transport indicates that the peak of sediment transport is commonly temporally offset from the peak of discharge – a phenomenon described as hysteresis. Sediment moving in suspension typically follows three distinct forms of hysteresis; (1) a clockwise loop where the peak sediment concentration precedes the peak discharge because available sediment is depleted before runoff peaks, (2) a counter-clockwise loop in which peak sediment concentration lags peak discharge, and (3) a figure-of-eight loop in which peak sediment concentration precedes peak discharge, but the shape of sediment output is

skewed relative to the flood peak (Williams, 1989). The details of hysteresis reflect sediment delivery processes (e.g., Smith and Dragovich, 2009) and influence scaling of transport with discharge and extrapolations and prediction of total suspended sediment transport (Aich et al., 2014). We assume that CPOM moving in suspension could display hysteresis, although the greater buoyancy of CPOM could create different patterns of hysteresis than those observed for sediment. As for suspended sediment, greater understanding of the temporal scales of hysteresis would improve estimates of total CPOM transport that are now being published and compared across sites (e.g., Bunte et al., 2016; Iroumé et al., 2020).

Here, we address some of the gaps in understanding CPOM transport in relatively small channels. Working in a snowmelt-dominated stream in the Southern Rockies of Colorado, USA, we measured CPOM moving in suspension and in contact with the stream bed at 4-hour intervals during the rising and recessional limbs of the snowmelt hydrograph. We measured CPOM transport at three sites: (1) in the backwater pool upstream from a channel-spanning logjam; (2) immediately downstream from the logjam; and (3) in a riffle about 10 bankfull-channel-widths downstream from any channel-spanning logjams. Our sampling strategy was designed to test four hypotheses.

H1: CPOM mass in suspension will be greater than CPOM mass moving as bedload.

We expect this relationship because of the generally lower density of CPOM relative to mineral sediment. If CPOM is moving predominantly in suspension and CPOM retention is important for biological uptake of nutrients, then river management and restoration intended to facilitate CPOM retention can focus on strategies that affect the movement of suspended material.

H2: Seasonal CPOM transport is greater during the rising limb of the annual snowmelt hydrograph than during equivalent discharge on the recessional limb.

We expect CPOM stored in the channel and overbank areas to be mobilized as stage rises and snowmelt runoff enters the channel, and thus we expect the supply of CPOM to be depleted as stage declines after peak flow.

H3: Daily CPOM transport will be greater during the daily rising limb of channel flows. During the snowmelt hydrograph, flow reaches a peak around midnight during each 24-hour cycle. We expect CPOM transport to precede or coincide with this daily discharge peak for similar reasons as seasonal transport (H2).

H4: CPOM transport will be lower in the backwater area of the channel-spanning logjam than at the sites downstream of the logjam.

The greater flow depth and lower downstream velocities in the backwater pool will limit the quantity and size of CPOM that can enter suspension and be transported. These characteristics of deeper backwater flow also increase the likelihood of CPOM storage instead of transport.

Previous studies have demonstrated greater storage of CPOM in logjam backwaters during baseflow but understanding the effect of a logjam on CPOM transport during peak flow could have management implications for anthropogenically altered streams with limited CPOM inputs.

We expect that the hypothesized patterns of CPOM transport in snowmelt systems have ecological and geomorphic implications. Ecologists have shown that abscission (leaf fall) is the time of greatest CPOM abundance in river systems draining deciduous forests (Weigelhofer and Waringer, 1994) and, although conifers do not have the same seasonal behavior, our qualitative observations of streams in the study area suggest that CPOM is heavily exported in suspension during the spring snowmelt rising limb and peak. Suspended transport may equate to greater travel distances and therefore headwater subsidies of CPOM to downstream portions of the river network. Understanding the relative locations and timing of CPOM transport at the reach scale is

critical to river management designed to enhance CPOM retention and processing (Lepori et al., 2005). If the majority of CPOM is moving in suspension, we can infer that river restoration designed to enhance CPOM retention should incorporate retention structures (i.e., logjams) that span the channel at high flows.

2.0 Field Area

Little Beaver Creek (LBC) is a third-order tributary of the South Fork of the Cache la Poudre River in the Colorado Front Range, USA (Figure 3.1). The catchment is underlain by Precambrian-age Silver Plume Granite (Cole et al., 2010), with a narrow valley flood and a floodplain that does not exceed 10 times the average bankfull channel width of 6 m. The area has a warm, semiarid climate with mean annual precipitation of 55 cm and mean annual temperature of 8.3°C (Barry, 1973). The creek drains 40 km² and flow is dominated by snowmelt, which produces an annual hydrograph with a sustained May–June peak. Channels in this elevation range of the study area have an annual snowmelt peak that seldom exceeds 1.1 m³/s/km², as well as infrequent (recurrence interval 10² years) summer floods associated with convective storms, which can create peak flows up to 40 m³/s/km² (Jarrett, 1990). Little Beaver Creek is ungauged but the snowmelt peak averages 1.26 m³/s at the study area based on long-term regional regression equations from US Geological Survey stream gages (streamstats.usgs.gov) and base flow is ~0.15 m³/s (Ader et al., 2021). The channel has a pool-riffle to low step-pool morphology, with steps forced by channel-spanning logjams. Channel gradient averages 0.02 m/m and D₅₀ of channel substrate averages 45–60 mm, except in logjam backwaters where sand and fine gravel are present.

Riparian vegetation in the study area is old-growth montane forest dominated by ponderosa pine (*Pinus ponderosa*), Engelmann spruce (*Picea engelmannii*), Douglas-fir

(*Pseudotsuga menziesii*), aspen (*Populus tremuloides*), and willows (*Salix* spp.). Stands of old-growth montane forest are small and patchy across the Front Range of Colorado but serve as valuable reference sites for understanding instream wood dynamics given their lack of flow alterations (Jackson & Wohl, 2015). Old-growth riparian forests have greater basal areas (density of forest and size of trees), which corresponds to greater instream wood loads (Richmond & Fausch, 1995; Warren et al., 2007) and more closely spaced channel-spanning logjams (Beckman & Wohl, 2014). Large wood is recruited to the creek primarily from bank erosion and individual tree fall and wood is abundant throughout the channel. The channel is densely shaded and both upland and riparian sources of CPOM are abundant. Coniferous vegetation produces litter fall throughout the year, whereas the riparian aspen and willows produce the greatest litter fall during leaf abscission in autumn.

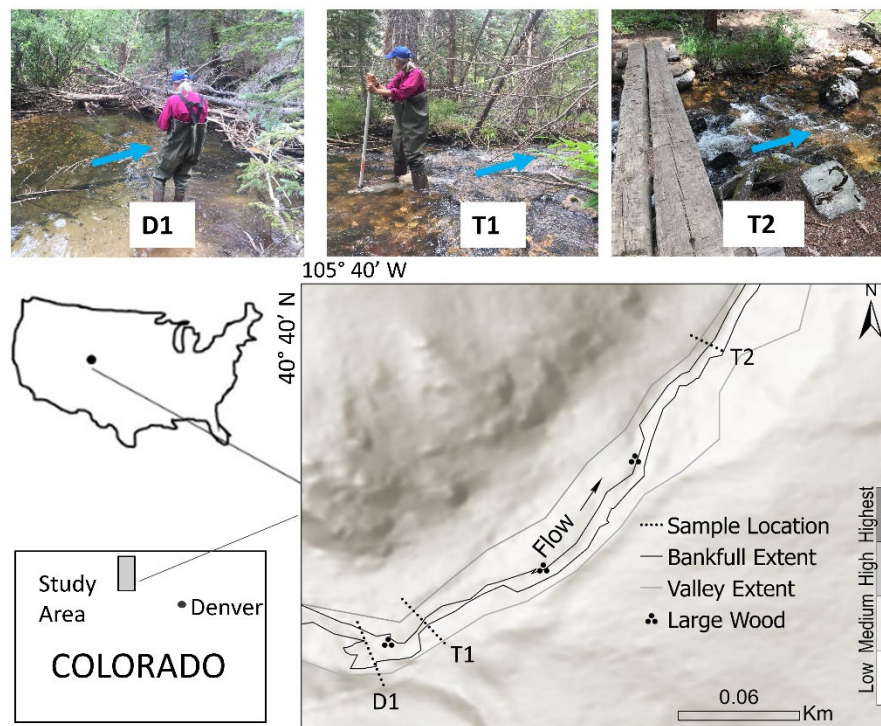


Figure 3.1. Little Beaver Creek sample locations: D1) backwater pool upstream from a channel-spanning logjam; T1) transport reach immediately downstream from the logjam; T2) transport reach in a riffle about 10 bankfull-channel-widths downstream from any channel-spanning

logjams. Sample locations are depicted by a black dotted line. Channel-spanning logjams are mapped as large wood in the figure and represented by the 3-dot symbology. Inset maps show the location of the study area within the contiguous United States and the State of Colorado.

3.0 Methods

3.1 Sample collection and processing

Three sampling locations were selected along the creek: a depositional reach in the backwater area of a channel-spanning logjam (D1), a transport reach below the logjam (T1), and a transport reach without a depositional feature downstream of the other two sites (T2; Figure 1). CPOM was collected in the thalweg at each location at three levels in the water column: surface, midpoint (60% below the water surface and approximate location of average flow velocity), and on the channel bed. Midpoint measurements were not taken at base flow due to a lack of sufficient flow depth to allow three distinct sampling points. CPOM at the surface and midpoint was sampled using seines constructed of polyester 0.25 mm mesh fabric with an expanded entrance (orifice diameter 13 cm, total area 120.4 cm²). The expanded orifice was effective in increasing hydraulic efficiency of the sampler, thereby preventing backflow that could otherwise result in the loss of suspended CPOM. CPOM was sampled from the bed of the stream with a Helley-Smith bedload sampler (Figure 3.2; orifice dimensions 8 cm x 8 cm, total area 58 cm², mesh size 0.25 mm) (Edwards & Glysson, 1988; Merritt & Wohl, 2006). At each site, all samples were collected simultaneously by affixing the surface and midpoint samplers to the rigid handle of the bedload sampler and allowing water to flow through the traps for 15 minutes.

Thalweg flow depth varied from ~40 cm at base flow to 110 cm at the highest stage measured during the snowmelt hydrograph. This suggests that during base flow the bedload and surface samplers together accounted for ~50% of the total flow depth, whereas at the highest stage the three samplers together accounted for ~30% of the total flow depth. However, the

surface sampler was not always completely submerged at base flow (it had a tendency to float with the upper portion above the water surface). Consequently, we likely sampled 30-40% of the total flow depth during all flows.



Figure 3.2. Helley-Smith bedload sampler and surface seine with expanded orifice used for CPOM sampling at surface, midpoint, and bed depths. Three nets were used at high flows at surface, midpoint, and bed depths and only surface and bed nets were used at low flows. This photo, taken at base flow, shows surface and bed nets.

Sampling events occurred in sequence with the snowmelt hydrograph from May through August 2020. Four samples were taken on the snowmelt hydrograph rising limb (5/22-23, 5/28-29, 6/1-2, 6/9-10), one during the receding limb (6/16-17), and two at base flow (7/22-23, 7/23-24). Because we do not know exactly when the seasonal peak flow occurred, the 6/9-10 samples may have coincided with peak flow. Samples were collected at roughly 4-hour intervals for a duration of 24 hours. Samples in the 12 am-4 am range were not collected during peak runoff due to hazardous conditions and were not collected at the second base flow sampling event due to a lack of change in stage. Vertical velocity measurements were taken at the bed, 0.6 depth, and

surface for each sampling location once per sampling event. Stage below the logjam was also recorded once per sampling event and was used as a proxy for discharge in this ungauged stream.

All surface, midpoint, and bedload samples were air-dried for a minimum of 96 hours at 21°C and then weighed. A qualitative assessment of sample compositions was recorded, with attention to the primary material in each sample (i.e., sand and gravel, leaf matter, pine needles). Samples that included sand and gravel were processed using an ash-free dry mass method (AFDM), which indicated the loss on ignition (LOI), or percent of weighted carbon that was burned out of the greater sediment sample. Samples undergoing AFDM were placed in crucibles and heated for one hour prior to testing in order to remove any moisture before being weighed empty. The crucible was then filled with a sample of sediment and weighed. The sediment-filled evaporating dishes were placed in a muffling furnace at 450°C for eight hours. The dried samples were weighed to determine LOI. A 10% subset of surface and midpoint samples were randomly selected for quality control to compare pre-and post-LOI weights. This control process confirmed that running LOI was only necessary for samples that had a significant amount of mineral sediment in them (visual estimate). All samples, regardless of LOI analysis or not, were weighed on a research balance with precision to the 0.001 g.

3.2 Data analysis

As with many studies that produce natural data, this dataset is non-normally distributed. The statistical data analysis thus requires alternative approaches that do not assume data normality. The median value, as opposed to the mean, is a better measure of center and is used in this analysis for comparisons. We used RStudio to perform the statistical analyses (R Core Team, 2020). To investigate H1 and H4, we used the Kruskal-Wallis Rank Sum Test and Dunn's Test (with no multiple testing adjustment) (`dunn.test` package; Dinno, 2017) to compare median

CPOM mass values. An alpha of 0.05 was used in all statistical analyses. No statistical tests were required to address H2 and H3.

4.0 Results

Seven sample sets, each 24 hours in duration, were collected from 22 May to 24 July 2020. With the missed mid-point samples at very shallow flows, a total of 298 samples were collected from the water column at the three channel locations along LBC (184 samples at the surface and midpoint, 114 at the bed). Table 1 in Appendix VI contains the raw data used for analyses and explains the distribution of samples through time.

Visual characterization of CPOM sample compositions during the seasonal hydrograph indicates that CPOM samples were primarily composed of leaf fragments and some conifer needles during the rising limb. At peak stage, more conifer needles were present as well as larger leaves in addition to leaf fragments. There was an overall increase in CPOM material size as well as the presence of aquatic macroinvertebrates moving downstream at peak stage. During the receding limb, some larger material remained but CPOM was primarily leaf fragments, conifer needles, and wood fragments, all of which were smaller and of a darker brown color compared to CPOM collected during peak stage. At base flow, CPOM samples primarily consisted of algal and leaf fragments.

Individual samples, each representing one 15-minute sampling interval for a specific date, time, and sampling depth, were retained for analyses. Samples were grouped differently for specific analyses, as described in individual figure captions below.

4.1 CPOM Transport (H1)

Boxplots of CPOM mass at the three depths of flow were used to compare where in the water column CPOM is transported (Figure 3.3). Comparison of the CPOM masses by depth via Kruskal-Wallis (p -value < 0.0001) and Dunn's tests (p -value for all three pairwise comparisons ≤ 0.0001) show that the masses at each depth of flow are significantly different from each other (indicated by the letters), with:

$$MASS_{Bed} < MASS_{Surface} < MASS_{60\% \text{ from Surface}}$$

Specifically, CPOM mass transported in suspension is significantly greater than mass transported as bedload. The results thus support the first hypothesis.

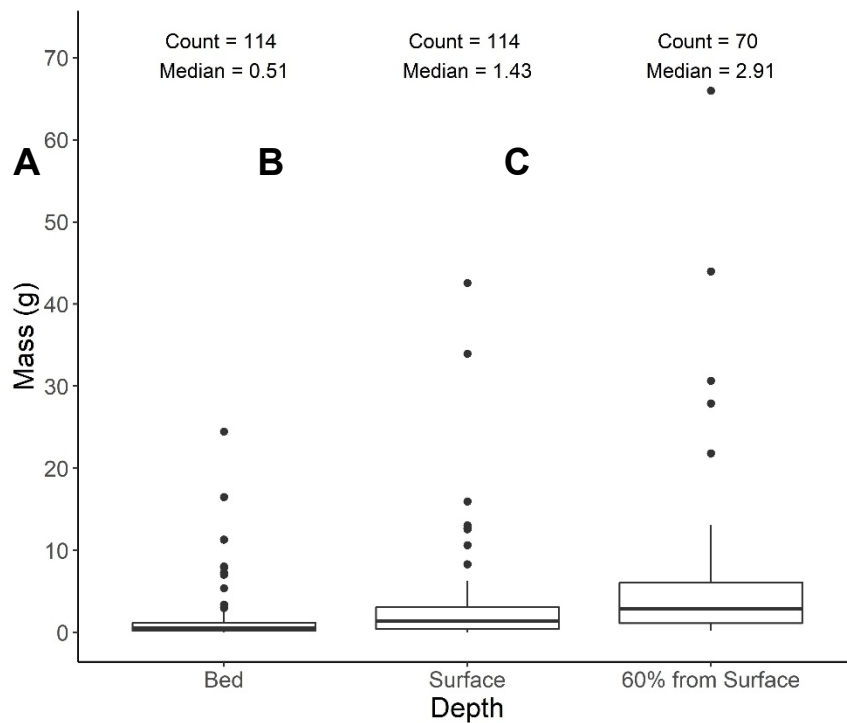


Figure 3.3. Boxplot of CPOM mass by sample depth showing a significant difference in the relationship between CPOM mass at each depth. Each population represents all samples taken at a particular depth for all sampling dates and times. Letters indicate statistically significant differences between median values of populations. The bold line represents the median. The box

top and bottom represent 75th and 25th percentiles, respectively. The ends of the vertical lines represent 1.5 times the interquartile range. The circles represent outliers.

4.2 Seasonal Hydrograph (H2)

Figure 3.4 illustrates seasonal CPOM trends. There is a more pronounced seasonal curve in the largest values of CPOM transport than in the average stage. Figure 3.5 depicts a clockwise hysteresis loop of CPOM mass over the seasonal hydrograph, where the peak CPOM precedes the peak stage (Williams, 1989). The most pronounced hysteresis curve occurs at T2, the transport reach without a depositional feature immediately upstream. The results thus support H2, indicating substantially greater CPOM transport during the final portion of the rising limb than at nearly equivalent stage on the falling limb of snowmelt hydrograph.

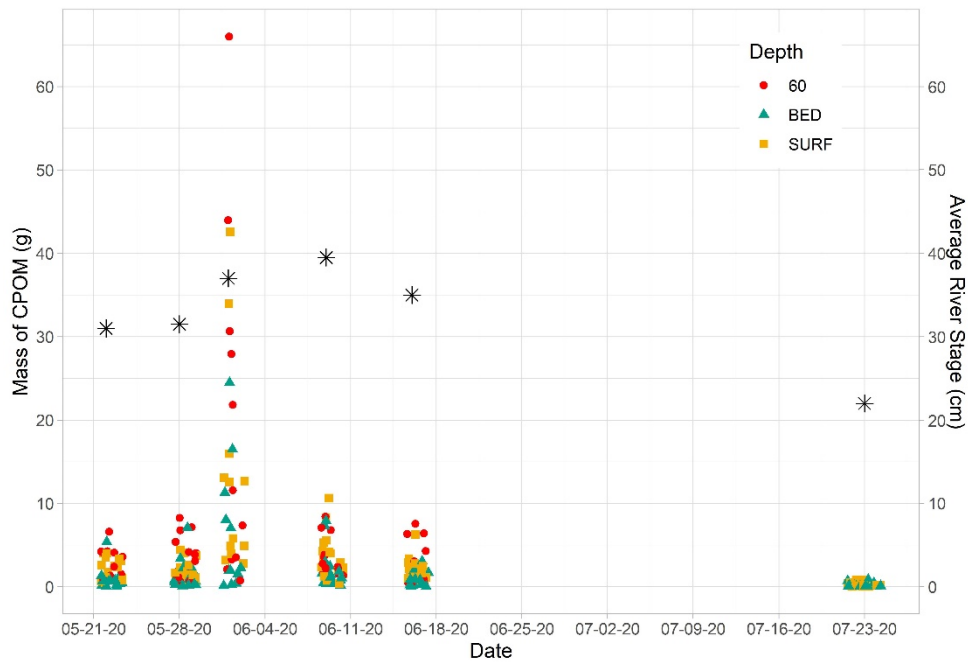


Figure 3.4. Mass of CPOM and corresponding average stage during sampling event. Black stars indicate average stage for each sampling period. Each data point in this plot represents an individual sample with respect to sampling depth, time interval, and date.

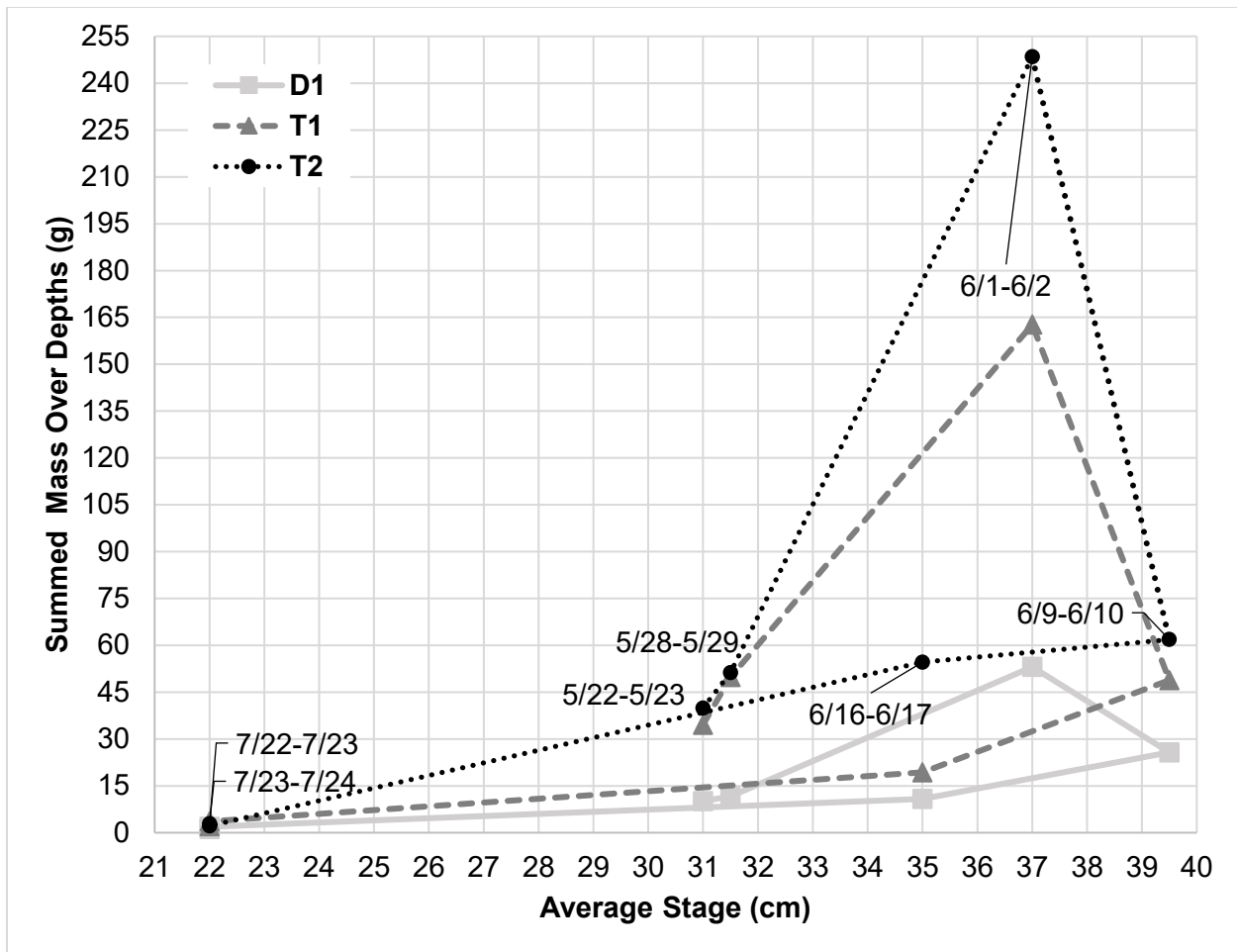


Figure 3.5. Hysteresis plot of mass corresponding with stage. Each data point represents the sum of all samples at a particular location during the 24-hour sampling period. The curves for each reach suggest clockwise hysteresis loops.

4.3 H3: Diurnal Cycle

There is no substantial change in CPOM mass in transport during the 24-hour hydrograph except during the highest stage each day. The difference is greatest at the transport reaches (Figure 3.6) but is also present at the depositional reach (Figure 3.7). The highest CPOM mass occurs before the highest stage during the diurnal cycle: CPOM mass peaks in the 5pm-11pm time window, while the peak stage was observed during the 11pm-3am time window, when CPOM masses were lower.

The diurnal stage changes were unexpectedly small during each 24-hour sample period. The downstream sample site has the most confined cross-section, with a steep bedrock bank along channel right. The greatest stage change during a 24-hour period here was 3 cm during the 6/1-2 and 6/9-10 sample periods. Over the course of the snowmelt hydrograph, stage changed by 18 cm at this site. The 6/1-2 time is the only sampling event with a pronounced diurnal hysteresis pattern (Figure 3.6 and 3.7). Diurnal trends during this sampling date match a clockwise hysteresis loop (Williams, 1989) where the peak CPOM precedes the peak stage. These results partly support the third hypothesis, indicating a diurnal hysteresis in CPOM transport only during the portion of the seasonal hydrograph with the greatest CPOM transport.

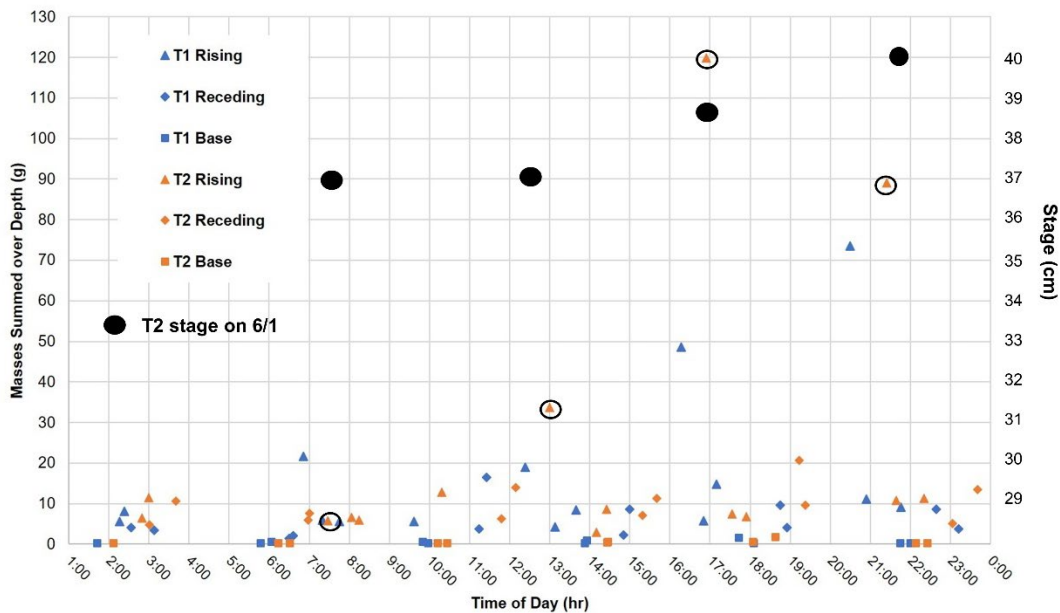


Figure 3.6. Sums of CPOM in transport reaches (T1 and T2) along the diurnal cycle. Each data point represents the sum of all sample depths taken at a particular sampling location, date, and time. Black ovals represent stage during the June 1-2 sampling period; circled CPOM masses collected during the June 1-2 sampling period.

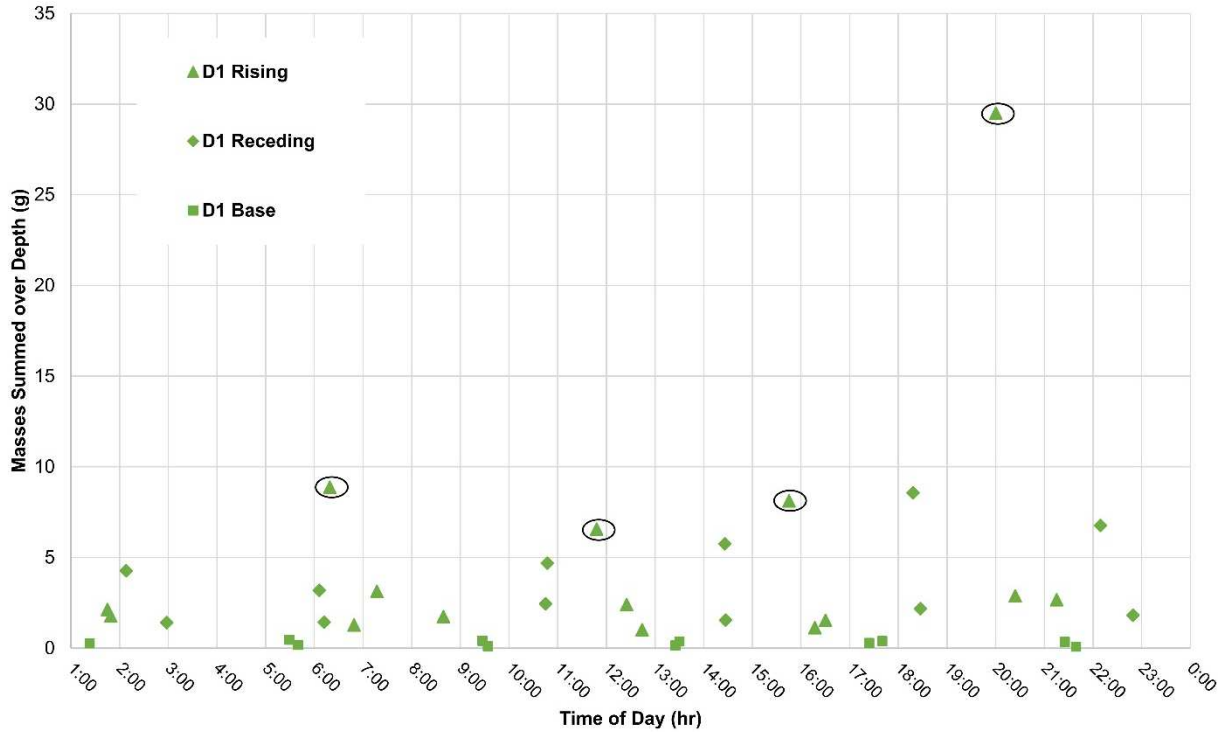


Figure 3.7. Sums of CPOM in the depositional reach along the diurnal cycle. Each data point represents the sum of all sample depths taken at a particular sampling location, date, and time. Circled data points are from the June 1-2 sampling interval.

4.4 H4: Local Storage Features

To address H4, we compared CPOM mass at the three distinct sampling locations (Figure 3.8). Kruskal-Wallis ($p\text{-value} < 1 \times 10^{-8}$) and Dunn's tests ($p\text{-value}_{(T2-D1)} = p\text{-value}_{(T1-D1)} = 0$, $p\text{-value}_{(T2-T1)} = 0.2908$) show that there is a statistically significant difference in CPOM masses between deposition and transport reaches, but not a statistically significant difference between the transport reach with and without a local storage feature (as indicated by the letters). The results thus support the fourth hypothesis in showing significantly different rates of CPOM transport in the logjam backwater than in the transport sites.

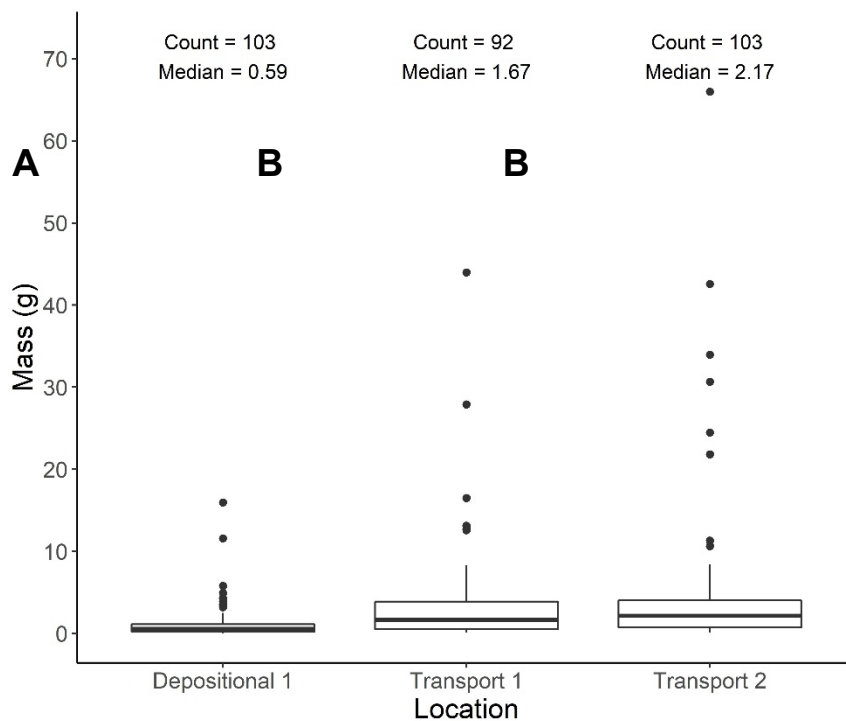


Figure 3.8. Boxplot of CPOM mass by location. Each population represents all samples taken at a site for all sampling dates and times. Letters A and B indicate statistical differences and similarities between the three sample sites. The bold line represents the median. The box top and bottom represent 75th and 25th percentiles, respectively. The ends of the vertical lines represent 1.5 times the interquartile range. The circles represent outliers.

5.0 Discussion

Because we sampled only at the channel thalweg, we did not attempt to calculate total CPOM flux in the creek. Suspended and bedload transport of mineral sediment commonly vary across a channel cross section. Sampling of CPOM using bedload traps also indicates cross-channel variations in transport, although these may be smaller than those commonly present for mineral sediment transport, with the majority of CPOM bedload transport (64-67%) occurring in and near the thalweg (K. Bunte, 18 Feb. 2021, pers. comm.). We chose to sample in the thalweg as likely having the highest concentrations of suspended and bedload CPOM transport.

The mass of CPOM in suspension (at depths of 0.6 and at the surface) is greater than the mass of CPOM moving as bedload. This relationship makes sense as CPOM generally has a low density and is therefore easily entrained by flow at a wide range of velocities. The greater mass of CPOM at 0.6 depth compared to the surface may reflect a decrease in CPOM concentration with distance from the bed, analogous to that commonly observed in suspended sediment (Kuhnle, 2013). The difference in suspended CPOM mass with depth may also reflect experimental design. The seines used to collect CPOM in suspension oscillated in the swift, turbulent flow of the transport reaches, sometimes even changing their relative vertical positions during a 15-minute sampling interval. Additionally, the flow in D1 was often too slow to maintain lift of the seines, causing them to drift lower in the water column than expected in the experimental design. These movements of the sample bags creates uncertainty in the relative masses of CPOM moving at 0.6 depths versus the surface. Therefore, our results support H1 that more CPOM is moving in suspension, but more data may need to be collected using a different sampler design to determine exactly where in the water column most suspended CPOM is being transported. Given the lack of diurnal fluctuations in CPOM transport during most sampling events, future studies might more effectively focus on additional sampling dates and/or sites rather than repeated sampling during 24-hour periods.

The observed seasonal hysteresis patterns suggest that CPOM stored in the channel and overbank areas is more likely to be mobilized as stage rises and snowmelt runoff enters the channel, whereas the supply of CPOM is depleted as the snowmelt hydrograph continues. A similar hysteresis in CPOM transport does not occur during diurnal fluctuations in discharge except during the sampling date of greatest CPOM movement. The extent to which these patterns

might represent those in rainfall-dominated streams and watersheds with more strongly seasonal abscission remains to be determined.

Our results show that the channel-spanning logjam has a significant effect on the mass of CPOM in transport above and below the jam. The statistical difference in masses indicates that the reach above the logjam is storing CPOM while the reaches below are transporting it. The lack of statistical significance between the two downstream transport reaches suggests that there is no local effect, or CPOM “shadow”, from the channel-spanning logjam. We infer that logjams act as storage features for CPOM and, despite the greater presence of stored CPOM in pool backwaters demonstrated in other studies (e.g., Beckman and Wohl, 2014; Livers et al., 2018), the lower velocities in the backwater limit CPOM suspension and transport.

6.0 Conclusions

Sampling CPOM at two to three depths of the water column during regular intervals throughout 24 hours at three locations and different portions of the annual snowmelt hydrograph reveals significant variations in transport of coarse particulate organic matter in relation to channel location (depositional vs transport reaches), depth within the water column, and portion of the seasonal hydrograph. The greatest mass of CPOM moves in suspension in transport-dominated locations of the channel and during the final portion of the rising limb of the snowmelt hydrograph. Diurnal fluctuations in CPOM transport are negligible except during the period of greatest CPOM transport.

Because a substantial portion of CPOM is transported in suspension, flow obstructions that have a vertical dimension similar to peak flow depth are likely to be more effective in trapping and retaining CPOM than are obstructions with a smaller protrusion height. Similarly, areas of flow separation with substantially reduced flow velocity are more likely to retain CPOM

in suspension. Current installations of large wood and engineered logjams, for example, typically do not include channel-spanning logjams (Roni et al., 2015; Grabowski et al., 2019), which greatly increase retention of CPOM if the logjam has limited porosity and permeability (Livers et al., 2018). Even relatively brief retention of CPOM over periods of hours to days can increase microbial processing of CPOM and render nutrients within the CPOM more available to organisms in the stream (Battin et al., 2008).

Considering that CPOM is a primary energy source in the food webs of shaded forest streams, management designed to foster the sustainability of stream ecosystems can benefit from maintaining or creating features that enhance CPOM retention. Understanding patterns of diurnal and seasonal hysteresis of CPOM transport can improve estimates of total CPOM export from watersheds (e.g., Bunte et al., 2016; Iroumé et al., 2020) that are based on extrapolations from measurements; improve associated estimates of carbon storage and exports from rivers (Battin et al., 2008; Turowski et al., 2016); and inform management designed to enhance CPOM retention in anthropogenically modified streams with limited CPOM inputs and simplified channel morphologies that limit CPOM retention (Peipoch et al., 2015; Livers et al., 2018). As river scientists increasingly integrate their research and understanding of rivers across disciplines (e.g., Polvi et al., 2011; Castro and Thorne, 2019; Johnson et al., 2020), enhanced mechanistic understanding of CPOM transport, paired with biogeochemical and ecological understanding of the role of CPOM in nutrient dynamics, trophic cascades, and carbon dynamics, can underpin management of rivers as ecosystems.

References

- Ader, E., Wohl, E., McFadden, S., & Singha, K. (2021). Logjams as a driver of transient storage in a mountain stream. *Earth Surface Processes and Landforms*. Doi.org/10.1002/esp.5057.
- Aich, V., Zimmermann, A., & Elsenbeer, H. (2014). Quantification and interpretation of suspended-sediment discharge hysteresis patterns: How much data do we need? *Catena*, *122*, 120-129.
- Aumen, N. G., Bottomley, P. J., Ward, G. M., & Gregory, S. V. (1983). Microbial decomposition of wood in streams: Distribution of microflora and factors affecting [¹⁴C] lignocellulose mineralization. *Applied and Environmental Microbiology*, *46*(6), 1409-1416.
- Barry, R.G. (1973). A climatological transect on the east slope of the Front Range, Colorado. *Arctic, Antarctic, and Alpine Research*, *5*, 89-110.
- Battin, T. J., Kaplan, L. A., Findlay, S., Hopkinson, C. S., Marti, E., Packman, A. I., Newbold, J. D., & Sabater, F. (2008). Biophysical controls on organic carbon fluxes in fluvial networks. *Nature Geoscience*, *1*(2), 95–100. <https://doi.org/10.1038/ngeo101>
- Beckman, N. D., & Wohl, E. (2014). Carbon storage in mountainous headwater streams: The role of old-growth forest and logjams. *Water Resources Research*, *50*(3), 2376–2393. <https://doi.org/10.1002/2013WR014167>
- Bilby, R. E., & Likens, G. E. (1980). Importance of Organic Debris Dams in the Structure and Function of Stream Ecosystems. *Ecology*, *61*(5), 1107–1113. <https://doi.org/10.2307/1936830>
- Bunte, K., Swingle, K. W., Turowski, J. M., Abt, S. R., & Cenderelli, D. A. (2016). Measurements of coarse particulate organic matter transport in steep mountain streams and estimates of decadal CPOM exports. *Journal of Hydrology*, *539*, 162–176. <https://doi.org/10.1016/j.jhydrol.2016.05.022>
- Castro, J.M., & Thorne, C.R. (2019). The stream evolution triangle: integrating geology, hydrology, and biology. *River Research and Applications*, *35*, 315-326.
- Cole, J.C., Trexler, J.H., Cashman, P.H., Miller, I.M., Shroba, R.R., Cosca, M.A., & Workman, J.B. (2010). Beyond Colorado's Front Range – a new look at Laramide basin subsidence, sedimentation, and deformation in north-central Colorado. *Geological Society of America Field Guide*, *18*, 55-76.
- Cummins, K.W., Sedell, J.R., Swanson, F.J., Minshall, G.W., Fisher, S.G., Cushing, C.E., Peterson, R.C., & Vannote, R.L. (1983). Organic matter budgets for stream ecosystems: problems in their evaluation. In, *Stream Ecology: Application and Testing of General Ecological Theory*, J.R. Barnes & G.W. Minshall, eds., Springer, pp. 299-353.
- Dinno, A. (2017). dunn.test: Dunn's test of multiple comparisons using rank sums. R package version 1.3.5. <https://CRAN.R-project.org/package=dunn.test>
- Edwards, T. K., & Glysson, G. D. (1988). Edwards, T. K., and G. D. Glysson. "Field methods for measurement of fluvial sediment, Department of the Interior. *US Geological Survey, Publications*, Washington, DC

- Fisher, S.G., & Likens, G.E. (1972). Stream ecosystem: organic energy budget. *BioScience*, 22, 33-35.
- Goebel, P. C., Pregitzer, K. S., & Palik, B. J. (2003). Geomorphic influences on large wood dam loadings, particulate organic matter and dissolved organic carbon in an old-growth northern hardwood watershed. *Journal of Freshwater Ecology*, 18(3), 479–490. <https://doi.org/10.1080/02705060.2003.9663984>
- Gorecki, V. I., Fryirs, K. A., & Brierley, G. J. (2006). The relationship between geomorphic river structure and coarse particulate organic matter (CPOM) storage along the Kangaroo River, New South Wales, Australia. *Australian Geographer*, 37(3), 285–311. <https://doi.org/10.1080/00049180600954757>
- Grabowski, R.C., Gurnell, A.M., Burgess-Gamble, L., England, J., Holland, D., Klaar, M.D., Uttley, C., & Wharton, G. (2019). The current state of the use of large wood in river restoration and management. *Water and Environment Journal*, 33, 366-377.
- Harvey, J., & Gooseff, M. (2015). River corridor science: Hydrologic exchange and ecological consequences from bedforms to basins. In *Water Resources Research* (Vol. 51, Issue 9, pp. 6893–6922). Blackwell Publishing Ltd. <https://doi.org/10.1002/2015WR017617>
- Hilton, R. G., Galy, A., & Hovius, N. (2008). Riverine particulate organic carbon from an active mountain belt: Importance of landslides. *Global Biogeochemical Cycles*, 22(1). <https://doi.org/10.1029/2006GB002905>
- Iroume, A., Ruiz-Villanueva, V., & Salas-Coliboro, S. (2020). Fluvial transport of coarse particulate organic matter in a coastal mountain stream of a rainy-temperate evergreen broadleaf forest in southern Chile. *Earth Surface Processes and Landforms*, 45, 3216-3230.
- Jackson, K. J., & Wohl, E. (2015). Instream wood loads in montane forest streams of the colorado front range, USA. *Geomorphology*, 234, 161–170. <https://doi.org/10.1016/j.geomorph.2015.01.022>
- Jarrett, R. D. (1990). Paleohydrologic techniques used to define the spatial occurrence of floods. *Geomorphology*, 3(2), 181–195. [https://doi.org/10.1016/0169-555X\(90\)90044-Q](https://doi.org/10.1016/0169-555X(90)90044-Q)
- Jochner, M., Turowski, J. M., Badoux, A., Stoffel, M., & Rickli, C. (2015). The role of log jams and exceptional flood events in mobilizing coarse particulate organic matter in a steep headwater stream. *Earth Surface Dynamics*, 3(3), 311–320. <https://doi.org/10.5194/esurf-3-311-2015>
- Johnson, M.F., Thorne, C.R., Castro, J.M., Kondolf, G.M., Mazzacano, C.S., Rood, S.B., & Westbrook, C. (2020). Biomic river restoration: a new focus for river management. *River Research and Applications*, 36, 3-12.
- Kuhnle, R.A. (2013). Suspended load. In, *Treatise on Geomorphology*, vol. 9, Fluvial Geomorphology, E. Wohl, ed., Academic Press, San Diego, CA, pp. 124-136.
- Lautz, L. K., & Fanelli, R. M. (2008). Seasonal biogeochemical hotspots in the streambed around restoration structures. *Biogeochemistry*, 91(1), 85–104. <https://doi.org/10.1007/s10533-008-9235-2>

- Lepori, F., Palm, D., & Malmqvist, B. (2005). Effects of stream restoration on ecosystem functioning: detritus retentiveness and decomposition. *Journal of Applied Ecology*, *42*, 228-238.
- Livers, B., Lininger, K. B., Kramer, N., & Sendrowski, A. (2020). Porosity problems: Comparing and reviewing methods for estimating porosity and volume of wood jams in the field. *Earth Surface Processes and Landforms*, esp.4969. <https://doi.org/10.1002/esp.4969>
- Livers, B., & Wohl, E. (2016). Sources and interpretation of channel complexity in forested subalpine streams of the Southern Rocky Mountains. *Water Resources Research*, *52*(5), 3910–3929. <https://doi.org/10.1002/2015WR018306>
- Livers, B., Wohl, E., Jackson, K. J., & Sutfin, N. A. (2018). Historical land use as a driver of alternative states for stream form and function in forested mountain watersheds of the Southern Rocky Mountains. *Earth Surface Processes and Landforms*, *43*(3), 669–684. <https://doi.org/10.1002/esp.4275>
- Merritt, D. M., & Wohl, E. E. (2006). Plant dispersal along rivers fragmented by dams. *River Research and Applications*, *22*(1), 1–26. <https://doi.org/10.1002/rra.890>
- Moliner, J., & Pozo, J. (2004). Impact of a eucalyptus (*Eucalyptus globulus* Labill.) plantation on the nutrient content and dynamics of coarse particulate organic matter (CPOM) in a small stream. *Hydrobiologia*, *528*, 143-165.
- Newbold, J. D., Bott, T. L., Kaplan, L. A., Sweeney, B. W., & Vannote, R. L. (1997). Organic matter dynamics in White Clay Creek, Pennsylvania, USA. *Journal of the North American Benthological Society*, *1*(16), 46–50.
- Peipoch, M., Brauns, M., Hauer, F.R., Weitere, M., & Valett, H.M. (2015). Ecological simplification: human influences on riverscape complexity. *BioScience*, *65*, 1056-1065.
- Pfeiffer, A., & Wohl, E. (2018). Where does wood most effectively enhance storage? Network-scale distribution of sediment and organic matter stored by instream wood. *Geophysical Research Letters*, *45*(1), 194–200. <https://doi.org/10.1002/2017GL076057>
- Polvi, L. E., Wohl, E. E., & Merritt, D. M. (2011). Geomorphic and process domain controls on riparian zones in the Colorado Front Range. *Geomorphology*, *125*(4), 504-516.
- Piégay, H., Thévenet, A., & Citterio, A. (1999). Input, storage and distribution of large woody debris along a mountain river continuum, the Drome River, France. *Catena*, *35*(1), 19–39. [https://doi.org/10.1016/S0341-8162\(98\)00120-9](https://doi.org/10.1016/S0341-8162(98)00120-9)
- R Core Team (2020). R: A language and environment for statistical computing. R Foundation for Statistical Computing, Vienna, Austria. URL <https://www.R-project.org/>.
- Raikow, D. F., Grubbs, S. A., & Cummins, K. W. (1995). Debris dam dynamics and coarse particulate organic matter retention in an Appalachian mountain stream. *Journal of the North American Benthological Society*, *14*(4), 535–546. <https://doi.org/10.2307/1467539>
- Ramos Scharrón, C. E., Castellanos, E. J., & Restrepo, C. (2012). The transfer of modern organic carbon by landslide activity in tropical montane ecosystems. *Journal of Geophysical Research: Biogeosciences*, *117*(3). <https://doi.org/10.1029/2011JG001838>

- Richmond, A. D., & Fausch, K. D. (1995). Characteristics and function of large woody debris in subalpine Rocky Mountain streams in northern Colorado. *Canadian Journal of Fisheries and Aquatic Sciences*, 52(8), 1789–1802. <https://doi.org/10.1139/f95-771>
- Roni, P., Beechie, T., Pess, G., & Hanson, K. (2015). Wood placement in river restoration: fact, fiction, and future direction. *Canadian Journal of Fisheries and Aquatic Sciences*, 72, 466–478.
- Small, M. J., Doyle, M. W., Fuller, R. L., & Manners, R. B. (2008). Hydrologic versus geomorphic limitation on CPOM storage in stream ecosystems. *Freshwater Biology*, 53(8), 1618–1631. <https://doi.org/10.1111/j.1365-2427.2008.01999.x>
- Smith, H.G., & Dragovich, D. (2009). Interpreting sediment delivery processes using suspended sediment-discharge hysteresis patterns from nested upland catchments, south-eastern Australia. *Hydrological Processes*, 23, 2415–2426.
- Tank, J. L., Rosi-Marshall, E. J., Griffiths, N. A., Entrekin, S. A., & Stephen, M. L. (2010). A review of allochthonous organic matter dynamics and metabolism in streams. *Journal of the North American Benthological Society*, 29(1), 118–146. <https://doi.org/10.1899/08-170.1>
- Turowski, J. M., Jochner, M., Zurich, E., Turowski, J. M., Badoux, A., Bunte, K., Rickli, C., Federspiel, N., & Jochner, M. (2013). The mass distribution of coarse particulate organic matter exported from an alpine headwater stream. *Earth Surf. Dynam. Discuss*, 1, 1–29. <https://doi.org/10.5194/esurfd-1-1-2013>
- Turowski, J.M., Hilton, R.G., & Sparkes, R. (2016). Decadal carbon discharge by a mountain stream is dominated by coarse organic matter. *Geology*, 44, 27–30.
- Wallace, J. B., Whiles, M. R., Eggert, S., Cuffney, T. F., Lugthart, G. J., & Chung, K. (1995). Long-term dynamics of coarse particulate organic matter in three Appalachian Mountain streams. In *Am. Benthol. Soc* (Vol. 14, Issue 2).
- Warren, D. R., Bernhardt, E. S., Hall, R. O., & Likens, G. E. (2007). Forest age, wood and nutrient dynamics in headwater streams of the Hubbard Brook Experimental Forest, NH. *Earth Surface Processes and Landforms*, 32(8), 1154–1163. <https://doi.org/10.1002/esp.1548>
- Webster, J. R., Covich, A. P., & Crockett, T. v. (1994). Retention of coarse organic particles in streams in the southern Appalachian Mountains. In *Am. Benthol. Soc* (Vol. 13, Issue 2).
- Weigelhofer, G., & Waringer, J.A. (1994). Allochthonous input of coarse particulate organic matter (CPOM) in a first to fourth order Austrian stream. *Internationale Revue der gesamten Hydrobiologie und Hydrographie*, 79, 461–471.
- Whiles, M.R., & Wallace, J.B. (1997). Leaf litter decomposition and macroinvertebrate communities in headwater streams draining pine and hardwood catchments. *Hydrobiologia*, 353, 107–119.
- Williams, G. P. (1989). Sediment concentration versus water discharge during single hydrologic events in rivers. *Journal of Hydrology*, 111, 89–106.

Worrall, F., Burt, T. P., & Howden, N. J. K. (2014). The fluvial flux of particulate organic matter from the UK: Quantifying in-stream losses and carbon sinks. *Journal of Hydrology*, 519(PA), 611–625. <https://doi.org/10.1016/j.jhydrol.2014.07.051>

SUPPLEMENTARY INFORMATION

CHAPTER 2

Appendix I

Longitudinal Spacing Flume Run Raw Data

Number of Jams	Location	Flow	Skew hr ³	Mean arrival time (hr)	Variance (hr ²)	Mass (lbs)	TSI
1	DS	High	4.98E-05	0.03	6.41E-04	0.14	7.5
1	UPS	High	4.1E-05	0.01	3.69E-04	0.47	13.2
1	DS	High	5.61E-05	0.03	6.41E-04	0.16	5.9
1	UPS	High	1.61E-05	0.05	1.93E-04	0.41	1.5
1	DS	Low	9.44E-05	0.04	1.20E-03	0.20	6.9
1	UPS	Low	3.6E-05	0.02	3.73E-04	0.18	9.5
1	DS	Low	9.14E-07	0.02	8.15E-05	0.12	2.0
1	UPS	Low	5.98E-05	0.03	6.16E-04	0.18	8.2
2	DS	High	1.75E-06	0.02	7.44E-05	0.23	2.7
2	UPS	High	1.45E-06	0.01	4.11E-05	0.48	3.5
2	DS	High	5.95E-05	0.02	6.58E-04	0.21	12.3
2	UPS	High	3.98E-05	0.01	3.67E-04	0.33	24.4
2	DS	High	2E-05	0.02	2.93E-04	0.17	5.2
2	UPS	High	2.44E-05	0.01	2.30E-04	0.37	7.3
2	DS	Low	0.000105	0.05	1.40E-03	0.21	7.0
2	UPS	Low	6.66E-05	0.02	6.46E-04	0.20	16.5
2	DS	Low	0.000108	0.04	1.30E-03	0.20	10.4
2	DS	Low	0.000113	0.05	1.50E-03	0.20	6.4
2	UPS	Low	7.05E-05	0.02	6.73E-04	0.23	16.8
4	DS	High	4.76E-05	0.04	6.06E-04	0.22	4.6
4	UPS	High	2.84E-05	0.02	2.87E-04	0.44	5.7
4	DS	High	4.68E-05	0.04	5.63E-04	0.20	5.1
4	UPS	High	2.7E-05	0.02	2.57E-04	0.35	5.4
4	DS	High	5.13E-05	0.04	6.21E-04	0.21	5.8
4	UPS	High	3.11E-05	0.02	3.14E-04	0.28	8.8
4	DS	Low	0.000109	0.06	1.50E-03	0.18	5.0
4	UPS	Low	8.02E-05	0.02	8.06E-04	0.19	13.2
4	DS	Low	0.000103	0.06	1.50E-03	0.19	5.0
4	UPS	Low	7.94E-05	0.02	8.30E-04	0.21	13.2
4	DS	Low	3.85E-05	0.10	8.47E-04	0.18	1.4
4	UPS	Low	4.78E-05	0.07	7.00E-04	0.22	2.1

5	DS	High	3.62E-05	0.04	5.06E-04	0.20	4.4
5	UPS	High	1.79E-05	0.01	1.75E-04	0.47	5.9
5	DS	High	5.49E-05	0.04	6.56E-04	0.20	5.3
5	UPS	High	2.56E-05	0.01	2.34E-04	0.56	7.6
5	DS	High	5.84E-05	0.03	6.90E-04	0.20	6.9
5	DS	Low	9.4E-05	0.06	1.40E-03	0.20	4.5
5	UPS	Low	6.01E-05	0.02	6.10E-04	0.21	9.6
5	DS	Low	0.000102	0.06	1.60E-03	0.18	5.6
5	UPS	Low	7.9E-05	0.02	7.79E-04	0.19	17.4
5	DS	Low	8.6E-05	0.06	1.40E-03	0.19	4.1
5	UPS	Low	7.95E-05	0.03	8.12E-04	0.19	8.9

Flume Replicate	Response Variable	Reason for Not Including in Analysis
1 jam, low flow*	Mean Arrival Time & Skew	ds data run starts above background conductivity even before injection and then drops. Faulty injection due to start time delay
1 jam, high flow, upstream only*	Mean Arrival Time & Skew	issue with ups start time. Tracer pulse is delayed. Delay doesn't have significant effect on ds data
2 jam, high flow	Skew	conductivity starts above background level even before tracer injection for one replicate. Threshold is still not within standard deviation after removing one replicate, but opted to keep remaining two replicates given a lack of justification for removing one vs. the other
2 jam, low flow, downstream only*	Mean Arrival Time	Values do not fall within uncertainty threshold**
4 jam, low flow	Mean Arrival Time & Skew	Values do not fall within uncertainty threshold**
5 jam, high flow, downstream only	Skew	Values do not fall within uncertainty threshold**
5 jam, low flow, upstream only	Skew	Values do not fall within uncertainty threshold**

* indicates flume runs that only had two replicates necessitating additional justification for removal.

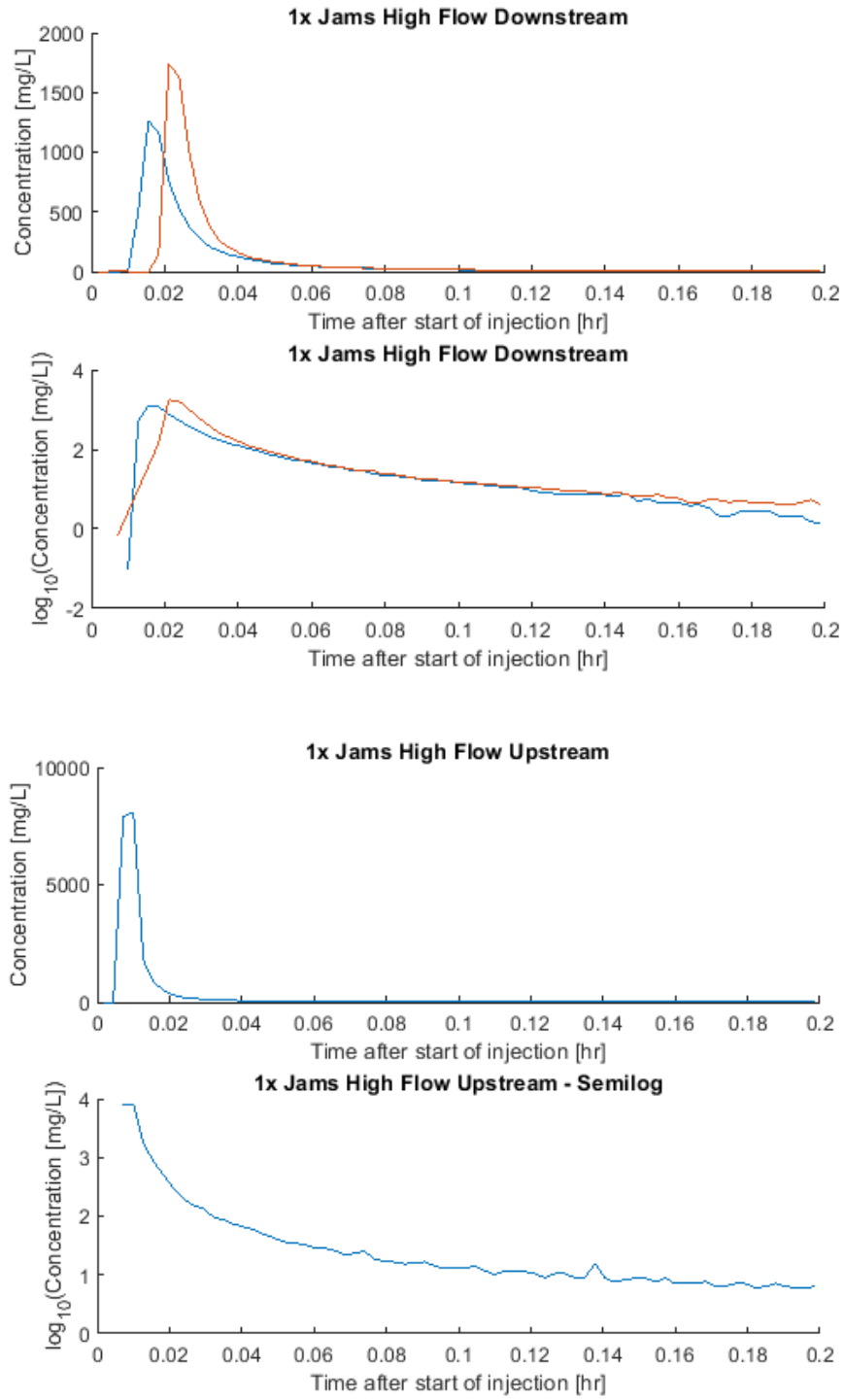
+indicates flume runs with 3 replicates which allowed for two replicates to remain.

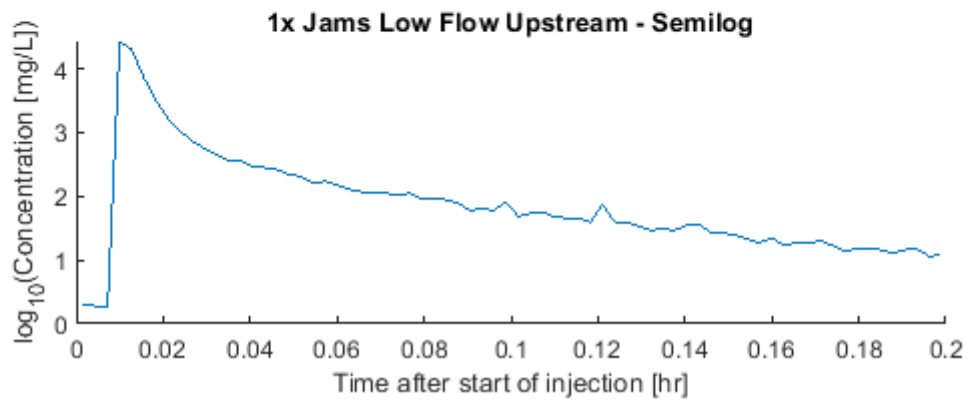
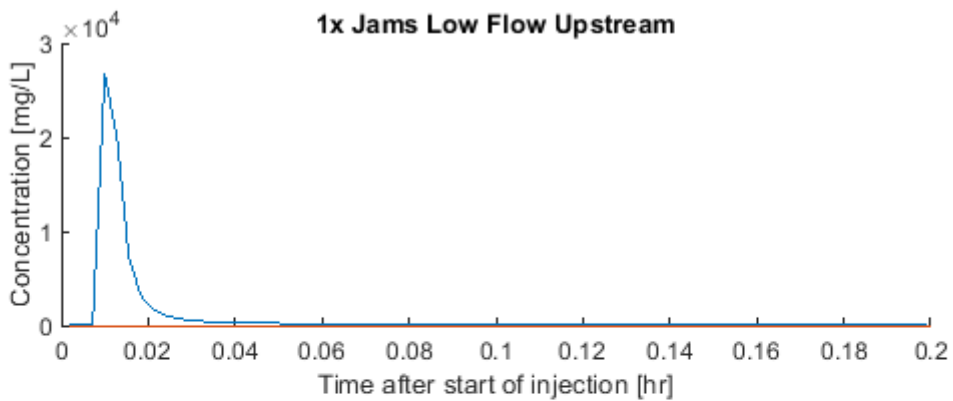
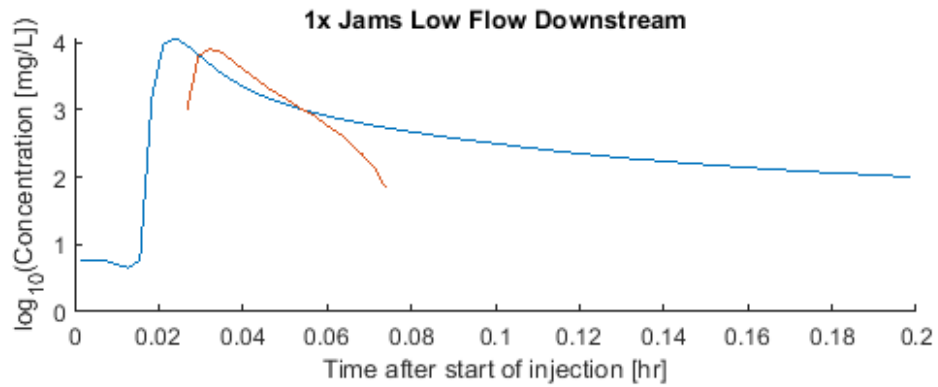
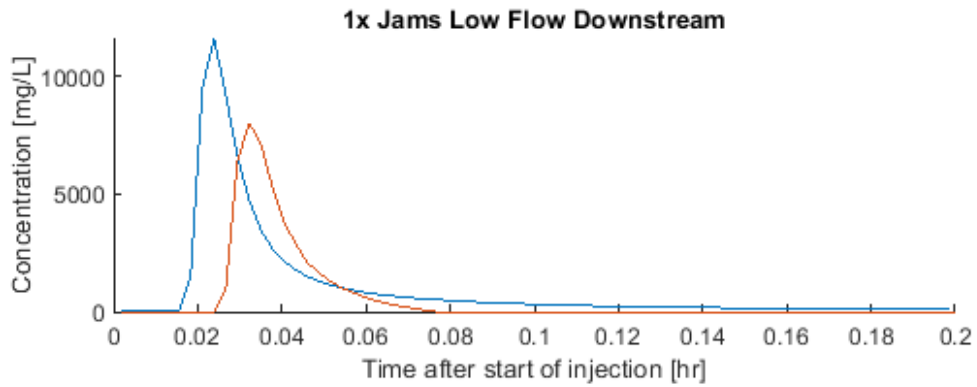
**uncertainty threshold is defined as >0.003 for mean arrival time and >8.15E-06 for skew.

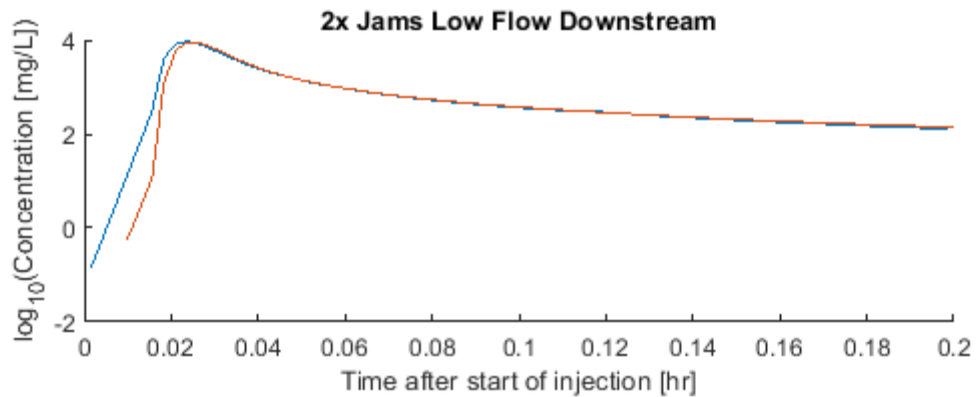
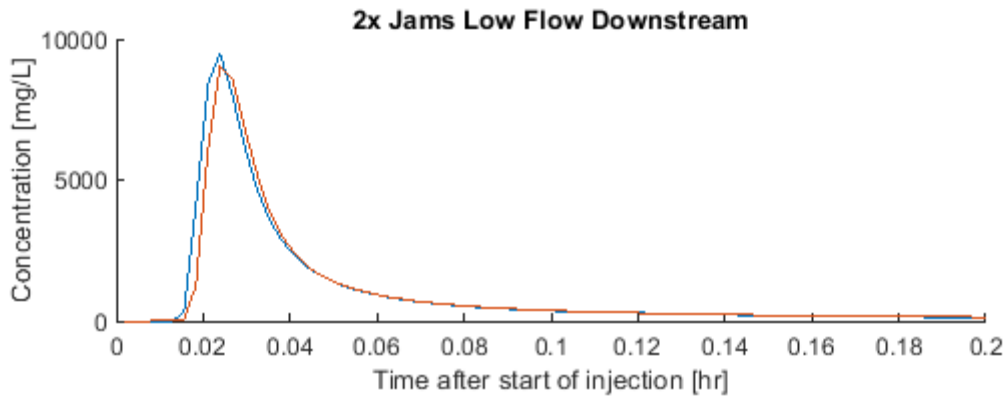
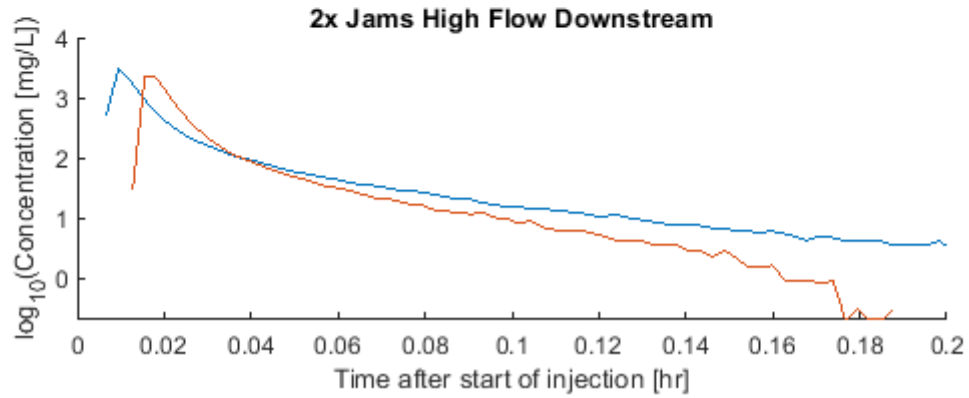
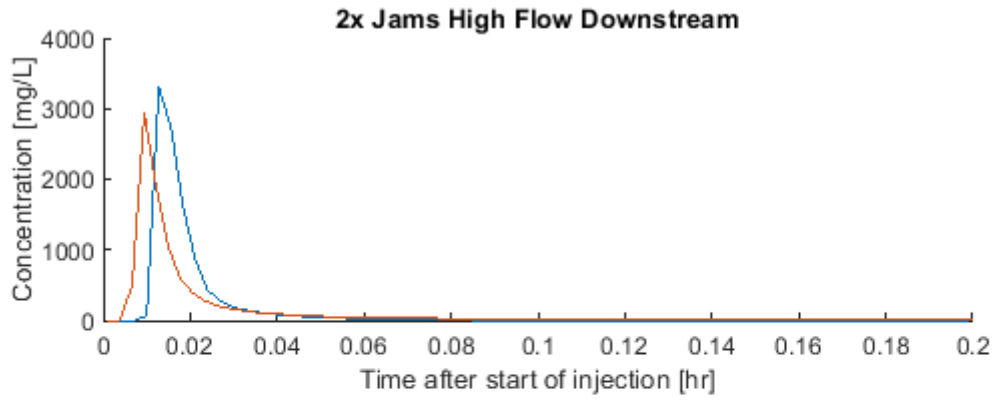
Appendix II

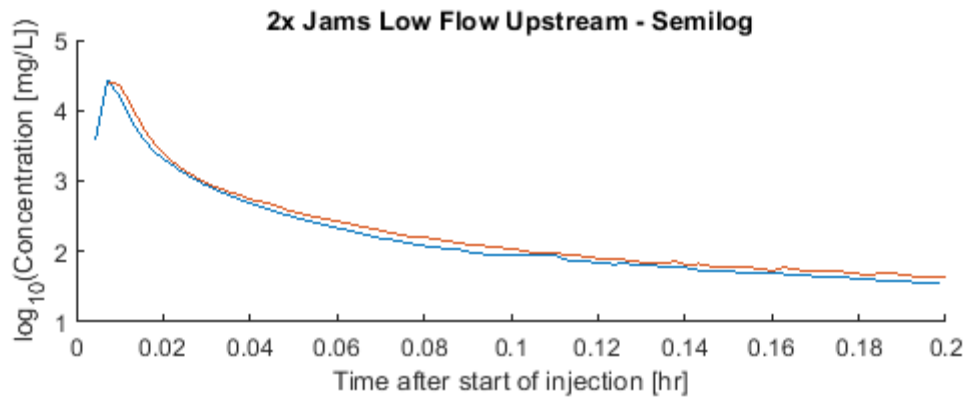
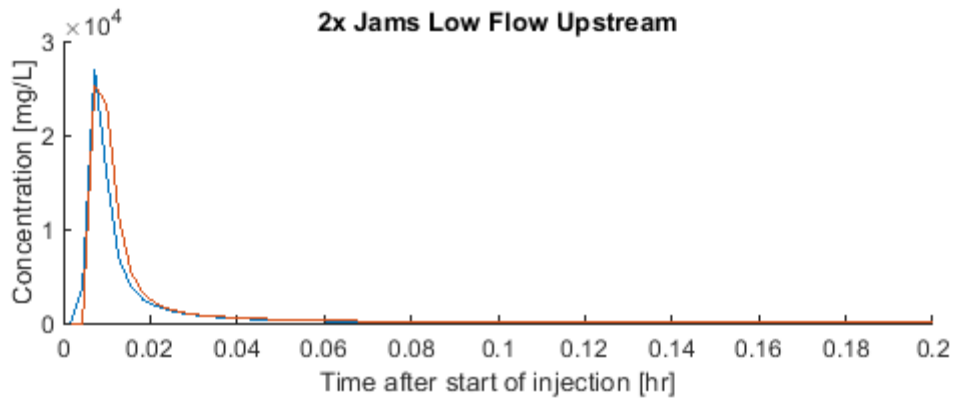
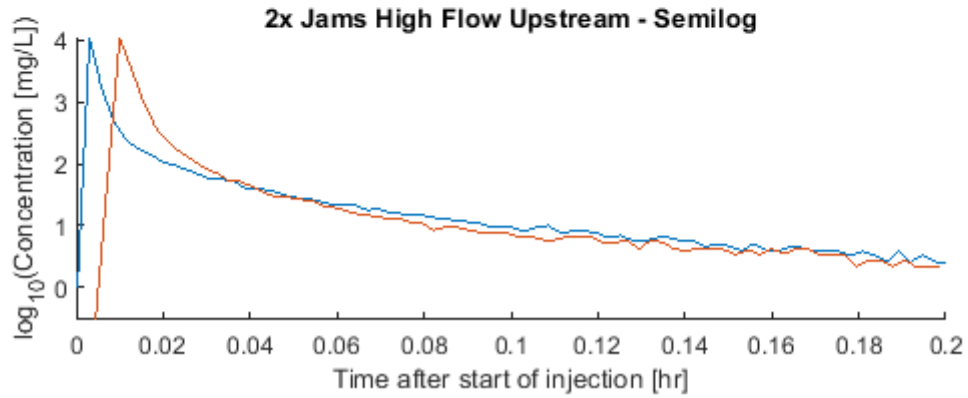
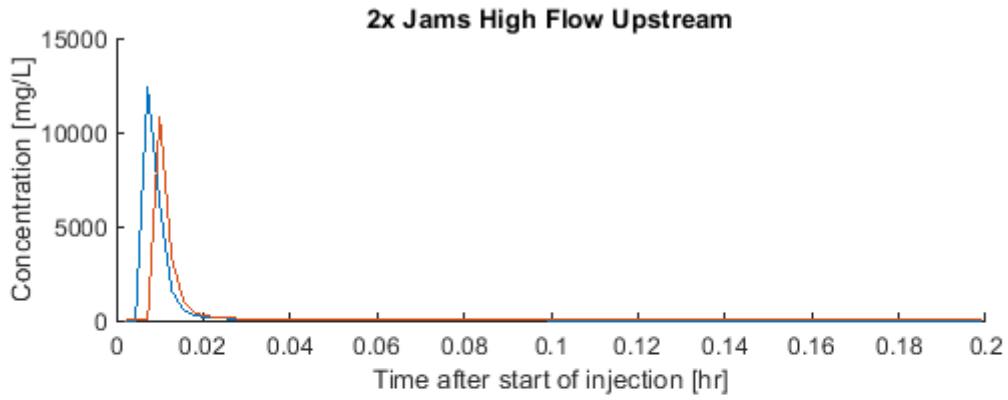
Longitudinal Spacing Flume Run Breakthrough Curves

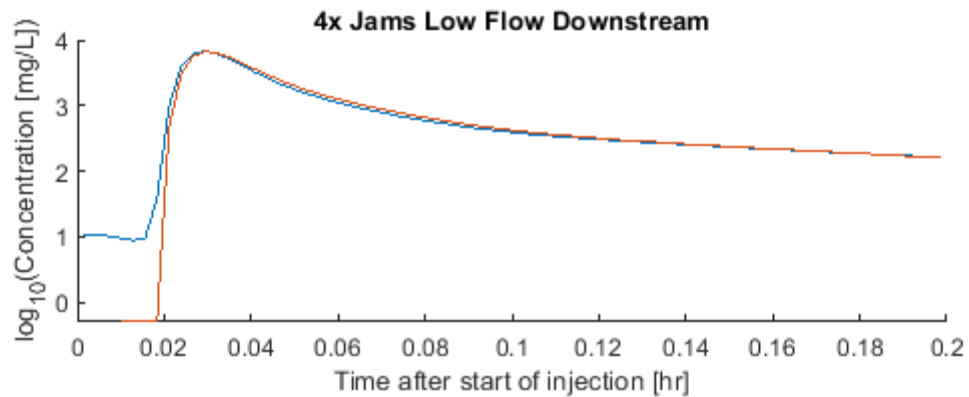
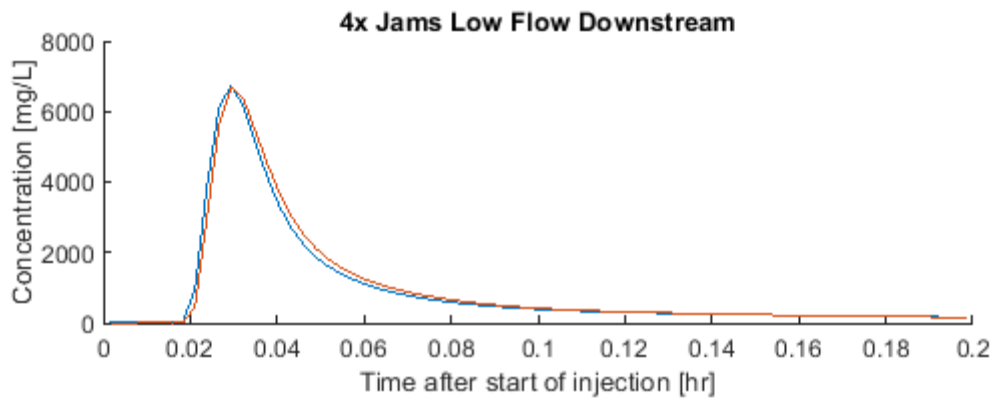
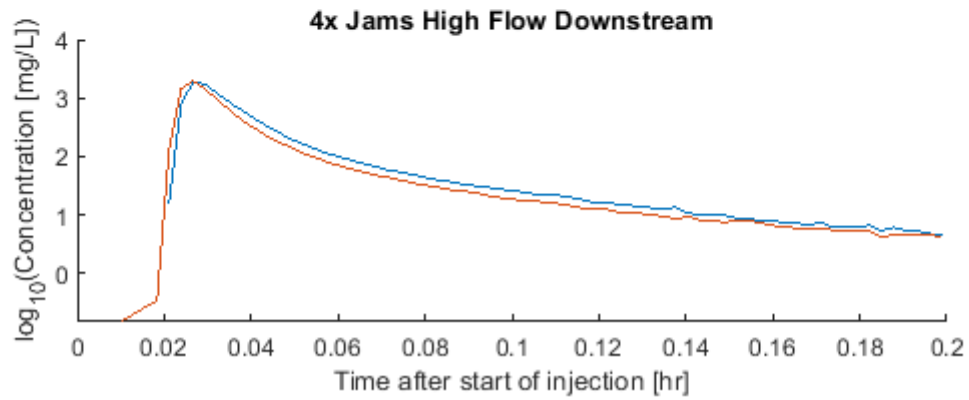
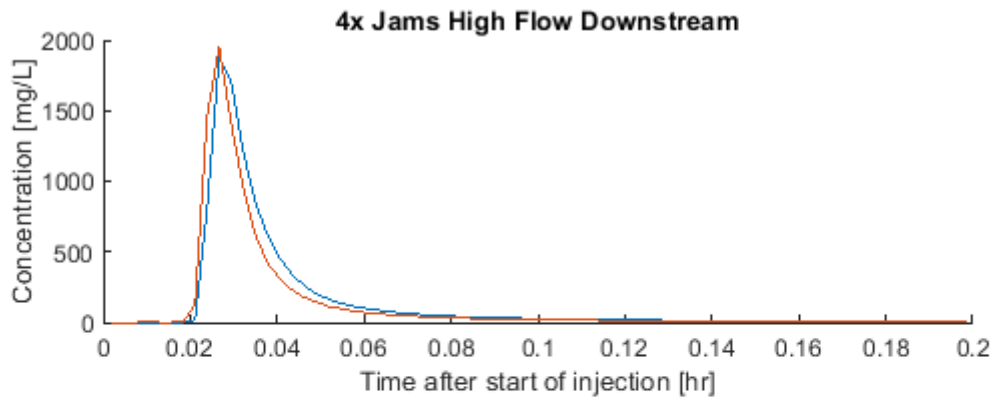
Note: colored lines indicate replicate runs in the flume.

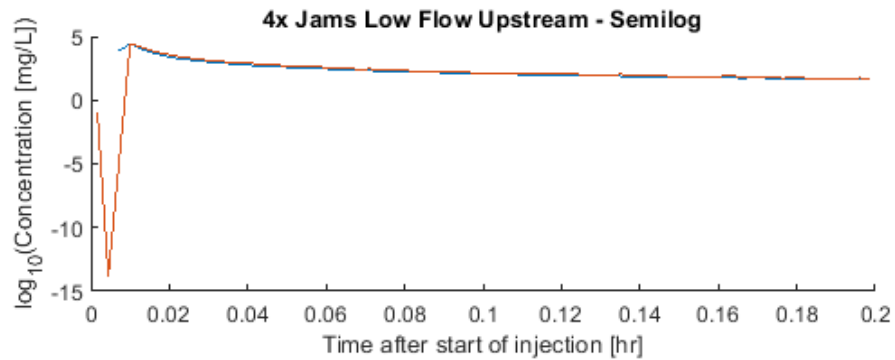
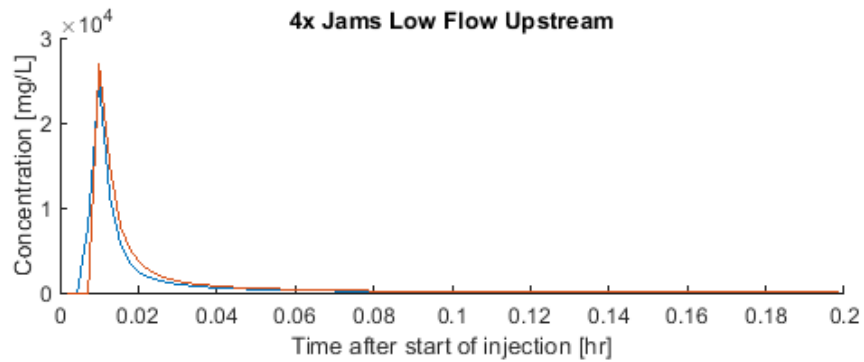
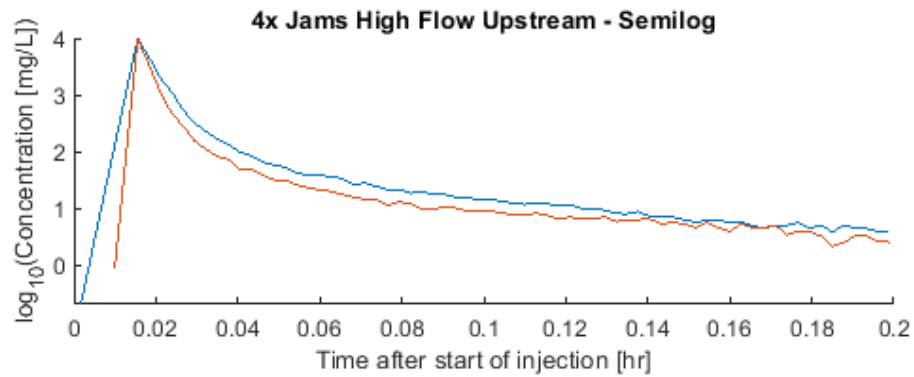
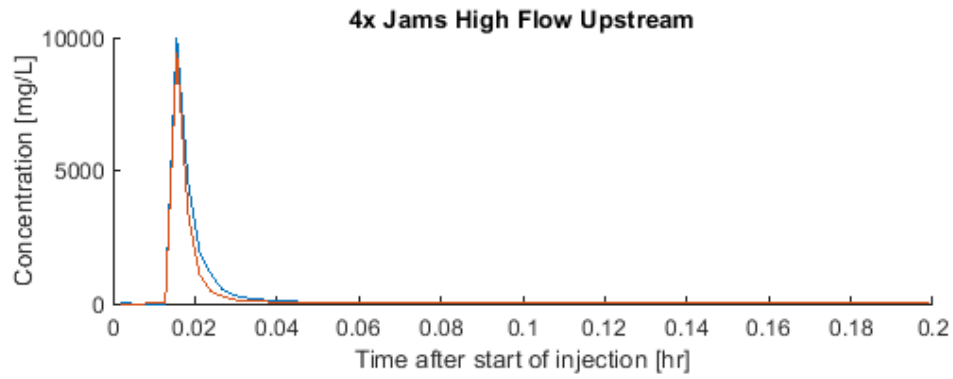


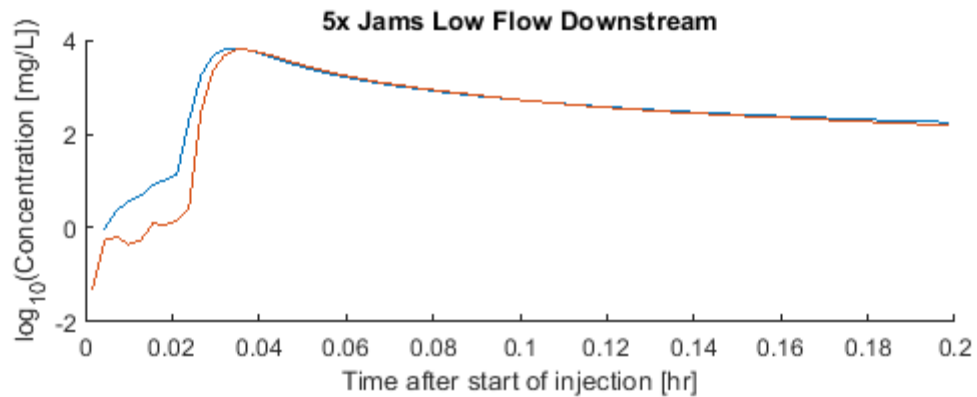
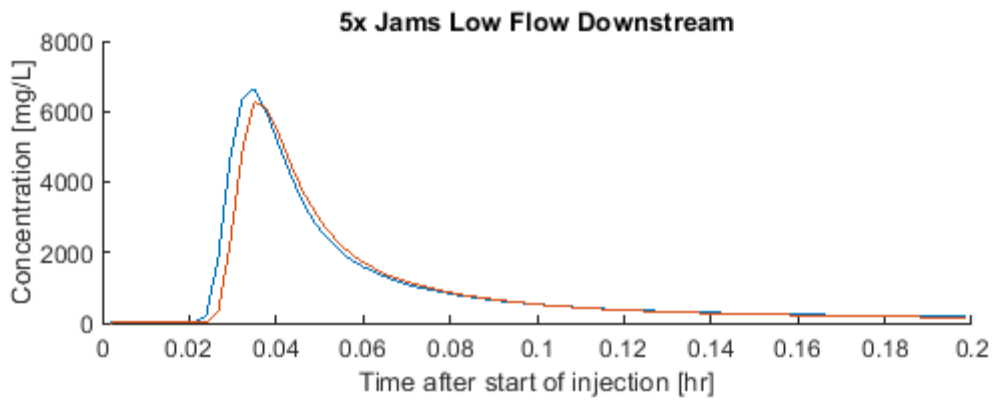
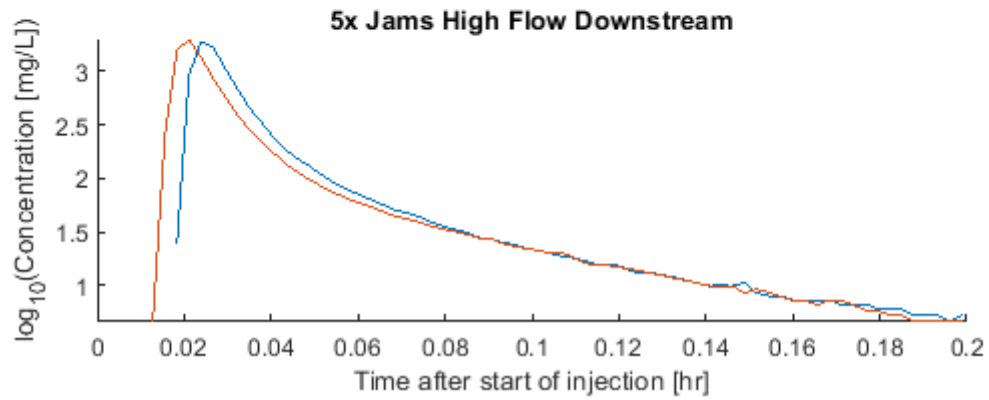
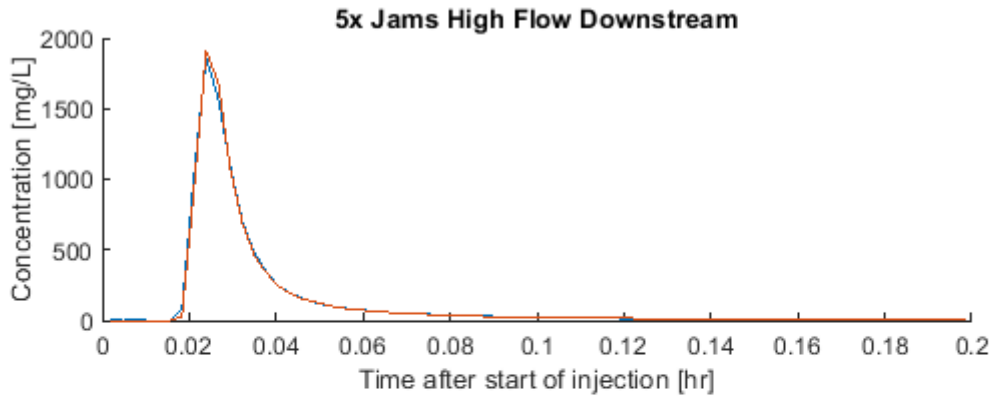


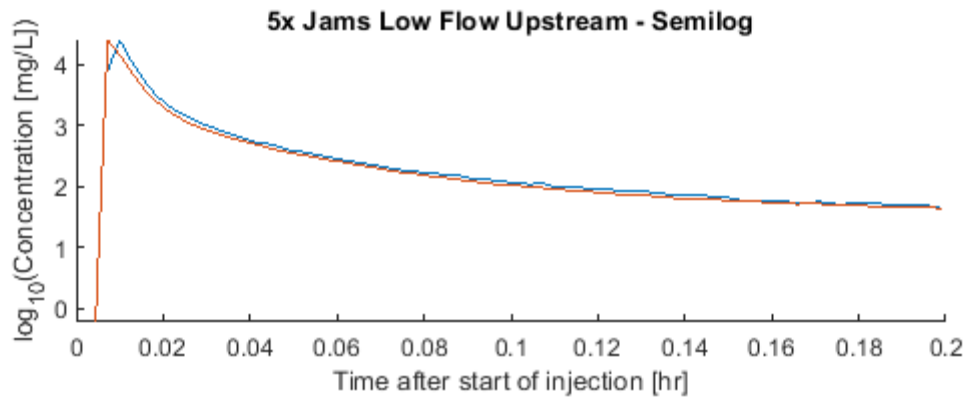
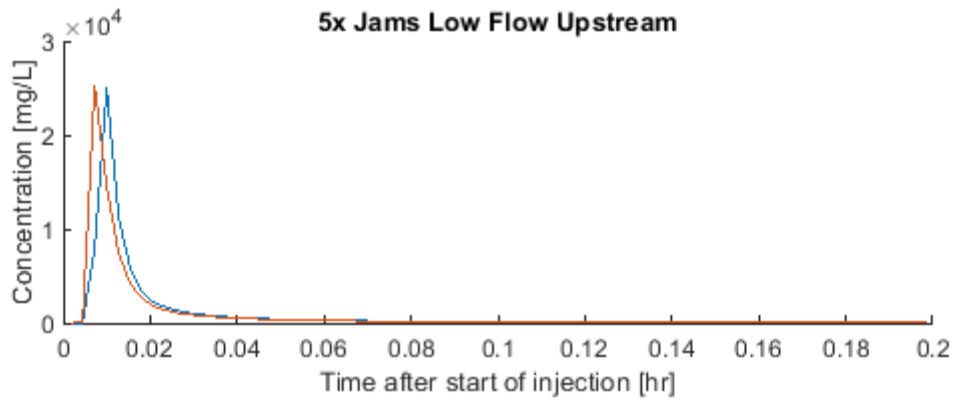
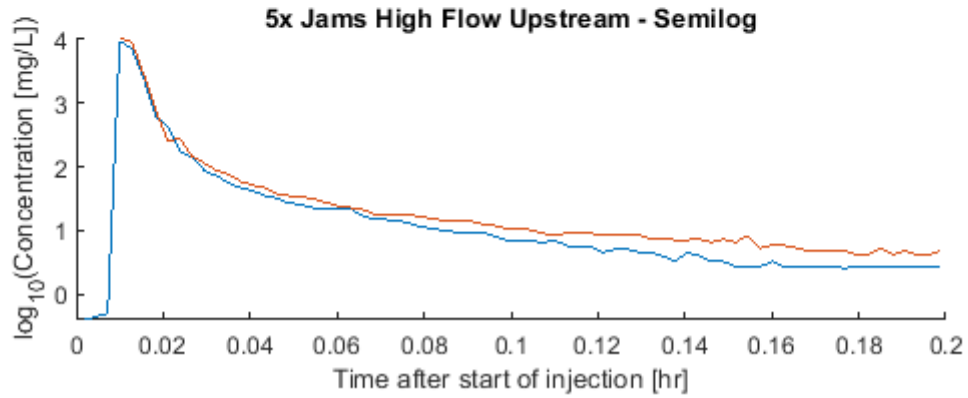
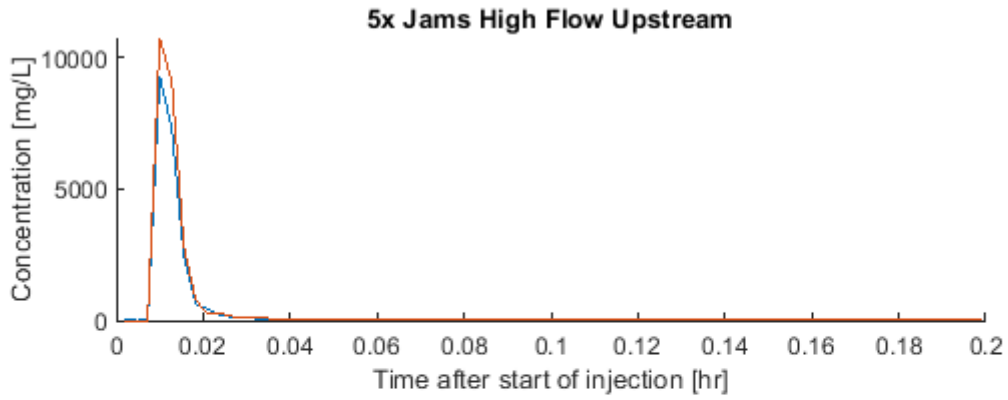


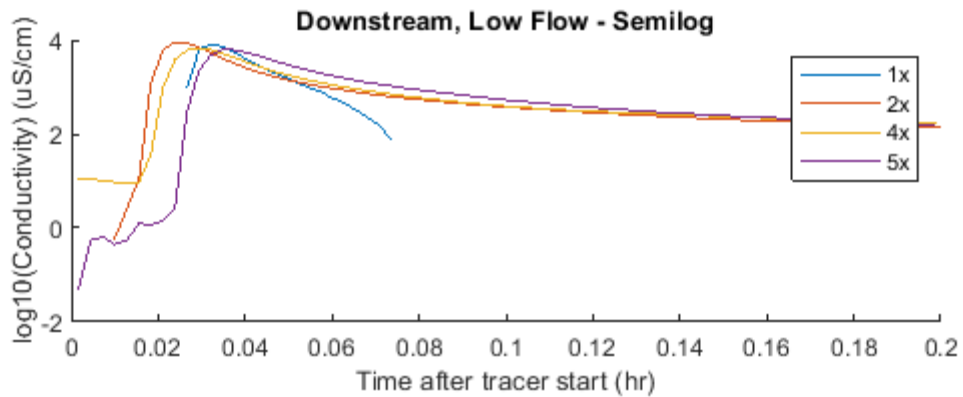
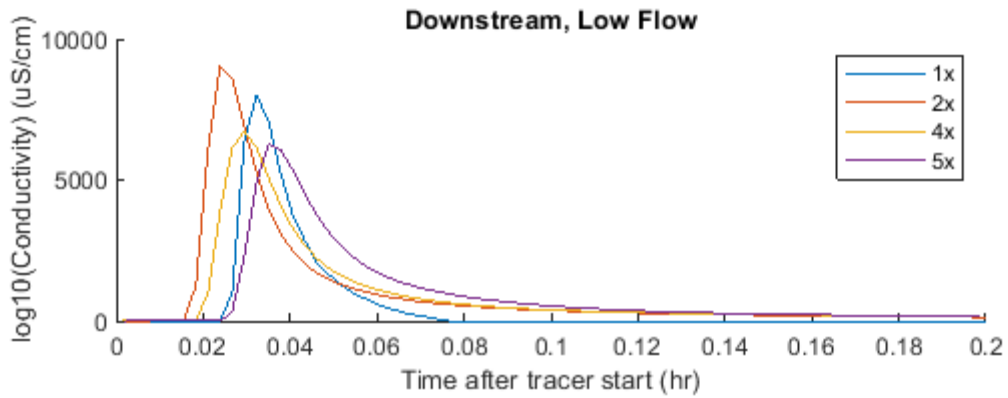
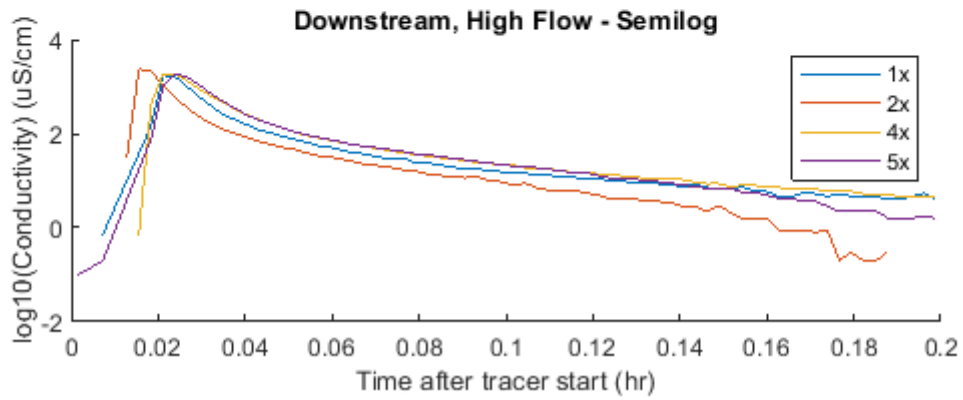
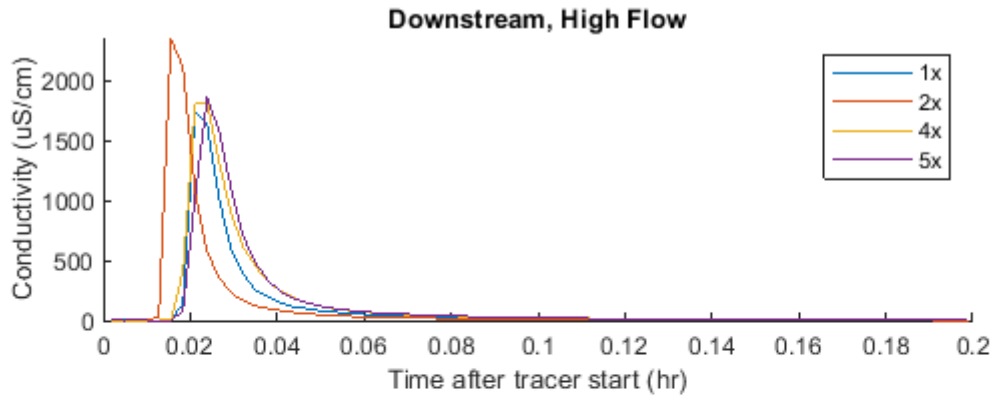


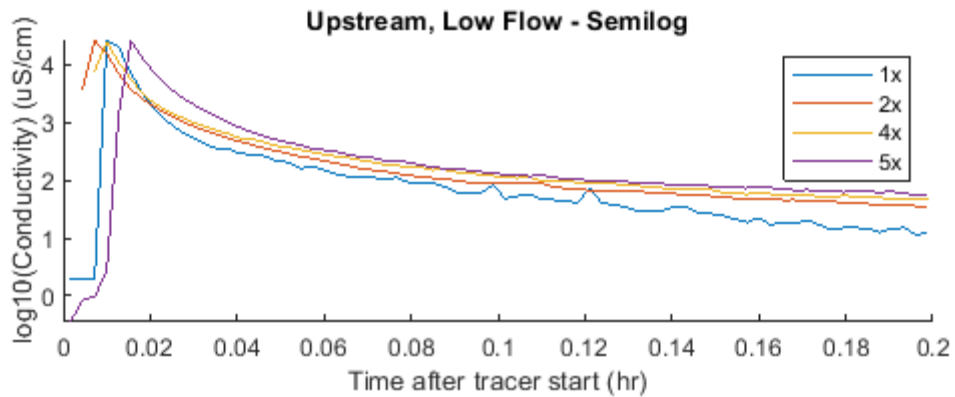
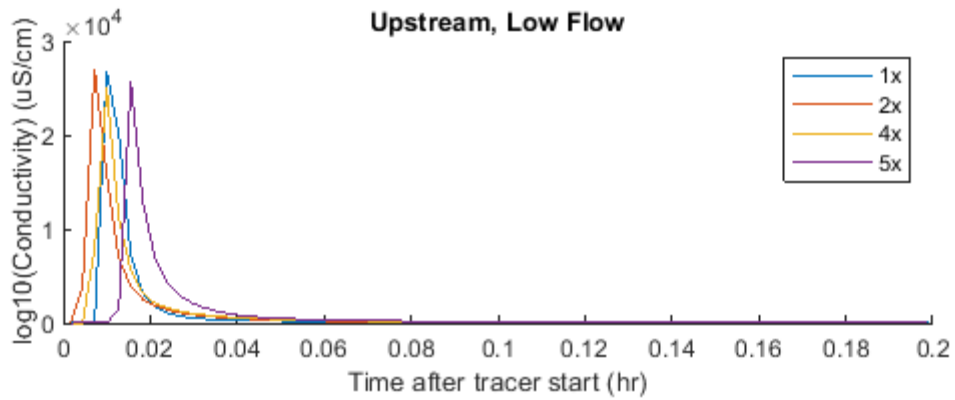
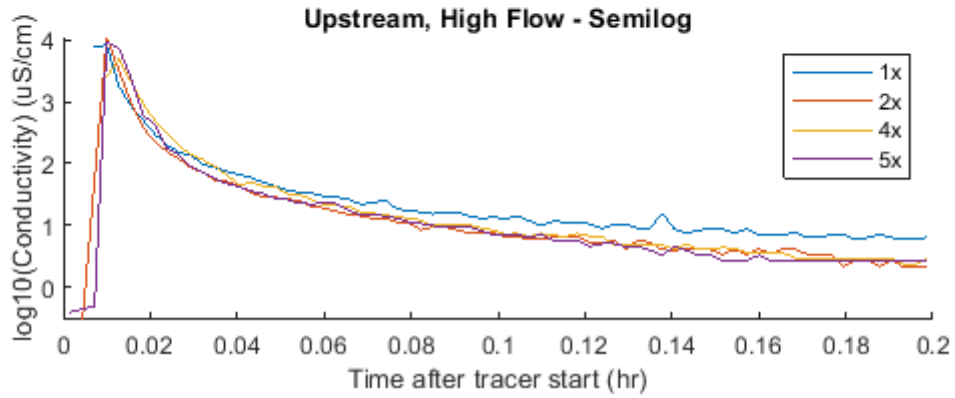
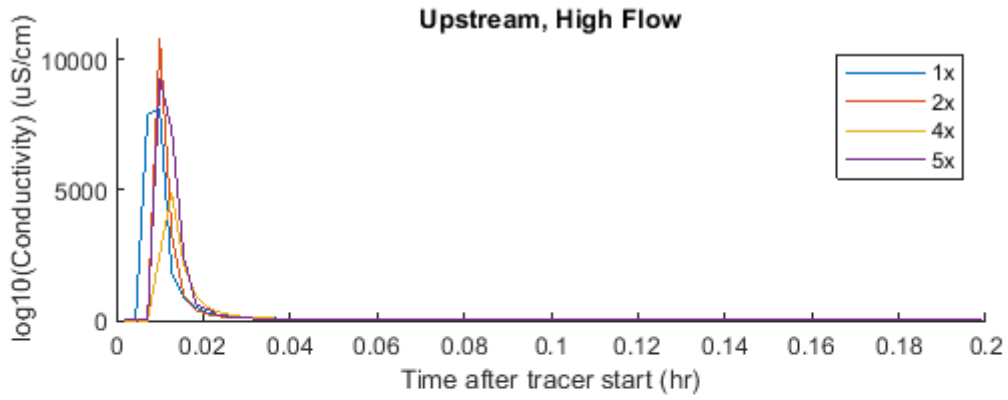












Appendix III

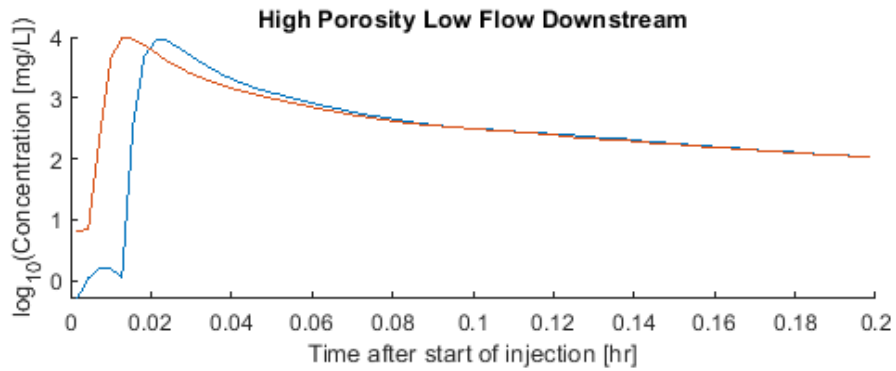
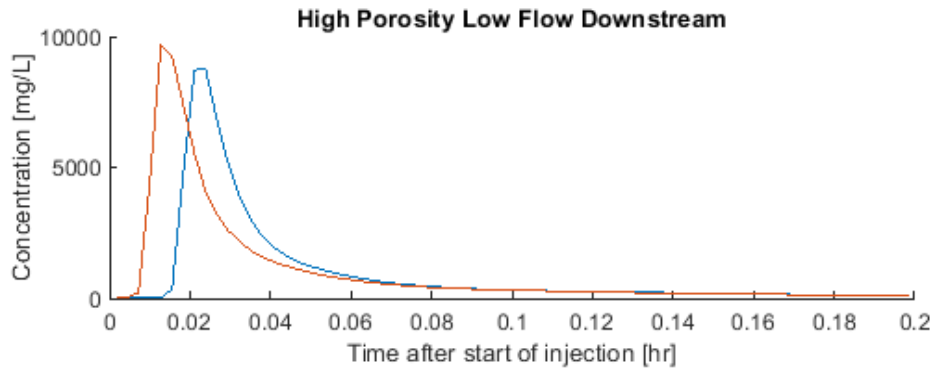
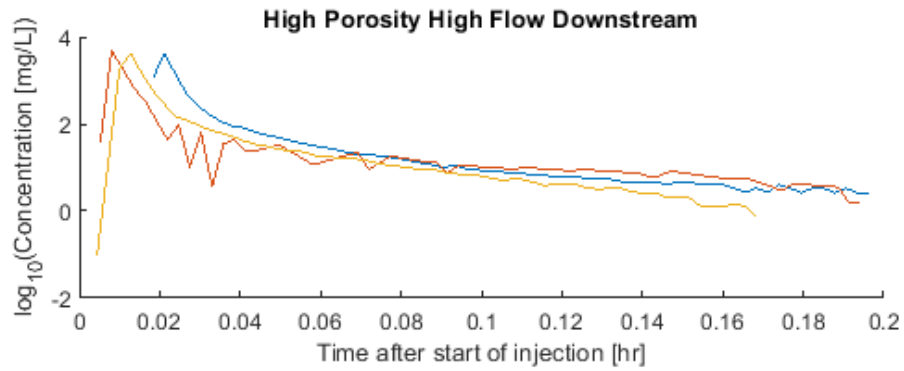
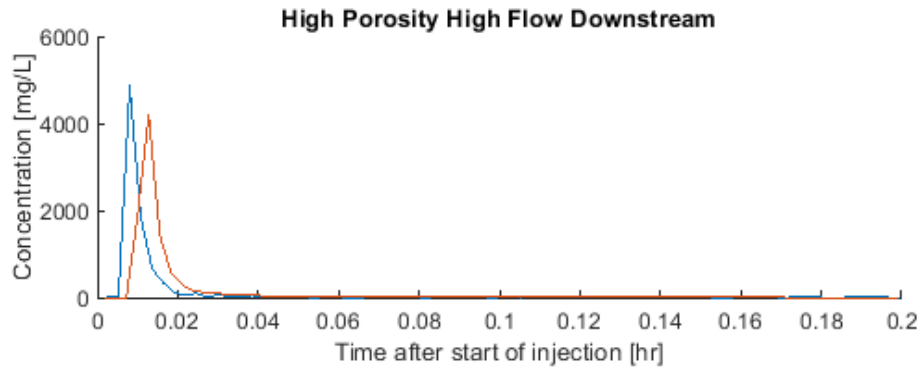
Porosity Flume Run Raw Data

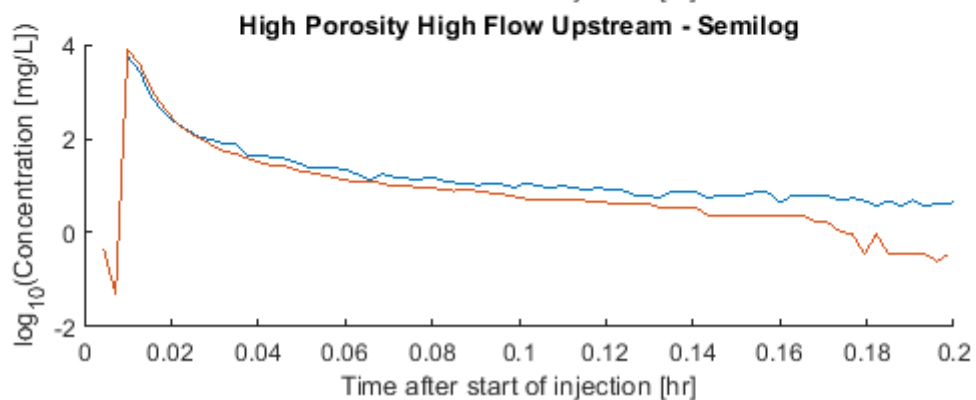
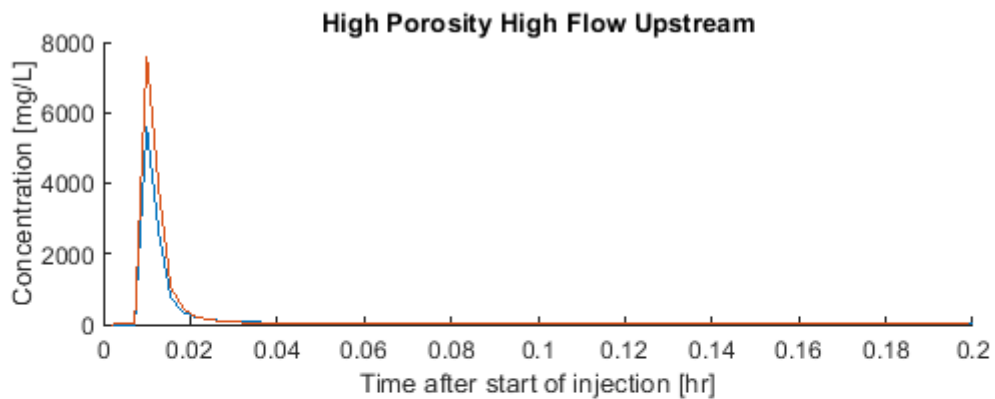
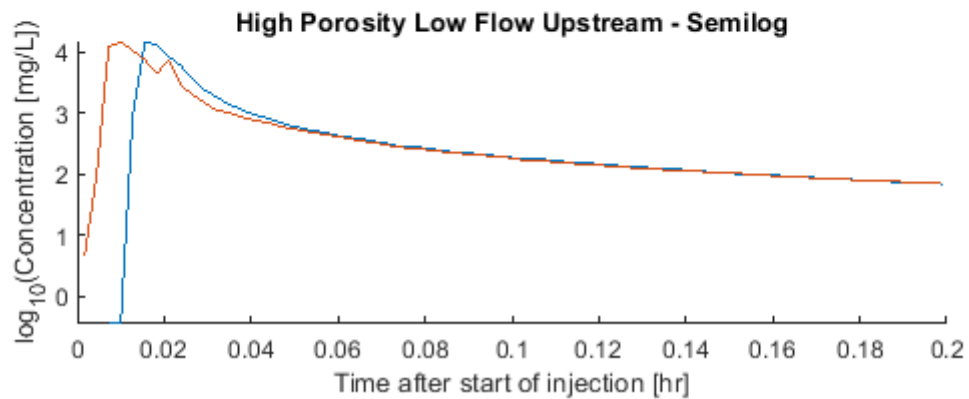
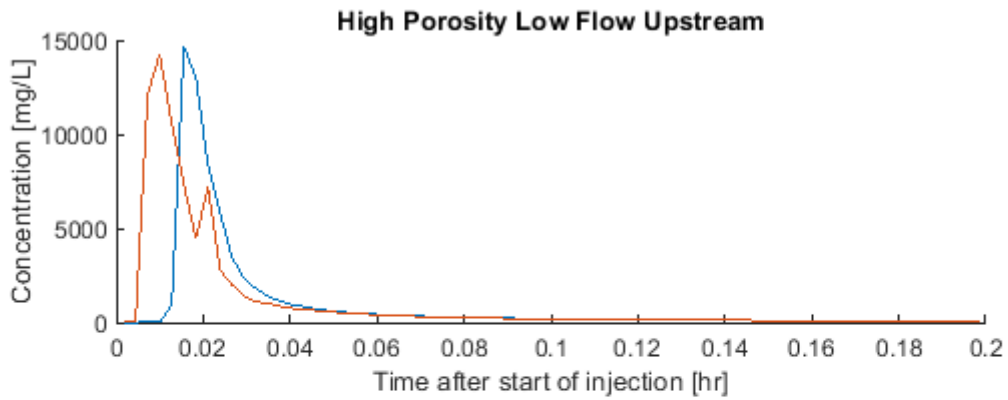
Note: High porosity=LW only, medium porosity=LW+twigs, low porosity=LW,twigs, CPOM

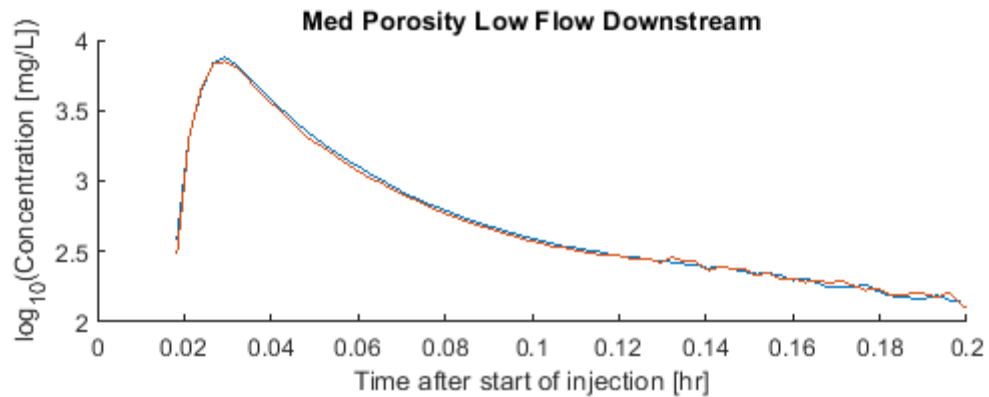
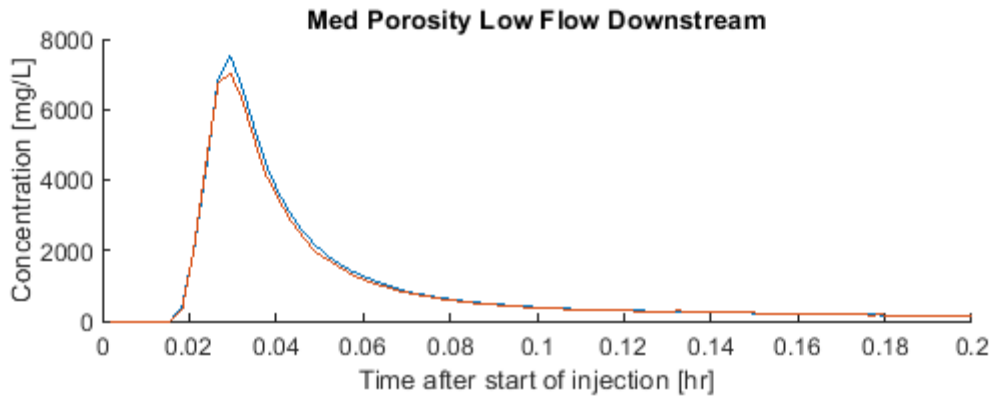
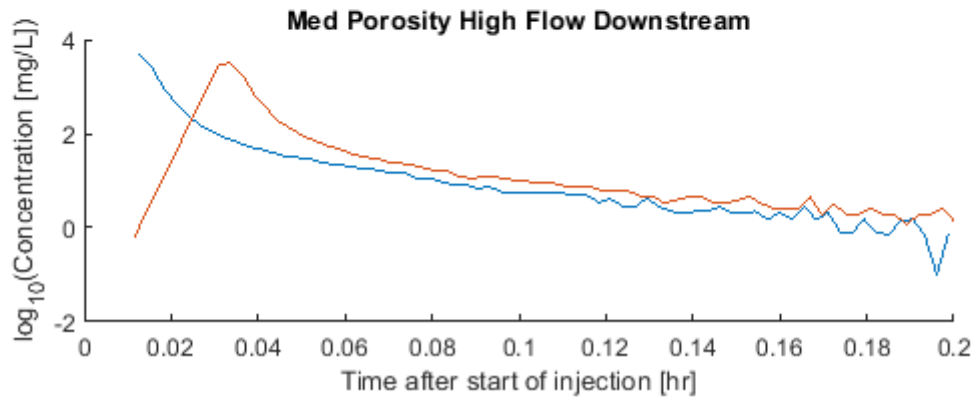
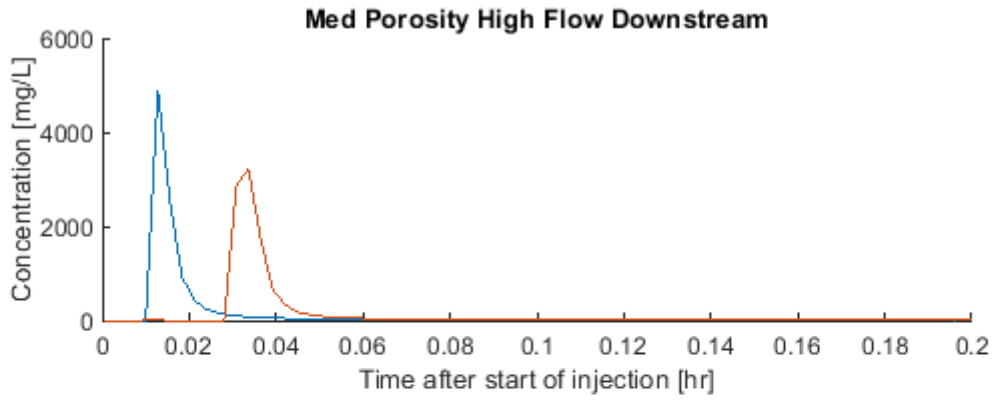
Porosity	Flow	Location	Skew (hr ³)	Mean arrival time (hr)	Variance (hr ²)	Mass (lbs)	TSI
High	High	DS	3.59E-05	0.03	3.75E-04	0.19	4.81
High	High	UPS	3.04E-05	0.02	2.93E-04	0.26	5.07
High	High	DS	4.32E-05	0.01	4.07E-04	0.19	12.65
High	High	UPS	5.59E-05	0.02	5.02E-04	0.24	11.71
High	High	DS	1.62E-05	0.02	2.16E-04	0.21	7.07
High	High	UPS	1.58E-05	0.01	1.72E-04	0.31	6.10
High	Low	DS	1.05E-04	0.05	1.40E-03	0.19	7.04
High	Low	UPS	9.55E-05	0.03	1.00E-03	0.18	9.18
High	Low	DS	1.17E-04	0.04	1.50E-03	0.20	11.76
High	Low	UPS	9.80E-05	0.03	1.00E-03	0.21	18.71
Medium	High	DS	2.02E-05	0.02	2.32E-04	0.22	5.69
Medium	High	UPS	2.23E-05	0.01	2.19E-04	0.35	7.94
Medium	High	UPS	4.38E-05	0.02	3.98E-04	0.34	12.29
Medium	High	DS	3.37E-05	0.04	3.10E-04	0.22	2.93
Medium	High	UPS	1.49E-05	0.03	1.58E-04	0.36	2.07
Medium	High	DS	4.16E-05	0.03	4.30E-04	0.25	5.92
Medium	High	UPS	5.10E-05	0.03	5.04E-04	0.20	6.48
Medium	Low	DS	9.88E-05	0.05	1.40E-03	0.20	5.54
Medium	Low	UPS	8.87E-05	0.04	1.10E-03	0.20	6.79
Medium	Low	DS	1.08E-04	0.05	1.50E-03	0.19	5.64
Medium	Low	UPS	9.76E-05	0.04	1.20E-03	0.19	7.04
Low	High	DS	1.31E-05	0.02	1.67E-04	0.21	5.61
Low	High	UPS	1.07E-05	0.01	1.24E-04	0.30	5.81
Low	High	DS	1.71E-05	0.02	1.98E-04	0.21	5.10
Low	High	UPS	1.77E-05	0.02	1.85E-04	0.28	6.10
Low	High	DS	1.58E-05	0.02	1.84E-04	0.20	4.71
Low	High	UPS	1.39E-05	0.02	1.52E-04	0.25	3.92
Low	High	DS	1.52E-05	0.01	1.79E-04	0.20	7.74
Low	High	UPS	1.52E-05	0.01	1.79E-04	0.20	3.92
Low	Low	DS	8.51E-05	0.04	1.10E-03	0.21	7.75
Low	Low	UPS	8.07E-05	0.03	9.25E-04	0.22	13.41
Low	Low	DS	1.01E-04	0.04	1.30E-03	0.20	8.03
Low	Low	UPS	9.18E-05	0.03	1.00E-03	0.21	10.98

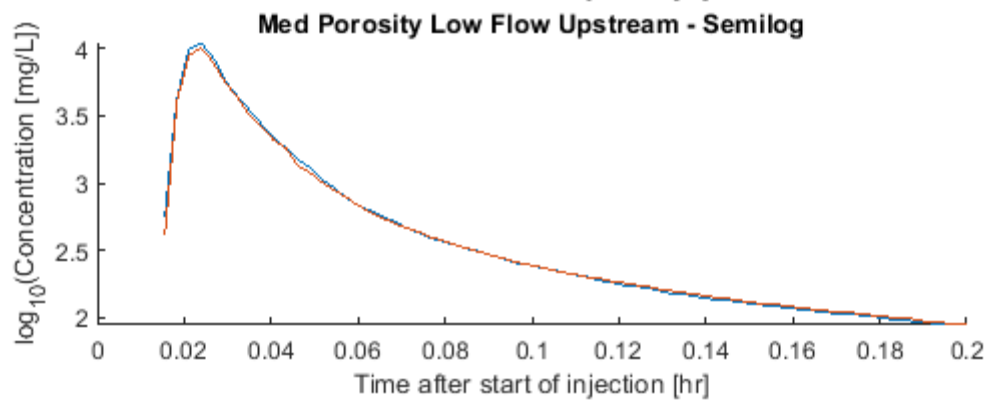
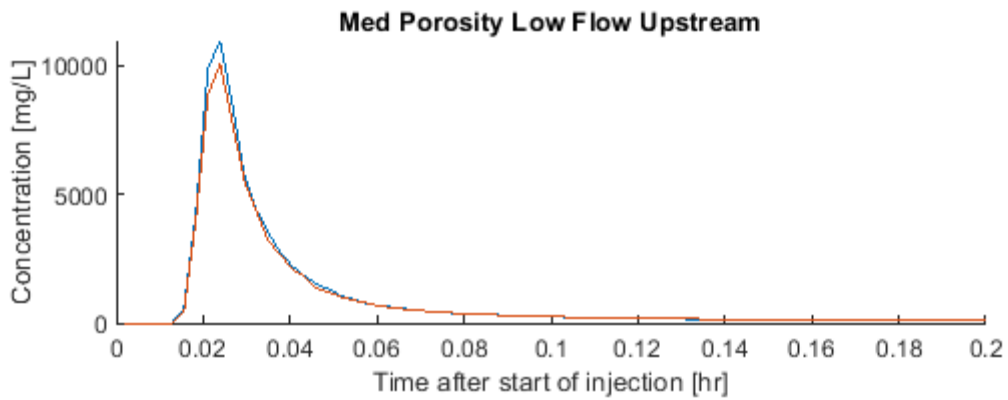
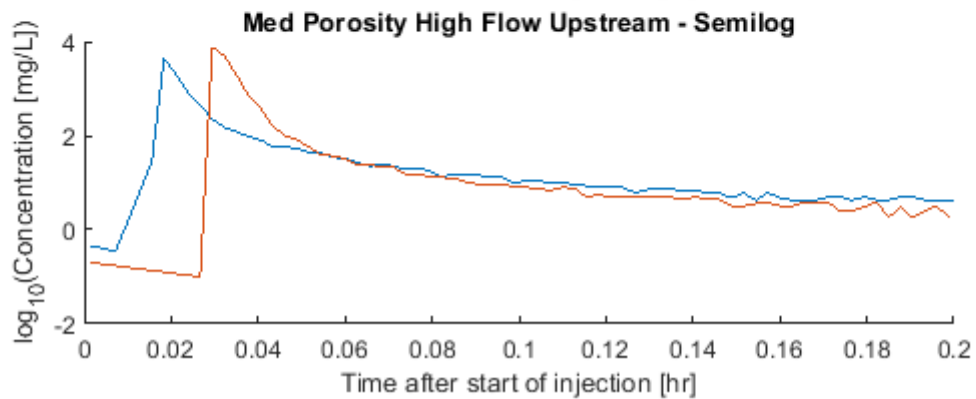
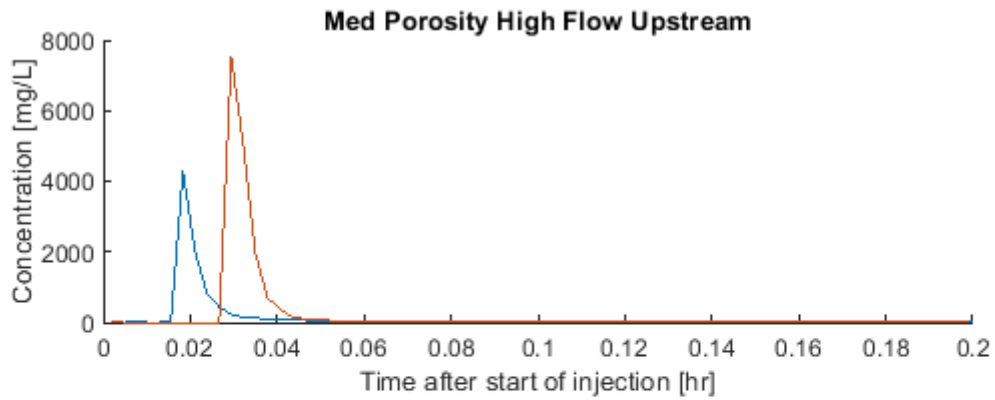
Appendix IV

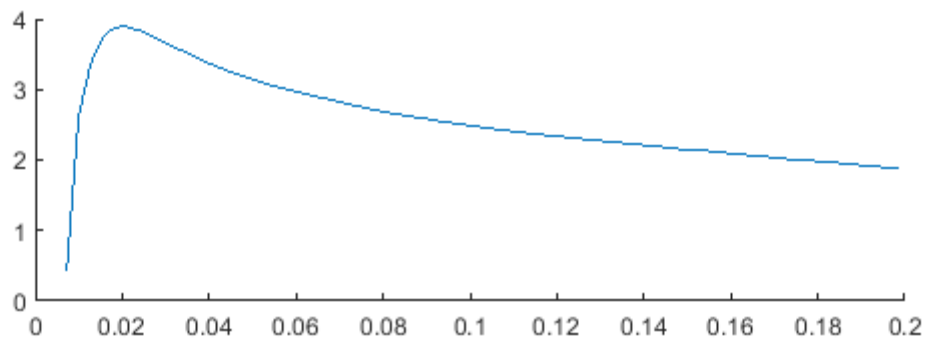
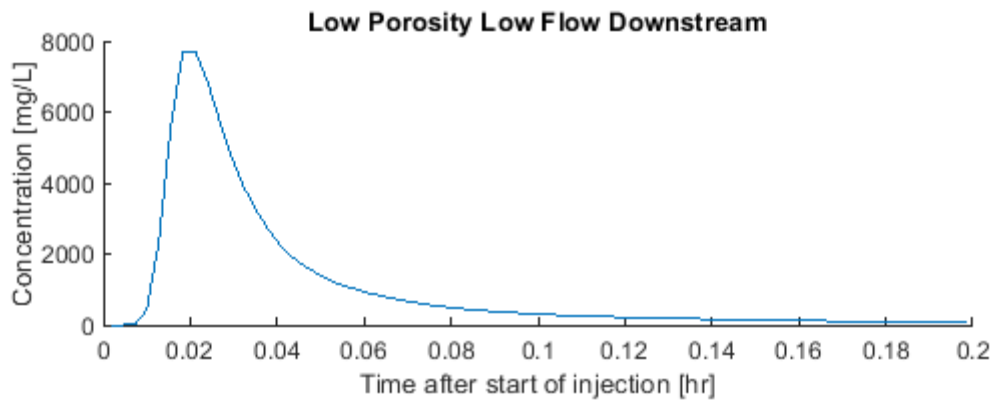
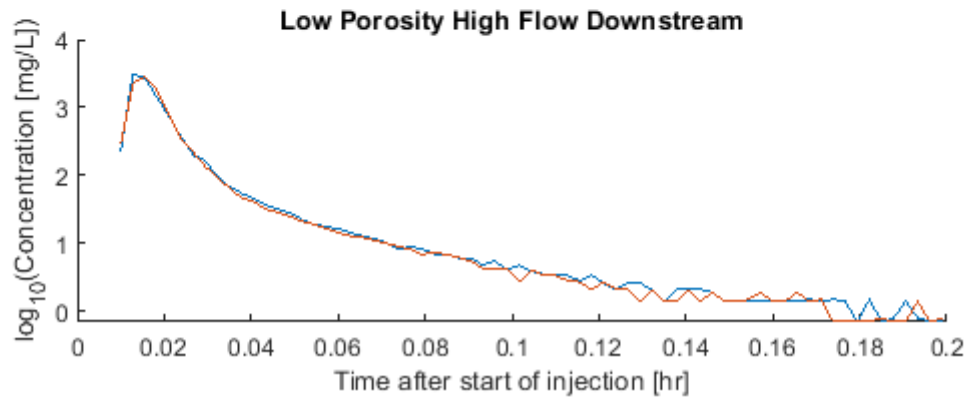
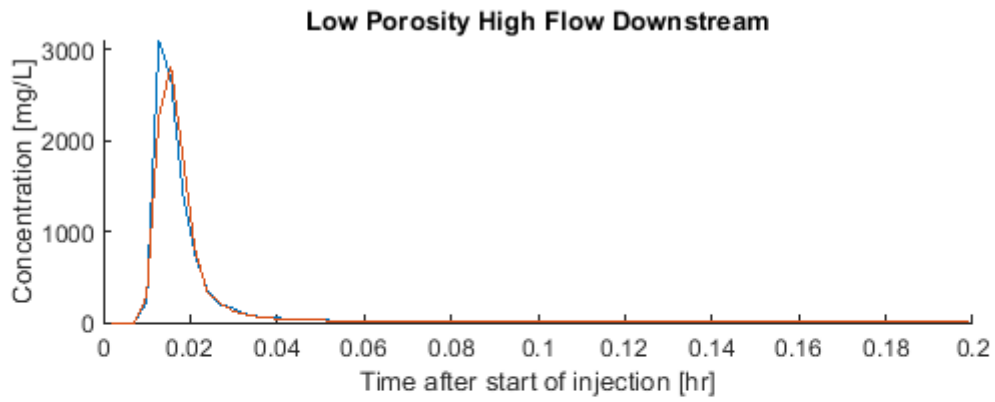
Porosity Flume Run Breakthrough Curves

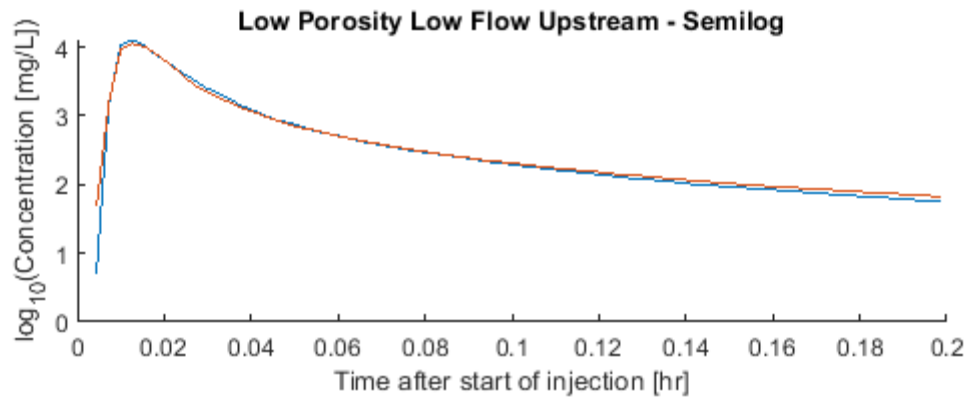
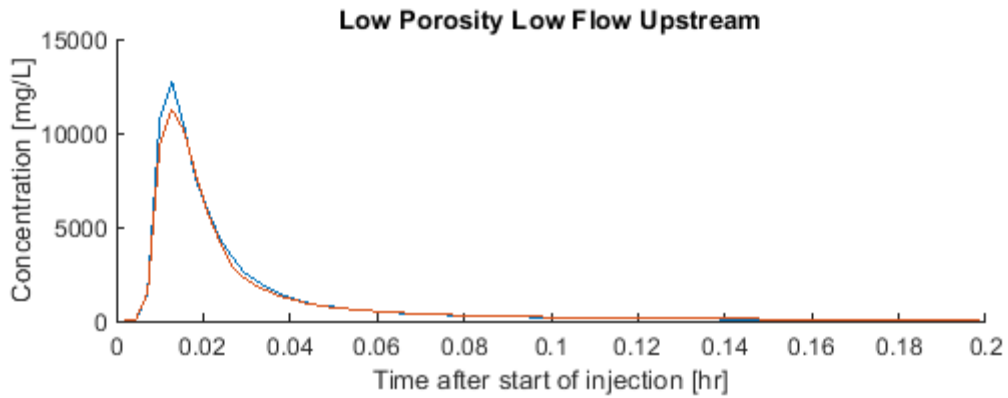
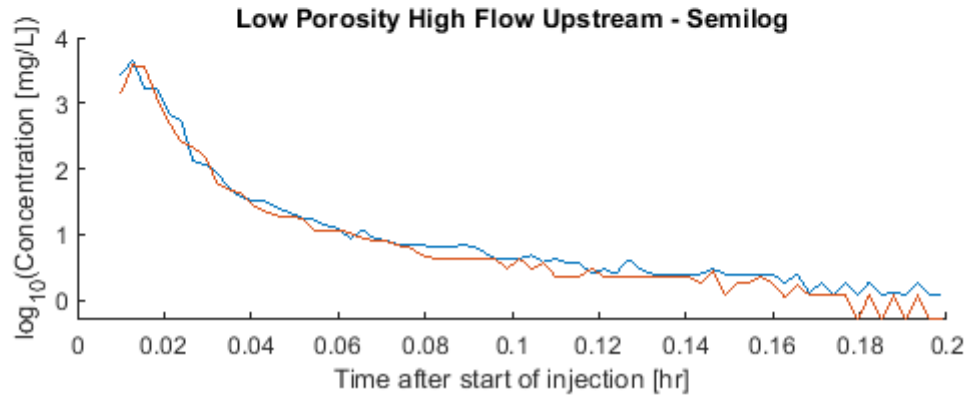
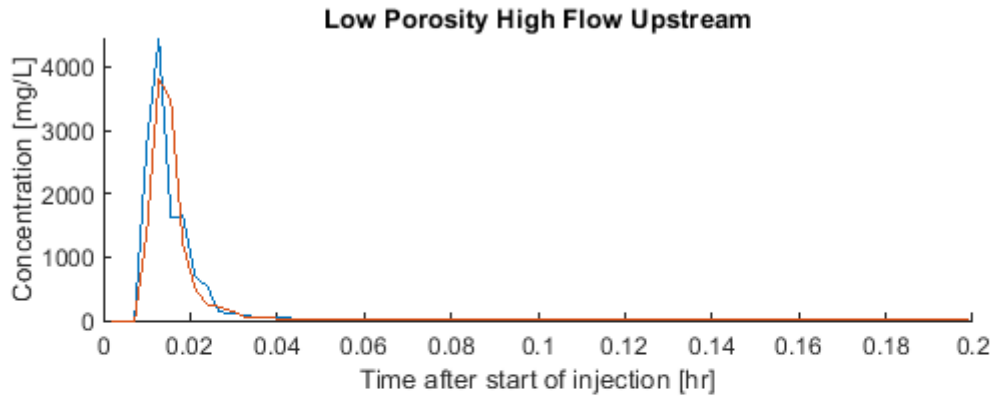












Appendix V

Porosity Flume Runs Results and Discussion

Results from the porosity experiment indicate no significant differences between skew or mean arrival time as the porosity declines. Transient storage is relatively unchanging as porosity changes, with the exception of a significant influence of flow. I expected to see greater transient storage with a decreasing porosity (i.e., as more material was added to the logjam) as well as greater transient storage with an increase in flow as backwater size increased. However, the results from the porosity flume runs cannot be physically interpreted with confidence given how fast the solute tracer moved through the system. Specifically, the scaling used in the flume was not effective in distinguishing the study effects and travel time for the tracer, regardless of flow, was too high to distinguish changes based on porosity. In other words, the tracer moved through the short flume reach too quickly to distinguish between changes in porosity. Sensors were placed less than 0.5-m above and below a single logjam. Thus, the “study reach” from upstream to downstream sensor was less than a meter in total distance. The results suggested that the tracer moves through the entire flume system very quickly, so when confined to a very small reach length (and high discharges), the results are not interpretable. Future configurations for the single jam with changing porosities would benefit with sensors located at the flume extents in tandem with lower overall discharges.

Additionally, the amount of material added between flume runs to change the porosity did not appear to be enough to show clear patterns in results. Future jam configurations should include larger changes in porosity between runs (i.e. changes by about 10% porosity) achieved by adding a greater quantity of organic material. This study decreased the porosity approximately 5% from high to low porosity and while that did increase the backwater, it was not enough of a change to influence transient storage significantly.

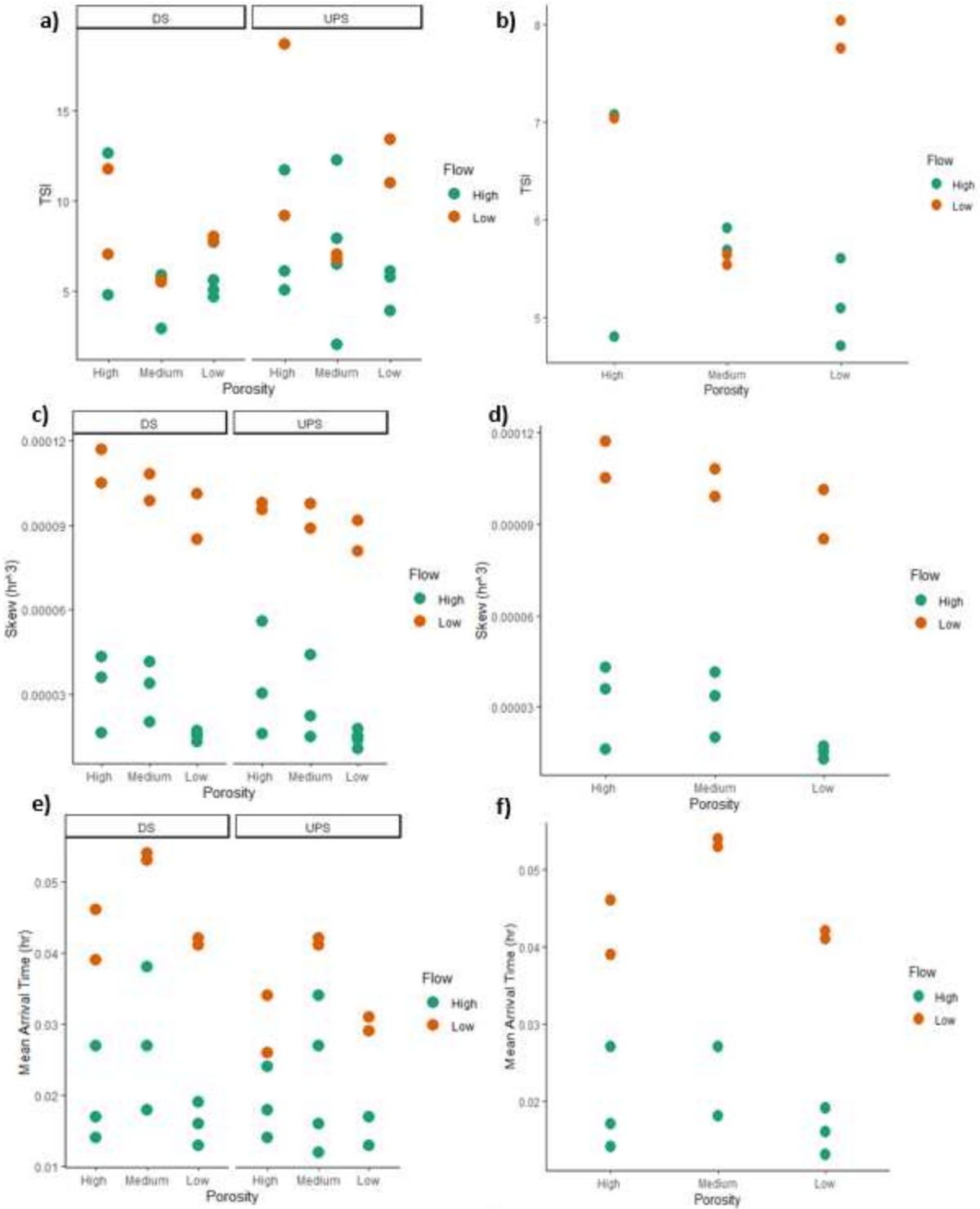


Figure 3.4. Skew, mean arrival time, and TSI values plotted for all flume runs (including replicates) with high, low, and medium porosities. Each porosity configuration was run at high and low flow scenarios and flow is indicated in the figure by color. Sensors measuring conductivity were placed at the upstream and downstream extents of the flume. Figure 3.4a,c,e

show all data points, split by location. Figure 3.4b,d,f show downstream data points that were the focus of analysis.

As porosity changes, what happens to transient storage at a point?

Results from Figure 3.4 suggest limited trends between changing porosity and transient storage. As porosity declines, visual interpretation of Figure 3.4 indicates an increase in TSI and a decrease in skew and mean arrival time at high flow. At low flow, we see a visual decrease in skew and no discernable trend in TSI and mean arrival time (Figure 3.4). Figure 3.5 shows that the backwater is increasing upstream of the logjam at high flow and as more material is added to the jam (decreasing the porosity). However, the data plotted in Figure 3.4 indicate that high porosity (LW only) has greater skew compared to low porosity (LW+twigs+CPOM) for a given flow. This is the opposite of what I hypothesized and what preliminary field data suggest. The lack of statistical significance seems to suggest that the increasing backwater size created by decreased porosity is not having much of an effect on transient storage.

Table 3.1. Calculated porosity values for the single logjam with changing porosity. Porosities remain consistent values between high and low flow.

Porosity Condition	Porosity Value (%)
High (LW only)	70
Medium (LW & twigs)	68
Low (LW, twigs, CPOM)	65

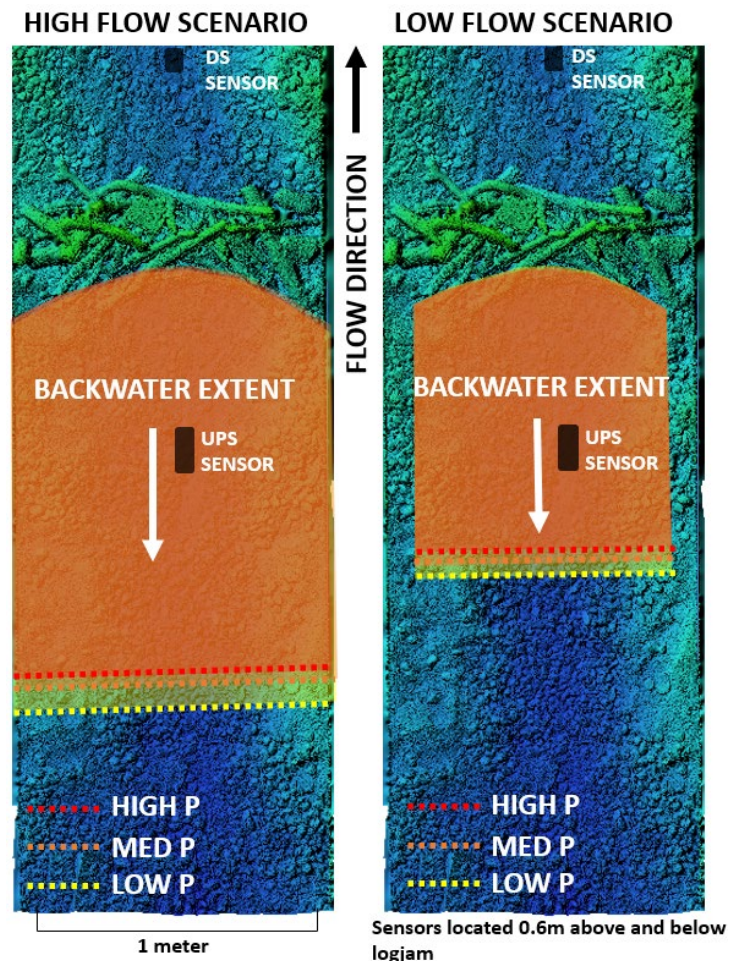


Figure 3.5. To reader's right, plotted backwater areas at high and low flow and at differing porosities.

As flow changes, what happens to transient storage at a point?

Overall, transient storage is higher at low flow compared to high flow. Mean arrival times are longer for all porosities at low flow compared to high flow, which suggests slower advection times through the logjams. In the simplified flume system at high flow, there is not enough time for exchange between the surface and subsurface flow paths before the salt mass is swept downstream. Some of the salt mass is also able to bypass the logjams via overtopping or preferential flow paths around the logjams, as observed during high flow runs and evidenced by the shorter mean arrival time. Transient storage is often greater at high flow in the field because flow paths are able to access the floodplain for storage. The flume cuts out the ability for water to access a floodplain as well as any much of the heterogeneity that exists in backwater pools.

CHAPTER 3

Appendix VI

CPOM Raw Data Table

Column Key:

Date= Date of sample

Location= depositional reach with storage feature (D1), transport reach with storage feature (T1), transport reach without storage feature (T2)

Time= Time of sample

Weight= Weight of CPOM sample after drying and LOI (if applicable)

A complete set of samples would be 7 dates x 3 sites x 3 depths per site x 6 time intervals = 378. Because of shallow flows (did not sample at 60% of depth) and unsafe conditions (early morning hours during high stage), we have a total of 298 samples: 45 from 5/22-23, 54 from 5/28-29, 36 from 6/1-2, 49 from 6/9-10, 48 from 6/16-17, and 33 each from 7/22-23 and 7/23-24. A complete set on a particular sampling date would be 54 samples.

Date	Location	Depth	Time	Weight (g)
5/22/2020	D1	60	12:44:00 PM	0.1674
5/22/2020	T1	60	1:40:00 PM	1.3309
5/22/2020	T2	60	2:25:00 PM	4.0112
5/22/2020	D1	60	4:17:00 PM	0.6102
5/22/2020	T1	60	4:50:00 PM	3.9990
5/22/2020	T2	60	5:33:00 PM	4.2007
5/22/2020	D1	60	9:15:00 PM	0.8766
5/22/2020	T1	60	9:46:00 PM	4.271
5/22/2020	T2	60	10:20:00 PM	6.6136
5/23/2020	D1	60	1:45:00 AM	0.7476
5/23/2020	T1	60	2:16:00 AM	1.5175
5/23/2020	T2	60	2:50:00 AM	3.5923
5/23/2020	D1	60	7:17:00 AM	0.6072
5/23/2020	T1	60	7:45:00 AM	4.0794
5/23/2020	T2	60	8:15:00 AM	2.4080
5/28/2020	D1	60	12:25:00 PM	0.9179
5/28/2020	T1	60	1:08:00 PM	1.9184
5/28/2020	T2	60	2:10:00 PM	1.1160

5/28/2020	D1	60	4:30:00 PM	0.6353
5/28/2020	T1	60	5:10:00 PM	8.2603
5/28/2020	T2	60	5:54:00 PM	1.4553
5/28/2020	D1	60	8:24:00 PM	1.1161
5/28/2020	T1	60	8:54:00 PM	5.3861
5/28/2020	T2	60	9:39:00 PM	6.7604
5/29/2020	D1	60	1:49:00 AM	0.3295
5/29/2020	T1	60	2:23:00 AM	4.0481
5/29/2020	T2	60	3:00:00 AM	7.1297
5/29/2020	D1	60	6:49:00 AM	0.4168
5/29/2020	T1	60	7:20:00 AM	2.4689
5/29/2020	T2	60	8:03:00 AM	4.1613
5/29/2020	D1	60	8:39:00 AM	0.6673
5/29/2020	T1	60	9:37:00 AM	3.8379
5/29/2020	T2	60	10:18:00 AM	3.0962
6/1/2020	D1	60	11:48:00 AM	3.2523
6/1/2020	T1	60	12:23:00 PM	13.1115
6/1/2020	T2	60	1:00:00 PM	21.8212
6/1/2020	D1	60	3:45:00 PM	2.0822
6/1/2020	T1	60	4:17:00 PM	27.9094
6/1/2020	T2	60	4:54:00 PM	65.9846
6/1/2020	D1	60	8:00:00 PM	11.584
6/1/2020	T1	60	8:30:00 PM	43.9709
6/1/2020	T2	60	9:25:00 PM	30.6415
6/2/2020	D1	60	6:19:00 AM	3.54
6/2/2020	T1	60	6:51:00 AM	7.36
6/2/2020	T2	60	7:28:00 AM	0.7585
6/9/2020	D1	60	10:47:00 AM	2.2157
6/9/2020	T1	60	11:26:00 AM	6.7895
6/9/2020	T2	60	12:09:00 PM	8.3983
6/9/2020	D1	60	2:26:00 PM	1.7112
6/9/2020	T2	60	3:40:00 PM	3.6042
6/9/2020	D1	60	6:18:00 PM	3.8386
6/9/2020	T2	60	7:14:00 PM	7.0901
6/9/2020	D1	60	10:09:00 PM	2.2593
6/9/2020	T2	60	11:03:00 PM	2.7809
6/10/2020	D1	60	2:08:00 AM	1.559
6/10/2020	T2	60	3:01:00 AM	2.3732
6/10/2020	D1	60	6:06:00 AM	1.3604
6/10/2020	T2	60	6:58:00 AM	2.1746
6/16/2020	D1	60	10:45:00 AM	1.0028

6/16/2020	T2	60	11:48:00 AM	2.6868
6/16/2020	D1	60	2:27:00 PM	0.4697
6/16/2020	T2	60	3:19:00 PM	3.0295
6/16/2020	D1	60	6:27:00 PM	0.9244
6/16/2020	T2	60	7:23:00 PM	7.5645
6/16/2020	D1	60	10:49:00 PM	0.5851
6/16/2020	T2	60	11:41:00 PM	6.3255
6/17/2020	D1	60	2:58:00 AM	0.2964
6/17/2020	T2	60	3:40:00 AM	6.4126
6/17/2020	D1	60	6:12:00 AM	0.7935
6/17/2020	T2	60	7:01:00 AM	4.2817
5/22/2020	D1	BED	12:44:00 PM	0.1414
5/22/2020	T1	BED	1:40:00 PM	5.3923
5/22/2020	T2	BED	2:25:00 PM	0.6181
5/22/2020	D1	BED	4:17:00 PM	0.0781
5/22/2020	T1	BED	4:50:00 PM	1.0059
5/22/2020	T2	BED	5:33:00 PM	0.6906
5/22/2020	D1	BED	9:15:00 PM	0.6401
5/22/2020	T1	BED	9:46:00 PM	1.3289
5/22/2020	T2	BED	10:20:00 PM	0.7120
5/23/2020	D1	BED	1:45:00 AM	0.3933
5/23/2020	T1	BED	2:16:00 AM	0.9322
5/23/2020	T2	BED	2:50:00 AM	0.5125
5/23/2020	D1	BED	7:17:00 AM	0.0324
5/23/2020	T1	BED	7:45:00 AM	0.7784
5/23/2020	T2	BED	8:15:00 AM	0.2499
5/28/2020	D1	BED	12:25:00 PM	0.6424
5/28/2020	T1	BED	1:08:00 PM	0.8199
5/28/2020	T2	BED	2:10:00 PM	0.5955
5/28/2020	D1	BED	4:30:00 PM	0.0928
5/28/2020	T1	BED	5:10:00 PM	2.5293
5/28/2020	T2	BED	5:54:00 PM	0.9398
5/28/2020	D1	BED	8:24:00 PM	0.2878
5/28/2020	T1	BED	8:54:00 PM	3.3926
5/28/2020	T2	BED	9:39:00 PM	2.2823
5/29/2020	D1	BED	1:49:00 AM	0.3141
5/29/2020	T1	BED	2:23:00 AM	2.2809
5/29/2020	T2	BED	3:00:00 AM	0.6282
5/29/2020	D1	BED	6:49:00 AM	0.2047
5/29/2020	T1	BED	7:20:00 AM	1.9829
5/29/2020	T2	BED	8:03:00 AM	0.893

5/29/2020	D1	BED	8:39:00 AM	0.2001
5/29/2020	T1	BED	9:37:00 AM	0.3367
5/29/2020	T2	BED	10:18:00 AM	7.0723
6/1/2020	D1	BED	11:48:00 AM	0.1199
6/1/2020	T1	BED	12:23:00 PM	1.9461
6/1/2020	T2	BED	1:00:00 PM	7.0396
6/1/2020	D1	BED	3:45:00 PM	0.2515
6/1/2020	T1	BED	4:17:00 PM	8.0393
6/1/2020	T2	BED	5:15:00 PM	11.2933
6/1/2020	D1	BED	8:00:00 PM	1.9696
6/1/2020	T1	BED	8:30:00 PM	16.503
6/1/2020	T2	BED	9:25:00 PM	24.473
6/2/2020	D1	BED	6:19:00 AM	0.4159
6/2/2020	T1	BED	6:51:00 AM	1.5541
6/2/2020	T2	BED	7:28:00 AM	2.2716
6/9/2020	D1	BED	10:47:00 AM	0.4703
6/9/2020	T1	BED	11:26:00 AM	1.4488
6/9/2020	T2	BED	12:09:00 PM	1.5915
6/9/2020	D1	BED	2:26:00 PM	0.6328
6/9/2020	T1	BED	3:00:00 PM	3.0157
6/9/2020	T2	BED	3:40:00 PM	2.4405
6/9/2020	D1	BED	6:18:00 PM	0.4434
6/9/2020	T1	BED	6:45:00 PM	7.2747
6/9/2020	T2	BED	7:14:00 PM	2.9866
6/9/2020	D1	BED	10:09:00 PM	0.3273
6/9/2020	T1	BED	10:39:00 PM	7.9163
6/9/2020	T2	BED	11:03:00 PM	1.1499
6/10/2020	D1	BED	2:08:00 AM	0.3911
6/10/2020	T1	BED	2:33:00 AM	1.1257
6/10/2020	T2	BED	3:01:00 AM	0.7575
6/10/2020	D1	BED	6:06:00 AM	0.17
6/10/2020	T1	BED	6:30:00 AM	1.0553
6/10/2020	T2	BED	6:58:00 AM	1.831
6/16/2020	D1	BED	10:45:00 AM	0.566
6/16/2020	T1	BED	11:14:00 AM	0.3039
6/16/2020	T2	BED	11:48:00 AM	1.1181
6/16/2020	D1	BED	2:27:00 PM	0.2035
6/16/2020	T1	BED	2:51:00 PM	0.5133
6/16/2020	T2	BED	3:19:00 PM	1.2028
6/16/2020	D1	BED	6:27:00 PM	0.1404
6/16/2020	T1	BED	6:55:00 PM	1.9592

6/16/2020	T2	BED	7:23:00 PM	1.0388
6/16/2020	D1	BED	10:49:00 PM	0.0517
6/16/2020	T1	BED	11:12:00 PM	0.90333
6/16/2020	T2	BED	11:41:00 PM	0.8834
6/17/2020	D1	BED	2:58:00 AM	0.2379
6/17/2020	T1	BED	3:08:00 AM	1.6866
6/17/2020	T2	BED	3:40:00 AM	3.0596
6/17/2020	D1	BED	6:12:00 AM	0.0378
6/17/2020	T1	BED	6:36:00 AM	0.456
6/17/2020	T2	BED	7:01:00 AM	0.8278
7/22/2020	D1	BED	9:34:00 AM	0.0796
7/22/2020	T1	BED	9:58:00 AM	0.1444
7/22/2020	T2	BED	10:27:00 AM	0.091
7/22/2020	D1	BED	1:30:00 PM	0.177
7/22/2020	T1	BED	1:56:00 PM	0.602
7/22/2020	T2	BED	2:27:00 PM	0.221
7/22/2020	D1	BED	5:24:00 PM	0.0894
7/22/2020	T1	BED	5:43:00 PM	0.7259
7/22/2020	T2	BED	6:05:00 PM	0.1438
7/22/2020	D1	BED	9:25:00 PM	0.072
7/22/2020	T1	BED	9:45:00 PM	0.1758
7/22/2020	T2	BED	10:08:00 PM	0.0921
7/23/2020	D1	BED	1:23:00 AM	0.0522
7/23/2020	T1	BED	1:43:00 AM	0.1926
7/23/2020	T2	BED	2:07:00 AM	0.0973
7/23/2020	D1	BED	5:29:00 AM	0.0462
7/23/2020	T1	BED	5:47:00 AM	0.1018
7/23/2020	T2	BED	6:14:00 AM	0.1078
7/23/2020	D1	BED	9:27:00 AM	0.3278
7/23/2020	T1	BED	9:50:00 AM	0.1666
7/23/2020	T2	BED	10:12:00 AM	0.0701
7/23/2020	D1	BED	1:25:00 PM	0.0917
7/23/2020	T1	BED	1:53:00 PM	0.2272
7/23/2020	T2	BED	2:26:00 PM	0.2107
7/23/2020	D1	BED	5:40:00 PM	0.0851
7/23/2020	T1	BED	6:06:00 PM	0.1135
7/23/2020	T2	BED	6:38:00 PM	0.8623
7/23/2020	D1	BED	9:39:00 PM	0.0568
7/23/2020	T1	BED	10:00:00 PM	0.2387
7/23/2020	T2	BED	10:25:00 PM	0.0962
7/24/2020	D1	BED	5:40:00 AM	0.0443

7/24/2020	T1	BED	6:04:00 AM	0.4571
7/24/2020	T2	BED	6:31:00 AM	0.096
5/22/2020	D1	SURF	12:44:00 PM	0.7083
5/22/2020	T1	SURF	1:40:00 PM	1.7633
5/22/2020	T2	SURF	2:25:00 PM	4.0306
5/22/2020	D1	SURF	4:17:00 PM	0.4376
5/22/2020	T1	SURF	4:50:00 PM	0.6981
5/22/2020	T2	SURF	5:33:00 PM	2.5888
5/22/2020	D1	SURF	9:15:00 PM	1.1615
5/22/2020	T1	SURF	9:46:00 PM	3.5488
5/22/2020	T2	SURF	10:20:00 PM	4.0021
5/23/2020	D1	SURF	1:45:00 AM	0.9888
5/23/2020	T1	SURF	2:16:00 AM	3.1382
5/23/2020	T2	SURF	2:50:00 AM	2.3690
5/23/2020	D1	SURF	7:17:00 AM	2.4987
5/23/2020	T1	SURF	7:45:00 AM	0.7979
5/23/2020	T2	SURF	8:15:00 AM	3.3560
5/28/2020	D1	SURF	12:25:00 PM	0.8444
5/28/2020	T1	SURF	1:08:00 PM	1.4389
5/28/2020	T2	SURF	2:10:00 PM	1.2136
5/28/2020	D1	SURF	4:30:00 PM	0.8044
5/28/2020	T1	SURF	5:10:00 PM	4.0644
5/28/2020	T2	SURF	5:54:00 PM	4.4389
5/28/2020	D1	SURF	8:24:00 PM	1.4868
5/28/2020	T1	SURF	8:54:00 PM	2.3504
5/28/2020	T2	SURF	9:39:00 PM	1.6822
5/29/2020	D1	SURF	1:49:00 AM	1.126
5/29/2020	T1	SURF	2:23:00 AM	1.8325
5/29/2020	T2	SURF	3:00:00 AM	3.7698
5/29/2020	D1	SURF	6:49:00 AM	0.6514
5/29/2020	T1	SURF	7:20:00 AM	1.4447
5/29/2020	T2	SURF	8:03:00 AM	1.4678
5/29/2020	D1	SURF	8:39:00 AM	0.8691
5/29/2020	T1	SURF	9:37:00 AM	1.412
5/29/2020	T2	SURF	10:18:00 AM	2.5718
6/1/2020	D1	SURF	11:48:00 AM	3.1990
6/1/2020	T1	SURF	12:23:00 PM	3.9631
6/1/2020	T2	SURF	1:00:00 PM	4.8657
6/1/2020	D1	SURF	3:45:00 PM	5.7919
6/1/2020	T1	SURF	4:17:00 PM	12.5703
6/1/2020	T2	SURF	4:54:00 PM	42.5752

6/1/2020	D1	SURF	8:00:00 PM	15.9513
6/1/2020	T1	SURF	8:30:00 PM	13.0711
6/1/2020	T2	SURF	9:25:00 PM	33.9501
6/2/2020	D1	SURF	6:19:00 AM	4.9203
6/2/2020	T1	SURF	6:51:00 AM	12.6767
6/2/2020	T2	SURF	7:28:00 AM	2.7752
6/9/2020	D1	SURF	10:47:00 AM	1.9998
6/9/2020	T1	SURF	11:26:00 AM	8.3116
6/9/2020	T2	SURF	12:09:00 PM	4.0089
6/9/2020	D1	SURF	2:26:00 PM	3.4108
6/9/2020	T1	SURF	3:00:00 PM	5.5644
6/9/2020	T2	SURF	3:40:00 PM	5.2905
6/9/2020	D1	SURF	6:18:00 PM	4.2804
6/9/2020	T1	SURF	6:45:00 PM	2.3263
6/9/2020	T2	SURF	7:14:00 PM	10.6205
6/9/2020	D1	SURF	10:09:00 PM	4.1812
6/9/2020	T1	SURF	10:39:00 PM	0.741
6/9/2020	T2	SURF	11:03:00 PM	1.2469
6/10/2020	D1	SURF	2:08:00 AM	2.3204
6/10/2020	T1	SURF	2:33:00 AM	2.9061
6/10/2020	T2	SURF	3:01:00 AM	1.577
6/10/2020	D1	SURF	6:06:00 AM	1.656
6/10/2020	T1	SURF	6:30:00 AM	0.3867
6/10/2020	T2	SURF	6:58:00 AM	1.9107
6/16/2020	D1	SURF	10:45:00 AM	0.8764
6/16/2020	T1	SURF	11:14:00 AM	3.3912
6/16/2020	T2	SURF	11:48:00 AM	2.4133
6/16/2020	D1	SURF	2:27:00 PM	0.8706
6/16/2020	T1	SURF	2:51:00 PM	1.6789
6/16/2020	T2	SURF	3:19:00 PM	2.8946
6/16/2020	D1	SURF	6:27:00 PM	1.1171
6/16/2020	T1	SURF	6:55:00 PM	2.1775
6/16/2020	T2	SURF	7:23:00 PM	1.0199
6/16/2020	D1	SURF	10:49:00 PM	1.1822
6/16/2020	T1	SURF	11:12:00 PM	2.7878
6/16/2020	T2	SURF	11:41:00 PM	6.2584
6/17/2020	D1	SURF	2:58:00 AM	0.8748
6/17/2020	T1	SURF	3:08:00 AM	1.7741
6/17/2020	T2	SURF	3:40:00 AM	1.1102
6/17/2020	D1	SURF	6:12:00 AM	0.5996
6/17/2020	T1	SURF	6:36:00 AM	1.6612

6/17/2020	T2	SURF	7:01:00 AM	2.4562
7/22/2020	D1	SURF	9:34:00 AM	0.0235
7/22/2020	T1	SURF	9:58:00 AM	0.1143
7/22/2020	T2	SURF	10:27:00 AM	0.1069
7/22/2020	D1	SURF	1:30:00 PM	0.1957
7/22/2020	T1	SURF	1:56:00 PM	0.3624
7/22/2020	T2	SURF	2:27:00 PM	0.3748
7/22/2020	D1	SURF	5:24:00 PM	0.1979
7/22/2020	T1	SURF	5:43:00 PM	0.8439
7/22/2020	T2	SURF	6:05:00 PM	0.4879
7/22/2020	D1	SURF	9:25:00 PM	0.2665
7/22/2020	T1	SURF	9:45:00 PM	0.1376
7/22/2020	T2	SURF	10:08:00 PM	0.1444
7/23/2020	D1	SURF	1:23:00 AM	0.2265
7/23/2020	T1	SURF	1:43:00 AM	0.1175
7/23/2020	T2	SURF	2:07:00 AM	0.2137
7/23/2020	D1	SURF	5:29:00 AM	0.4157
7/23/2020	T1	SURF	5:47:00 AM	0.1113
7/23/2020	T2	SURF	6:14:00 AM	0.1062
7/23/2020	D1	SURF	9:27:00 AM	0.0838
7/23/2020	T1	SURF	9:50:00 AM	0.3662
7/23/2020	T2	SURF	10:12:00 AM	0.1342
7/23/2020	D1	SURF	1:25:00 PM	0.0557
7/23/2020	T1	SURF	1:53:00 PM	0.0734
7/23/2020	T2	SURF	2:26:00 PM	0.185
7/23/2020	D1	SURF	5:40:00 PM	0.3045
7/23/2020	T1	SURF	6:06:00 PM	0.1997
7/23/2020	T2	SURF	6:38:00 PM	0.8232
7/23/2020	D1	SURF	9:39:00 PM	0.0298
7/23/2020	T1	SURF	10:00:00 PM	0.0593
7/23/2020	T2	SURF	10:25:00 PM	0.1851
7/24/2020	D1	SURF	5:40:00 AM	0.1441
7/24/2020	T1	SURF	6:04:00 AM	0.1951
7/24/2020	T2	SURF	6:31:00 AM	0.1945